Faculty of Science and Engineering
Department of Exploration Geophysics

Investigation of Pressure and Saturation Effects on Elastic Parameters: an Integrated Approach to Improve Time-Lapse Interpretation

Marcos Hexsel Grochau

This thesis is presented for the Degree of
Doctor of Philosophy
of
Curtin University of Technology

March 2009

Declaration

To the best of my knowledge and belief this thesis contains no material previously published by any other person except where due acknowledgment has been made.

This thesis contains no material which has been accepted for the award of any other degree or diploma in any university.

Signature: …….

Date: ……...

To my parents, Harry and Ruth, whose efforts permitted my education.

ABSTRACT

Time-lapse seismic is a modern technology for monitoring production-induced changes in and around a hydrocarbon reservoir. Time-lapse (4D) seismic may help locate undrained areas, monitor pore fluid changes and identify reservoir compartmentalization. Despite several successful 4D projects, there are still many challenges related to time-lapse technology. Perhaps the most important are to perform quantitative time-lapse and to model and interpret time-lapse effects in thin layers. The former requires one to quantify saturation and pressure effects on rock elastic parameters. The latter requires an understanding of the combined response of time-lapse effects in thin layers and overcoming seismic vertical resolution limitation.

This thesis presents an integrated study of saturation and pressure effects on elastic properties. Despite the fact that Gassmann fluid substitution is standard practice to predict time-lapse saturation effects, its validity in the field environment rests upon a number of assumptions. The validity of Gassmann equations, ultimately, can only be tested in real geological environments. In this thesis I developed a workflow to test Gassmann fluid substitution by comparing saturated P-wave moduli computed from dry core measurements with those obtained from sonic and density logs. The workflow has been tested on a turbidite reservoir from the Campos Basin, offshore Brazil. The results show good statistical agreement between the P-wave elastic moduli computed from cores using the Gassmann equations and the corresponding moduli computed from log data. This confirms that all the assumptions of the Gassmann theory are adequate within the measurement error and natural variability of elastic properties. These results provide further justification for using the Gassmann theory to interpret time-lapse effects in this sandstone reservoir and in similar geological formations.

Pressure effects on elastic properties are usually obtained by laboratory measurements, which can be affected by core damage. I investigated the magnitude of this effect on compressional-wave velocities by comparing laboratory experiments and

log measurements. I used Gassmann fluid substitution to obtain low-frequency saturated velocities from dry core measurements taken at reservoir pressure, thus mitigating the dispersion effects. The analysis is performed for an unusual densely cored well from which 43 cores were extracted over a 45 m thick turbidite reservoir. These computed velocities show very good agreement with the sonic-log measurements. This is encouraging because it implies that core damages that may occur while bringing the core samples to the surface are small and do not adversely affect the measurement of elastic properties on these core samples. Should core damage have affected our measurements, we would have expected a systematic difference between properties measured in situ and on the recovered. This confirms that, for this particular region, the effect of core damage on ultrasonic measurements is less than the measurement error. Consequently, stress sensitivity of elastic properties as obtained from ultrasonic measurements are adequate for quantitative interpretation of time-lapse seismic data.

In some circumstances, stress sensitivity may not be obtained by ultrasonic measurements. Cores may be affected by damage, bias in the plugging process and scale effects and therefore may not be representative of the in situ properties. Consequently it is desirable to obtain this dependence from an alternative method. This other approach ideally should provide the pressure – velocity dependence from an intact rock. Few methods can sample the in situ rock. Seismic, for instance, provides in situ information, but lacks vertical resolution. Well logs, on the other hand, can provide high vertical resolution information, but usually are not available before and after production changes. I propose a method to assess the in situ pressure - velocity dependence using well data. I apply this method to a reservoir made up of sandstone. I used 23 wells drilled and logged in different stages of development of a hydrocarbon field providing rock and fluid properties at different pressures. For each well logged at a specific time, pore pressure, velocity and porosity, among other properties, are known. Pore pressure is accessed from a Repeat Formation Tester (RFT). As a field depletes and new wells are drilled and logged, similar data sets related to different stages of depletion are available.

I present an approach expanding Furre et al. (2009) study incorporating porosity and obtaining a three dimensional relationship with velocity and pressure. The idea is to help to capture rock property variability.

Quantitative time-lapse studies require precise knowledge of the response of rocks sampled by a seismic wave. Small-scale vertical changes in rock properties, such as those resulting from centimetre scale depositional layering, are usually undetectable in both seismic and standard borehole logs (Murphy et al., 1984). I present a methodology to assess rock properties by using X-ray computed tomography (CT) images along with laboratory velocity measurements and borehole logs. This methodology is applied to rocks extracted from around 2.8 km depth from offshore Brazil. This improved understanding of physical property variations may help to correlate stratigraphy between wells and to calibrate pressure effects on velocities, for seismic time-lapse studies.

Small scale intra-reservoir shales have a very different response from sands to fluid injection and depletion, and thus may have a strong effect on the equivalent properties of a heterogeneous sandstone reservoir. Since shales have very low permeability, an increase of pore pressure in the sand will cause an increase of confining pressure in the intra-reservoir shale. I present a methodology to compute the combined seismic response for depletion and injection scenarios as a function of net to gross (NTG or sand – shale fraction). This approach is appropriate for modelling time-lapse effects of thin layers of sandstones and shales in repeated seismic surveys when there is no time for pressure in shale and sand to equilibrate. I apply the developed methodology to analyse the sand - shale combined response to typical shale and sandstone stress sensitivities for an oil field located in Campos Basin, Brazil. For a typical NTG of 0.6, there is a difference of approximately 35% in reflection coefficient during reservoir depletion from the expected value if these shales are neglected. Consequently, not considering the small shales intra-reservoir may mislead quantitative 4D studies.

The results obtained in this research are aimed to quantify pressure and saturation effects on elastic properties. New methodologies and workflows have been proposed and tested using real data from South America (Campos Basin) datasets. The results of this study are expected to guide future time-lapse studies in this region. Further investigations using the proposed methodologies are necessary to verify their applicability in other regions.

ACKNOWLEDGEMENTS

I would like to thank my supervisor Professor Boris Gurevich for his guidance, patience, availability and inspiring ideas. Without his support completing this thesis would not have been easy. I also appreciate the assistance of Dr. Bruce Hartley, Dr. Christian Dupuis and Dr. Tobias Müller. Their careful reading has greatly improved the accuracy and clarity of this thesis.

I would like to thank all the staff members of the Department of Exploration Geophysics, who have assisted me in the course of my research, with special thanks to Ms. Deirdre Hollingsworth for her administrative help and Mr. Robert Verstandig for his computing help.

I would also like to thank my colleagues at the Department of Exploration Geophysics, Curtin University of Technology and CSRIO for their useful discussions and friendship throughout my PhD research, especially Ben Clennell, Dariush Nadri, Marina Pervukhina, Maxim Lebedev, Mohammed Alhussain and Putri Wisman.

I would also like to acknowledge Andre Gerhardt for his encouragement in the early phase of this project. My thanks also go to David Lumley for his suggestion to use combined analysis of core and log data in conjunction with seismic data.

I am also grateful for the financial assistance of Petrobras, the state-owned Brazilian oil company, through the commitment of the following E&P-managers who endorsed this project: Sebastião Benedito Martins, Paulo Marcos Tinoco, Sueli Ueta, Gilson Ferreira, Jose Adilson Tenorio, Paulo Johann, Carlos Eugênio da Ressureicão, Carlos Bruhn, Jose Antonio Figueiredo, Alberto Sampaio de Almeida and Guilherme Estrella. Their encouragement and support during all stages of this journey was extremely important and very much appreciated.

Thanks are due to to the efficient and extremely helpful secretary Maria Goretti who was always available to assist me with organizational requirements and the paper

work involved. I should also thank Julio Machado, Marcos Gomes and Edno Souza for helping me to organize the 4D papers database. Thank you to my tennis friends Dr. and Mrs. David Thwaites for suggesting grammatical improvements for this thesis.

Thank you to my colleagues of Petrobras with whom I have exchanged ideas and experience: Ana Moliterno, Armando Scarparo Cunha, Elisabete Campos, Gilberto Albertão, Gilberto Lima, Guilherme Vasquez, Marcos Sebastião, Osni de Paula and Silvia Malagutti. I really have appreciated the technical discussions and I acknowledge your help. Petrobras surely has a highly qualified group and can take great pride in this.

Special thanks to my sons Artur and Hugo for their understanding of the long hours spent studying hard; and to my wife, Lise, who provided support to continue my studies at Curtin.

Finally, a very special thank you to my parents, Harry Rodolfo Grochau and Ruth Guilhermina Hexsel Grochau for the opportunities their sacrifices have provided me with. Since my childhood they have shown me the importance of knowledge and have provided motivation and support.

TABLE OF CONTENTS

LIST OF FIGURES

LIST OF TABLES

LIST OF APPENDICES

Chapter 1

INTRODUCTION

1.1 Time-Lapse Seismic Technology

Seismic technology has been used in hydrocarbon exploration for over half a century. Initially only 2D seismic lines were acquired. Then, from the 1970's 3D seismic surveys were introduce to investigate the subsurface in three dimensions. The 3D seismic data began to be used not only for exploration, but also for characterization of reservoirs, thus assisting the development of oil and gas fields. 3D seismic usually helps to optimize reservoir management maximizing economic return from hydrocarbon fields.

In the 1980s and 1990s substantial progress in seismic technology and computer power led to the introduction development of 4D or time-lapse technology, in which repeated seismic (usually 3D) surveys were carried out to monitor changes in and around the reservoir induced by hydrocarbon production. This technology started to be tested in the early 1980's and commercialized in the late 1990's (Amundsen and Landro, 2007). Each seismic survey represents a snapshot of reservoir conditions at a certain time. 4D signals could reveal changes in rock elastic properties due to reservoir production, assisting in reservoir characterization. The differences between surveys may be attributed to changes in saturation, pressure, temperature, and other effects.

The benefits of time-lapse monitoring are many and occur in different stages of the production life of a hydrocarbon field. 4D seismic may assist in locating undrained

areas to be drilled increasing the recovery factor (Anderson et al., 1997), monitoring pore fluid pressure changes (Jenkins et al., 1997), guiding pressure maintenance (injection) programs (Staples et al., 2007), monitoring fluid movement (Sonneland et al., 1997), including CO_2, and identifying fault compartmentalization (Weisenborn and Hague, 2005). The potential benefits go beyond identifying saturation and pressure changes within the reservoir. Changes in overburden rock strength and subsidence due to reservoir compaction may also be identified (Tura et al., 2005), and thus help reduce risk from hazardous effects on wells and facilities.

Time-lapse seismic has become a new practice in monitoring reservoir production, reducing reservoir uncertainties and identifying additional reserves. Figure 1.1 shows the major technologies used in hydrocarbon exploration and production. Industry-wide market surveys identify 3D and 4D (time-lapse) seismic technologies as having a major impact on ultimate recovery and drilling efficiency, providing more accurate predictions of future reservoir production (Pickering, 2006).

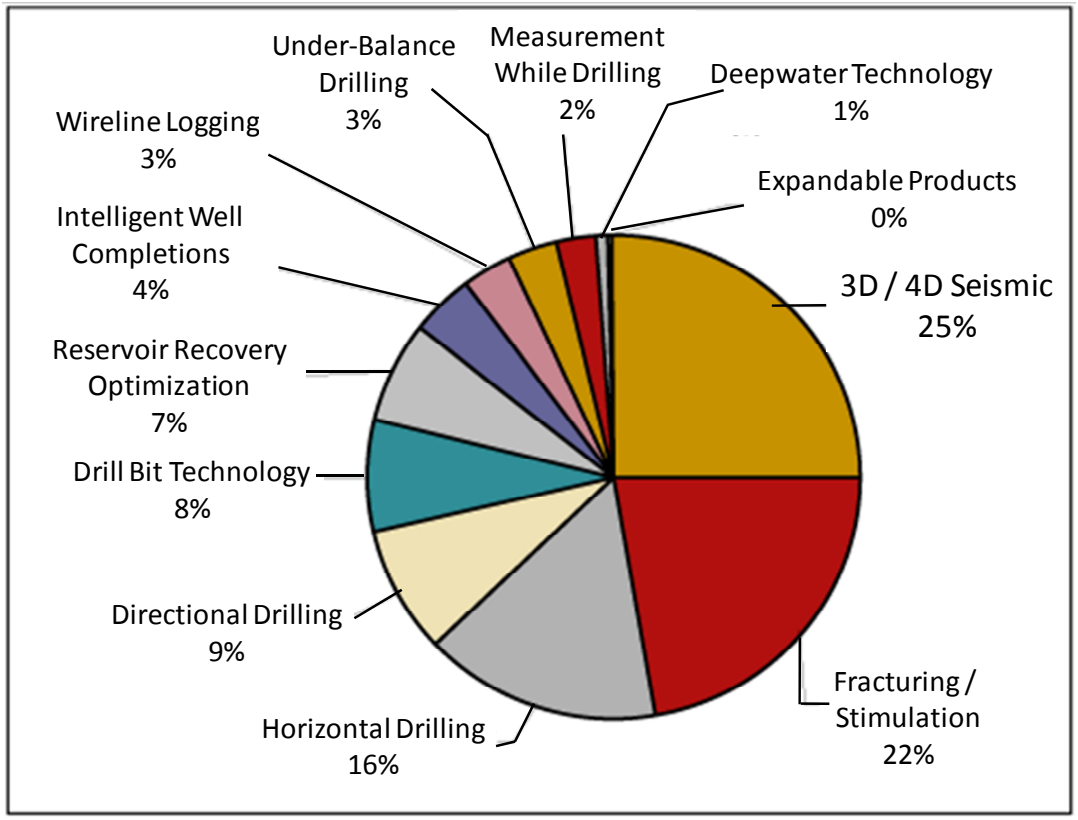

Figure 1.1: Illustration of the most important technologies influencing E&P spending (Lehman Brother E&P Spending Summary: Most Influential 2006 Technology).

Some of the early successful 4D projects, related to monitoring steam injection, were conducted by Pullin et al. (1987), Eastwood et al. (1994), Lumley (1995a) and Jenkins et al. (1997). Greaves and Fulp (1987) succeeded in their experiment design and analysis of a 4D seismic project to monitor a fireflood EOR process. Important projects related to gas monitoring include a North Sea gas cap expansion project by Johnstad et al. (1995), a west Texas CO_2 injection project by Harris et al. (1996), and a Paris basin gas storage project by Meunier and Huguet (1998).

Notable investments and interesting results in time-lapse projects occurred in Norwegian and UK North Sea: Oseberg field (Johnstad et al., 1995; Rutledal et al., 2003), the Magnus field (Watts et al., 1996), the Gullfaks field (Sonneland et al., 1997; Veire et al., 1998), the Draugen field (Gabriels et al., 1999), the Statfjord field (Al-Naijjar et al., 1999), and the Snorre field (Smith et al., 2001). In other regions around the world there are also many successful studies such as in carbonates in Canada (Hannah et al., 2005), a gas field (Maui) in New Zealand (Staples et al., 2006), Gulf of Mexico, USA (Burkhart et al., 2000; Johnston et al., 1999); Oman in Middle East (Waal and Calvert, 2003) and North West Shelf of Australia (Smith et al., 2007; Smith et al., 2008). In the last 10-15 years time-lapse seismic has become a proven technology based on successes around the world.

The vast number of publications demonstrates a keen interest in this technology by the scientific community and industry. Appendix A shows a list of papers related to time-lapse (4D) studies prepared in the initial stage of this PhD program. This database includes all the related pdf format files and has been made available to students and staff from Curtin University and may be available to anyone else upon request to the author. These publications show examples of application of 4D technology to clastic and carbonate fields; thin and thick reservoir; onshore and offshore in different regions.

Successful applications of 4D projects depend on the time-lapse signal strength, non-repeatable noise, and the complexity of interpreting the signal to be able to make conclusions about reservoir conditions (Staples et al., 2006). Figure 1.2 shows a maturity

S-curve for different 4D applications. The position on the maturity curve represents a combination of the signal strength and the complexity of the reservoir conditions. Pore pressure increase, for instance, sits high in this maturity S-curve, whereas depletion sits lower. This curve is general and only a general guideline of time-lapse maturity level to different field conditions. Simple assessments of technical risk of 4D projects have already been proposed in the literature (Lumley et al., 1997; Lumley et al., 2000). Following the basics assessments, I suggest performing a full technical feasibility study considering rock and fluid properties.

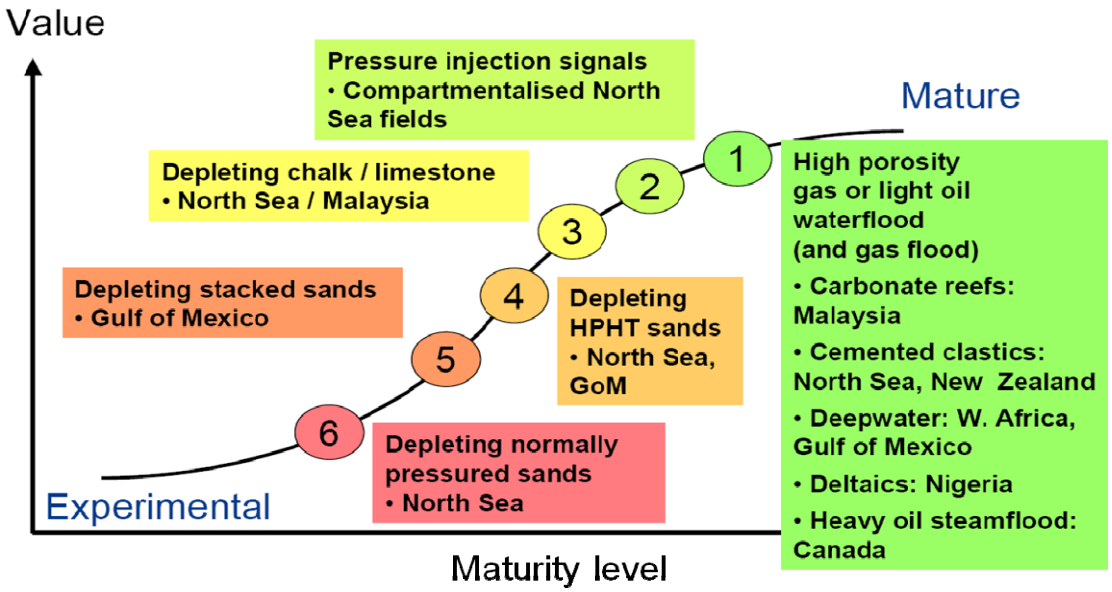

Figure 1.2: Maturity S-curve for different 4D applications (adapted from Staples et al., 2006).

Developments in this technology over the past few years indicate the potential of obtaining quantitative information rather than only qualitative. This quantitative approach is highly desirable by the oil industry in order to maximize profits, and is also important for humankind in terms of making better usage of our non renewable resources. In order to obtain useful quantitative information from time-lapse seismic data, however, it is necessary to better understand the seismic response to changes in rock and fluid properties as discussed in the Section 1.3.

1.2 Time-Lapse Seismic – Market and Economics Aspects

To analyse the value of 4D projects, costs and benefits should be taken into account. According to a study undertaken by the French Institute of Petroleum for the period 2000-2003 (Lumley, 2004), the expenditures of contractor and service companies related to 4D seismic were dominated mainly by North Sea projects (Figure 1.3). These expenditures include acquisition, processing and interpretation services, and the main component is acquisition costs. Today, the picture is almost the same (Amundsen and Landro, 2007). Other important geographical areas are offshore West Africa (Angola and Nigeria), offshore North America (Gulf of Mexico), and offshore South America (predominantly Brazil).

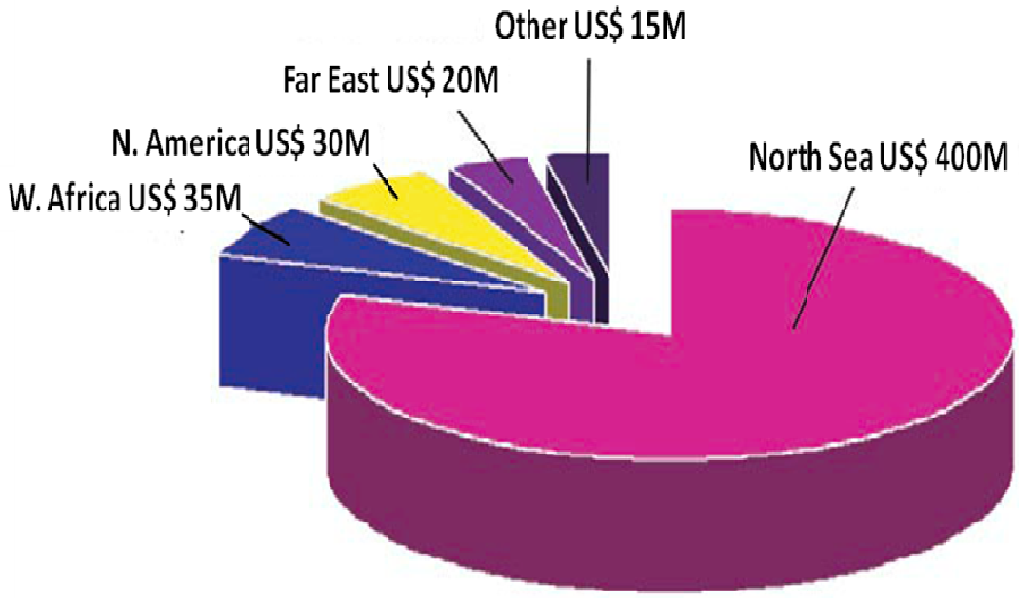

Figure 1.3: Cumulative expenditures on 4D seismic services to contractor and service companies for 2000-2003. Of $500 million cumulative 4D service expenditures, about $400 million (80%) has been spent in the North Sea, $35 million (7%) in West Africa, $30 million (6%) in North America, $20 million (4%) in the Far East, and $15 million (3%) elsewhere. This estimate of expenditures is for 4D seismic acquisition, processing and interpretation/analysis services (from Lumley, 2004).

In terms of benefits, the economic impact of 4D seismic has been significant, especially in the North Sea. Open sources, however, estimate the added value of North Sea 4D to be more than US$ 4 billion, with the added value at Gullfaks alone calculated to be close to US$ 1 billion. Furthermore, 4D is estimated to have reduced drilling costs by more than 6%, and contributed to additional reserves averaging 5% per field (Amundsen and Landro, 2007).

The dominant player in the 4D acquisition market today is StatoilHydro. More than twenty 4D streamer surveys were acquired during 2006. The other two big players are BP and Shell. BP has decided to invest strongly in permanently buried sensors for 4D, with installations at the North Sea Valhall field, the Caspian Sea Chiraz field and the US Clair field. The other main companies are ExxonMobil, ConocoPhillips, Chevron, Total and Petrobras (Amundsen and Landro, 2007).

1.3 Technical Challenges using Time-Lapse Seismic

Despite several successful 4D projects there are still many challenges related to time-lapse seismic technology. Applications in hard reservoirs, particularly in carbonates, often yield a small 4D signal (Waal and Calvert, 2003). Development of new acquisition technologies to enhance 4D repeatability and signal-to-noise ratio (Landro, 2008; Lumley, 2004), integrate time-lapse seismic data with reservoir engineering (Oldenziel, 2003) and 4D in thin-bedded clastic reservoirs (Amundsen and Landro, 2007) are also required. The main focus of the research presented in this thesis is related to another important challenge: quantitative analysis of 4D seismic responses of producing reservoirs. More specifically, to investigate pressure and saturation effects on elastic parameters.

The idea of repeating seismic surveys to monitor changes is an old one; however, the first quantitative data came from rock physics measurements at Stanford University in the mid 1980's (Lumley, 2001). These laboratory measurements on heavy-oil

saturated core samples showed large decreases in seismic rock velocity when the viscous oil was heated (Nur, 1989; Nur et al., 1984; Wang et al., 1990). Despite many studies investigating the relationships between changes in reservoir (rock and fluid) properties and seismic response, quantitative interpretation of time-lapse data is still a challenge and a very important research subject. In this thesis I focus on quantification of both saturation and pressure effects on rock elastic properties. Usually these are the most relevant effects on the 4D signal (Calvert, 2005; Eiken and Tondel, 2005; Hatchell and Bourne, 2005; Tura et al., 2005).

The effect of saturation changes on elastic properties is usually described by Biot-Gassmann theory of poroelasticity (Biot, 1956a, b; Gassmann, 1951). However, the validity of this theory on real (in situ) data has not been widely tested and requires further investigation.

The effect of pressure changes on elastic properties is usually obtained from ultrasonic measurements on core samples (Nes et al., 2002; Grochau and Gurevich, 2007b, 2008a). Issues such as core damage (Holt et al., 2005; Grochau and Gurevich, 2007a) and velocity dispersion always arise and need to be accounted for in order to provide reliable pressure-velocity relationship for time-lapse studies. Another approach to obtain this relationship is from in situ measurements (Furre et al., 2009; Hansen et al., 2006). A more reliable in situ measurement is provided by logs. In this thesis, feasibility of obtaining pressure sensitivity of rock properties from both logs and core measurements is investigated.

To fully understand 4D effects on seismic data, it is appropriate to start from small scale and move to larger scales. Interpretation of 4D data at a field scale may lead to ambiguous or even erroneous results when it is not calibrated with other more detailed data. The reason for this is due to the typical wavelengths of the seismic signals recorded in surface seismic surveys, which are often too large to separate different rock-fluid systems. Instead, seismic waves normally average over the heterogeneous systems and consequently add more unknowns to the inverse problem for each system.

Consequently, another technological challenge is to characterize thin stratification to help 4D interpretation. Moreover, this thin stratification and its combined seismic response should be understood both inside and in the surrounding of a reservoir. Small scale shales in clastic reservoirs may affect 4D seismic response during production and depletion. Fine layers with distinct elastic properties may impact the time-lapse response as well.

1.4 Aim of the Research

The main objective of this PhD thesis is to investigate saturation and pressure effects on elastic properties of rocks. These effects are commonly the most important ones in a time-lapse study.

Although it is possible to assess theoretically the validity of each of the assumptions and the impact of their violations on the predictions of Gassmann equations, they can ultimately be validated by in situ testing in real geological environments. One of the goals of this research is to verify the adequacy of Gassmann fluid substitution to the properties of in situ rocks.

Regarding the stress sensitivities of elastic parameters, they can be obtained from laboratory and from in situ measurements. Stress sensitivity of elastic properties as obtained from ultrasonic measurements can be affected, among other effects, by core damage. Velocity-pressure relationship can also be obtained from in situ measurements using well data. Another aim of this research is to investigate the reliability and limitations of obtaining this relationship from laboratory and from well data (in situ).

Considering the potential impact of thin stratification on 4D interpretation, another objective of this research is improve its characterization. This research proposes to use X-ray CT scan combined with ultrasonic and log measurements to better understand reservoir and overburden rocks, which may contribute to modelling and interpretation of 4D seismic data. The spatial resolution provided by the standard data

type (seismic and logs) may not be enough to fully capture and understand small scale geologic variations. Taking into consideration that typical Brazilian offshore clastic reservoirs contain small scale shales and considering the importance of 4D studies in this region, I also aim to investigate the combined seismic response of sandstone – shale due to pressure variation in a sandstone reservoir.

Meticulous analysis of time-lapse effects on different scales and a variety of tools provide better understanding and higher confidence for time-lapse interpretations. Development of new workflows and tests using real data increases the robustness of 4D interpretation and validate theoretical research towards a consistent application for field scale 4D studies.

1.5 Thesis Configuration

This thesis is composed of five chapters. After this introductory chapter, Chapter 2 provides some background regarding fluid effects on elastic properties. The effect of saturation changes on elastic properties is properly described by Gassmann (1951) theory. Despite being widely used to predict and interpret fluid changes, the validity of Gassmann theory in a real environment is not always evident since assumptions and limitations of this theory are often violated when considering real geology. After providing background information on Gassmann equations and assumptions, I present and apply a workflow to test the adequacy of this theory to a real environment.

Chapter 3 presents pressure effects on elastic parameters. Firstly, the velocity dependence on stress is obtained from core measurements. Core damage, velocity dispersion and under-representation of cores are discussed. I investigate the magnitude of core damage on compressional-wave velocities by comparing laboratory experiments and log measurements. All the experiments and results related to this approach are shown in this chapter. Secondly, the velocity dependence on stress is obtained from well data. In this in situ approach I present cross plots of velocity, confining stress and

porosity obtained from well logs and RFT (Repeated Formation Tester) data. Finally, the limitations of this approach for application in a real and complex environment are discussed.

The characterization of thin stratification and its impact on time-lapse response is discussed in Chapter 4. I use X-ray CT to obtain detailed information from small scale geologic variations, which were not fully captured using logs. Besides providing climatic insights and potentially assist accurate stratigraphic correlation, this high resolution technique may help to model and interpret time-lapse effects in the reservoir overburden rocks. The effect of the combined seismic response of shales inside sandstone during depletion and injection of a given reservoir is also discussed in this chapter.

In Chapter 5, I discuss the conclusions drawn from this research, the possible applicability of the results and make recommendations regarding directions of future research.

CHAPTER 2

FLUID EFFECTS ON ELASTIC PROPERTIES

One of the main aims for hydrocarbon reservoir management is to better map the fluid distribution during the production process. The development design is based on the a priori reservoir model, which initially has high uncertainty due to insufficient information about geometry and properties of the reservoir. The use of time-lapse (4D) seismic to monitor fluid distribution may allow optimization of the production layout and increase the recovery factor.

Time-lapse seismic requires understanding of the change of elastic wave velocities due to changes in fluid saturation. The elastic properties of a saturated rock are often predicted using Gassmann's equations (Gassmann, 1951; Landro, 2001). Gassmann fluid substitution has been used for various purposes: e. g. time-lapse effect prediction and mud filtrate corrections (Walls and Carr, 2001).

Gassmann theory is based on a number of assumptions. Although it is possible to assess theoretically the validity of each of these assumptions (Brown and Koringa, 1975; Wang, 2000; Artola and Alvarado, 2006) and the impact of their violations on the predictions of Gassmann equations, they can only, ultimately, be validated by in situ testing in real geological environments. According to Wang (2000), the rock-fluid system is so complicated that virtually all the theories for such a system have to make major assumptions in order to simplify the mathematics. Considering the above mentioned complexity, more studies testing Gassmann theory in real oil fields are important, particularly in South America where there are no or only a few in situ studies.

In this chapter, I present a brief theoretical background about elastic moduli of materials as well as Gassmann theory and its assumption. Subsequently I describe a workflow proposed to apply its equations and to test the underlying assumptions of this theory. The strategy is to compare saturated P-wave moduli computed from dry core measurements against those obtained from sonic and density logs.

2.1 Theoretical Background

2.1.1 Elastic moduli

According to Sheriff and Geldart (1995), elasticity deals with deformations that vanish entirely upon removal of the stresses that cause them. For small deformations, Hooke's law holds and strain is proportional to stress. The stress-strain properties of materials that obey Hooke's law are specified by elastic moduli. The relationship between stress and strain can be expressed by the elasticity tensor. In a general anisotropic media this tensor has up to 21 independent constants. In this research I consider isotropic media; therefore there are only two independent elastic constants.

The stress-strain ratio under hydrostatic pressure is given by the bulk modulus (K), and expresses the ratio of pressure change to relative volume strain ($\Delta V/V$)

$$K = \frac{\Delta P}{\Delta V/V}, \tag{2.1}$$

where ΔP is the pressure change, V is the initial volume and ΔV is the volume change.

The stress-strain ratio for single shear is given by the shear modulus, rigidity modulus or Lame's constant (μ)

$$\mu = \frac{\Delta F/A}{\Delta L/L}, \tag{2.2}$$

where ΔF is the shearing (tangential) force, A is the cross-sectional area, L is the distance between shear planes and ΔL is the shear displacement.

2.1.2 Gassmann theory and assumptions

Gassmann's fluid-substitution relation is commonly applied to predict the bulk modulus, and the expected changes in velocities, for rocks saturated with different fluids (Mavko et al. 1998). The saturated bulk modulus K_{sat} is computed using the Gassmann equation (Gassmann, 1951):

$$K_{sat} = K_{dry} + \frac{\left(1 - \frac{K_{dry}}{K_{\min}}\right)^2}{\frac{\phi}{K_{fluid}} + \frac{1-\phi}{K_{\min}} - \frac{K_{dry}}{(K_{\min})^2}}, \tag{2.3}$$

where

$$K_{dry} = \rho_{dry}\left(V_{Pdry}^2 - 4V_{Sdry}^2/3\right) \tag{2.4}$$

is the bulk modulus of the frame or dry rock, $K_{\min}$ is the effective modulus of the solid mineral grains, K_{fluid} is the effective modulus of the saturating fluid, ϕ is the porosity, ρ_{dry} is the density of the dry sample, V_{Pdry} and V_{Sdry} are the compressional and shear wave velocities measured in a dry sample.

Gassmann equations can also be expressed as follows:

$$\frac{K_{sat}}{K_{\min} - K_{sat}} = \frac{K_{dry}}{K_{\min} - K_{dry}} + \frac{K_{fluid}}{\phi\left(K_{\min} - K_{fluid}\right)}. \tag{2.5}$$

Gassmann equation allows transforming the bulk modulus from one fluid to another and calculating the expected change in velocities as a result of a change in pore fluid (Mavko et al., 1998):

$$\frac{K_{sat2}}{K_{\min}-K_{sat2}}-\frac{K_{fluid2}}{\phi\left(K_{\min}-K_{fluid2}\right)}=\frac{K_{sat1}}{K_{\min}-K_{sat1}}-\frac{K_{fluid1}}{\phi\left(K_{\min}-K_{fluid1}\right)}. \tag{2.6}$$

Gassmann predicted no change for the shear modulus due to saturation (Mavko and Jizba, 1991):

$$\mu_{sat}=\mu_{dry}, \tag{2.7}$$

where K_{sat1} and K_{sat2} are bulk moduli with fluids 1 and 2; K_{fluid1} and K_{fluid2} are bulk moduli of fluids 1 and 2; μ_{sat} and μ_{dry} are bulk modulus of the saturated and dry rock, respectively;

The saturated P- and S-waves velocities are expressed by the following equations:

$$V_p=\sqrt{\frac{(K+4\mu/3)}{\rho}}, \tag{2.8}$$

$$V_S=\sqrt{\frac{\mu}{\rho}}. \tag{2.9}$$

Gassmann's derivation is based on the following assumptions (Berryman, 1999):

- Pore pressure is in equilibrium between pores. This can be achieved at very low frequencies, usually at seismic frequencies or lower, where the fluid has enough time to reach relaxation or equilibrium. However, the relaxation time depends also on fluid viscosity and density, and rock permeability;
- The porous frame consists of a single solid material (monomineralic). If more than one mineral is present, an average mineral (called effective grain) must be derived;
- The rock is isotropic, however modifications have been discussed for anisotropic conditions (Brown and Gurevich, 2004);
- Pores are in flow communication and are homogeneously fully filled with a single fluid;

- The system is closed undrained;
- The pore fluid does not chemically influence the solid frame.

2.2 Testing Gassmann Fluid Substitution: Sonic Logs versus Ultrasonic Measurements

In this section, I present a workflow to test Gassmann fluid substitution in a real geological environment. The most obvious way to test the adequacy of Gassmann fluid substitution to the properties of the in situ rocks is to use repeated velocity measurements before and after fluid saturation changes in the reservoir. However such testing is not easy because time-lapse seismic lacks resolution while time-lapse sonic logs are seldom available. Gommesen et al. (2007) presented an analysis of the Gassmann prediction that was restricted to well log data.

One other option is to use dry velocities measured in the lab, perform Gassmann fluid substitution and compare the result with in situ sonic velocities (Mavko and Mukerji, 1998). This can be done in almost any well where sonic logs of good quality and ultrasonic measurements on cores are available. However, such testing also presents certain challenges, as the Gassmann fluid substitution effect on sonic velocities may be obscured by scale effects (well log measurements represent much larger volume than the core measurements). A way to overcome these effects is to use a large number of samples and apply statistical analysis to discern the deterministic effect from the random variability. A simple workflow (Figure 2.1) aimed at such analysis is proposed and tested on 43 samples taken from a 45 m turbidite reservoir from the Campos Basin, offshore Brazil.

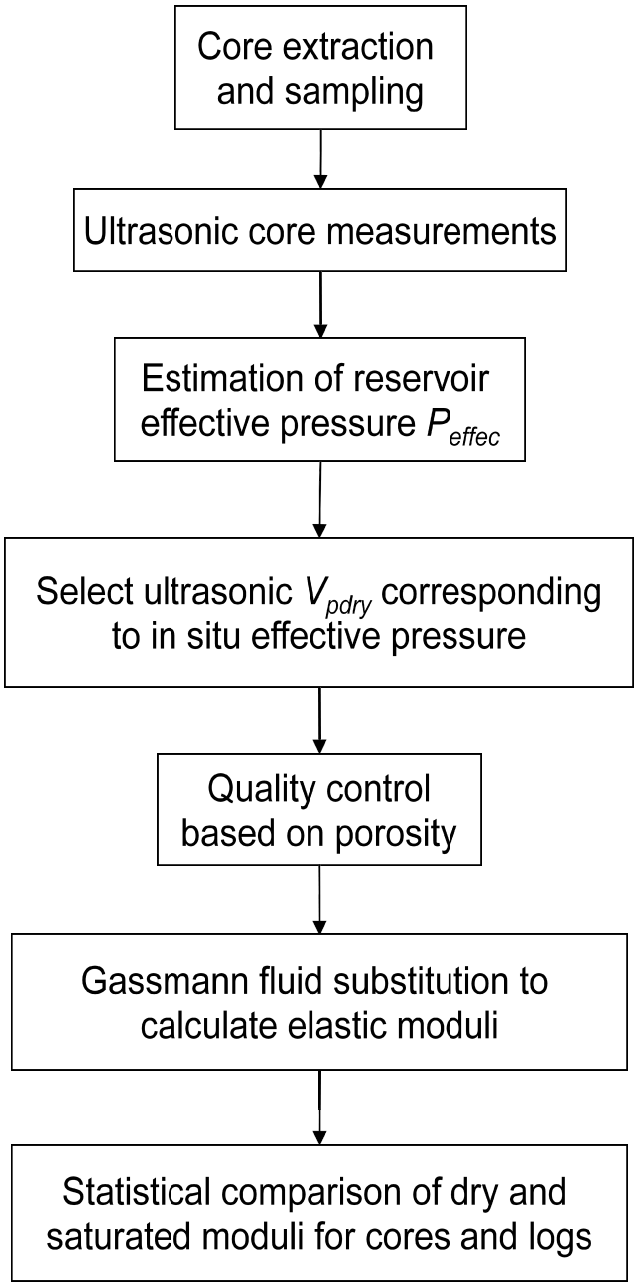

Figure 2.1: Workflow used for preparing the data and for testing Gassmann fluid substitution.

2.2.1 Core extraction and sampling

The well logs and cores analysed were obtained in the south portion of Campos Basin, around 100 km off the coast of Rio de Janeiro (south eastern Brazil), in a water depth of approximately 700 meters. In this basin there are more than 40 oil fields of different ages, representing a variety of reservoir properties (Figure 2.2). Each field and each reservoir has its own characteristics in terms of lithology, grain size, and cementation.

The first step is to ensure that the cores are extracted from a representative reservoir interval. For this study I use cores extracted continuously from a 45 m interval within and close to the reservoir zone from an oil field. The reservoir is composed of sandstone from turbidites deposited in the Cretaceous Period. Special care is required to ensure that the cores are not subject to significant damage during the drilling and extraction processes (Nes et al., 2002). As soon as samples are extracted, it is usual to follow these procedures. Cores are freezing by putting it in an ice container. After that, a small piece of the core is immersed in liquid nitrogen and the frozen rock is cored in a cylinder sample (plug). The plug is jacketed with a tin sleeve with screens at the faces of the cylinder in order to allow the measurement of porosity and permeability.

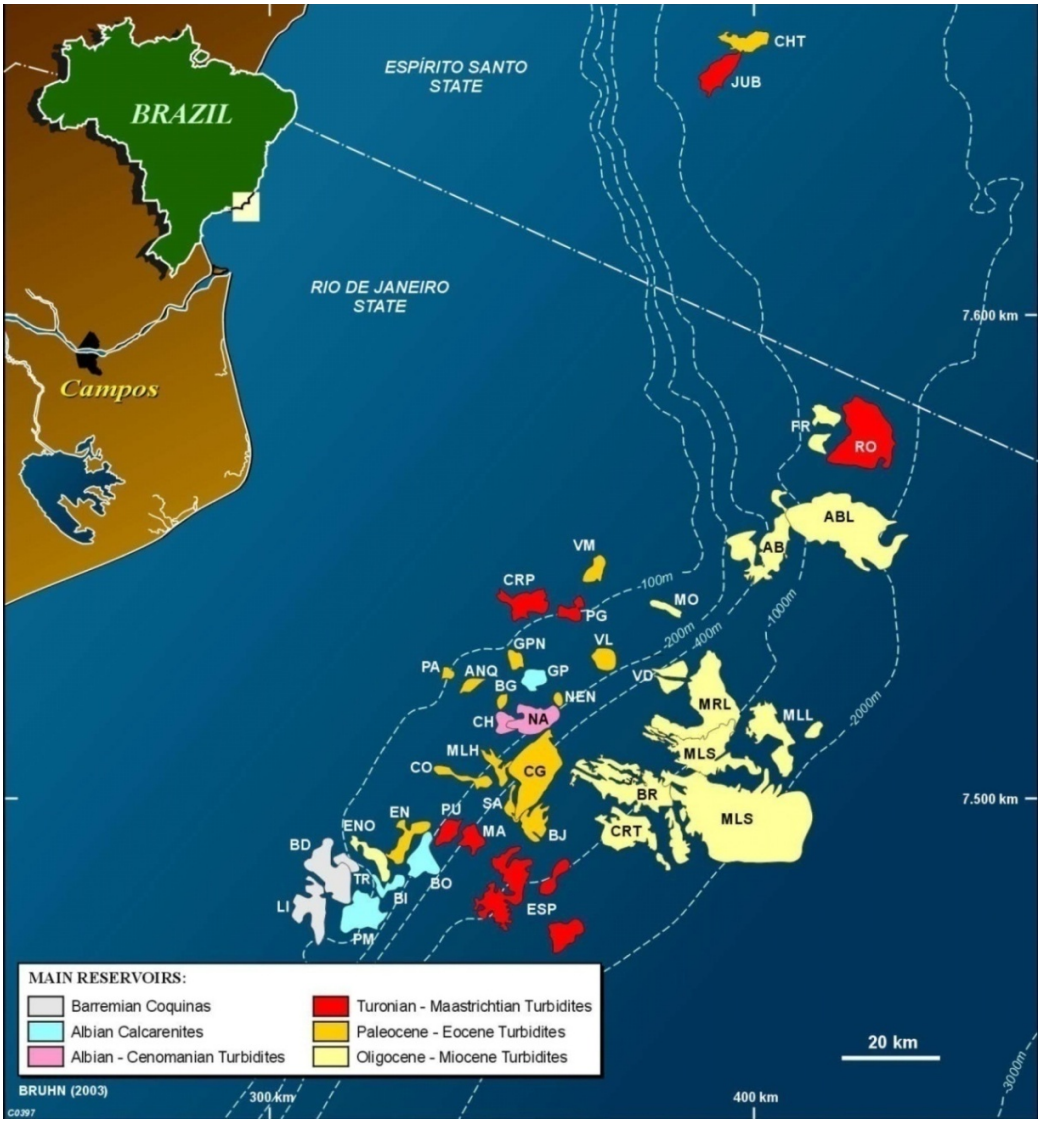

Figure 2.2: Map of the Campos Basin oilfields showing the location and age of the main reservoirs (Bruhn et al., 2003).

2.2.2 Ultrasonic core measurements

Ultrasonic measurements need to be performed on dry samples to exclude (or minimize) the effect of dispersion (Winkler, 1986), which can affect ultrasonic velocities. To this end 43 samples were extracted over a 45m thick reservoir and were dried under room-temperature conditions. The ultrasonic measurements were performed by positioning samples between two pairs of piezoelectric transducers (for P and S-waves) and immersed in a pressure chamber with hydraulic oil. The confining pressure was varied between 1000 and 6000 psi. A sinusoidal pulse with the central frequency 500 kHz was propagated through the sample and for each step of pressure increment velocities were determined (courtesy of J.E. Lira, A. Sobrinho and J. Pinheiro, Petrobras).

2.2.3 Estimation of reservoir effective pressure

In order to make an adequate comparison between log and lab data, both log and laboratory velocities need to be taken at the same effective pressure. Since in situ pressure is fixed we need to ensure that lab velocity is taken at the reservoir pressure. The effective pressure P_{effec} can be estimated from the lithostatic pressure and pore pressure using the equation

$$P_{effec} = Ah_w + B(h_r - h_w) - \eta P_{por} \ , \tag{2.10}$$

where η is the effective stress coefficient, P_{por} is the pore pressure, A and B are ocean water and lithostatic pressure gradients, h_w and h_r are water and reservoir depths, respectively. Pore pressure was obtained from well RFT (Repeat Formation Tester) measurements, which were made at the time when logs were acquired, and provided constant values over the reservoir interval. The effective stress coefficient η for velocities was assumed to be 1. The resulting value of effective pressure was taken to be 34.5 MPa (5000 psi) for the interval under investigation.

Formation testing is the final evaluation step before the well is put into production and provides essential information to design the well completion and production facilities. Among the applications of RFT are static pressure measurement and depletion determination, determination of reservoir fluid contacts and fluid density from gradients, and reservoir permeability (Schlumberger, Fundamentals of Formation Testing, internal report).

2.2.4 Quality control

Tests of Gassmann fluid substitution should be performed on porous rocks and should exclude low porosity and low permeability intervals where full draining of the core samples is not technically possible. Kahraman (2007) shows that P-wave velocities, estimated by applying the Gassmann equations, can widely differ from measured ones for rocks with very low porosities. Furthermore, it seems reasonable to exclude the cores extracted from strongly heterogeneous zones, since these are impossible to sample adequately with a few core measurements. For instance, the reservoir interval from the Campos Basin contains very thin low-porosity and high-velocity layers (concretions), which are under-sampled (smoothed over) by both porosity and sonic logs. At the same time, core samples can be taken either from concretions or from the surrounding sand. In both cases this may result in large discrepancies between log and core porosities. Such samples can be excluded from the test by comparing the core porosity against the total porosity from the well log. Figure 2.3 shows log and core porosities versus depth, and we can see that for 27 out of 43 samples the agreement between laboratory and log porosity is very good (discrepancy is within 0.03). Log porosities are systematically higher than core porosities. This difference may be caused by the presence of fractures in the vicinity of the well. Regarding the quality of log measurements, the caliper log shows integrity of the borehole over the interval under study.

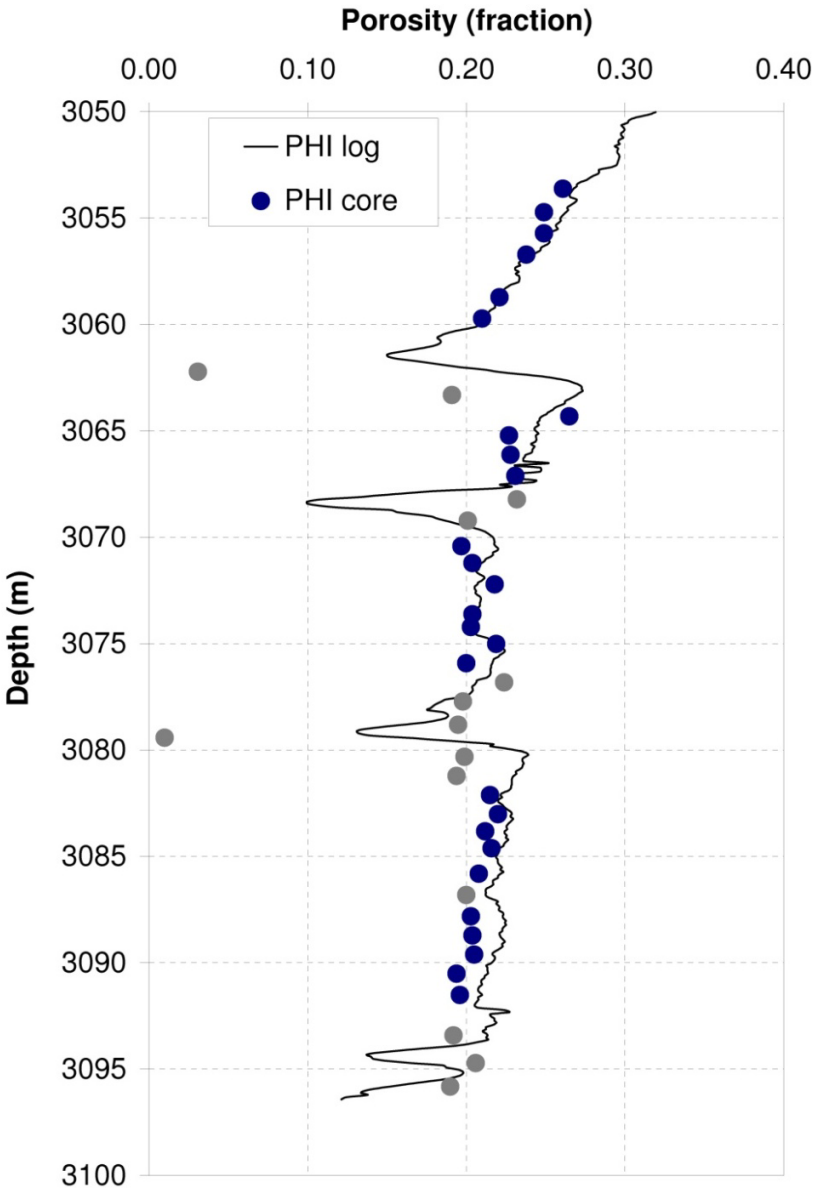

Figure 2.3: Porosity from log and cores showing the samples (blue) that meet the quality control criteria (discrepancy is within 0.03).

2.2.5 Gassmann fluid substitution to calculate elastic moduli

The most direct way to estimate the validity of Gassmann fluid substitution is to compare dry and saturated (obtained using Gassmann equation) bulk moduli K_{dry}, K_{sat} against the bulk moduli obtained from sonic log data $K_{\log}$. However, to compute these moduli, the knowledge of both *P* and *S* velocities is required. If *S*-wave velocities are not available, the comparison can be made of dry and saturated *P*-wave core velocities V_{Pdry}, V_{Psat} or *P* wave moduli $M_{dry} = \rho_{dry} V_{Pdry}^2$, $M_{sat} = K_{sat} + 4\mu/3$, against sonic velocity $V_{P\log}$ or *P* wave modulus $M_{\log} = \rho_{\log} V_{P\log}^2$, respectively. The use of *P* wave moduli is preferable to the use of velocities, as the effect of fluid substitution on velocities can be partially offset by the density effects, which increase relative errors and make precise comparison more difficult. The saturated bulk modulus K_{sat} is computed using Gassmann (equation (2.3)). If the saturation log is available, fluid modulus can be computed using Wood's equation (Mavko and Jizba, 1991):

$$1/K_{fluid} = (1 - S_w)/K_o + S_w/K_w , \tag{2.11}$$

where S_w is water saturation, K_o and K_w are the bulk moduli of the oil and water phases. The fluid substitution was performed using two-phase system: water and oil. The water saturation was taken directly from saturation log (Figure 2.4) at each core sample position.

2.2.6 Statistical analysis and results

The results of the workflow described above for the well data analysed are shown in Figures 2.5 and 2.6. Figure 2.5 shows the dry and saturated *P*-wave moduli M_{dry} and M_{sat} computed from laboratory data as well as the $M_{\log}$ obtained from the sonic log. These moduli are plotted against core porosity. We see that the differences between dry

and saturated moduli for the same samples are of the same order of magnitude as variation of velocities for a given porosity, or the average error between moduli obtained from laboratory and log data. This demonstrates that we cannot obtain a reliable conclusion about validity of fluid substitution from comparison of individual data points.

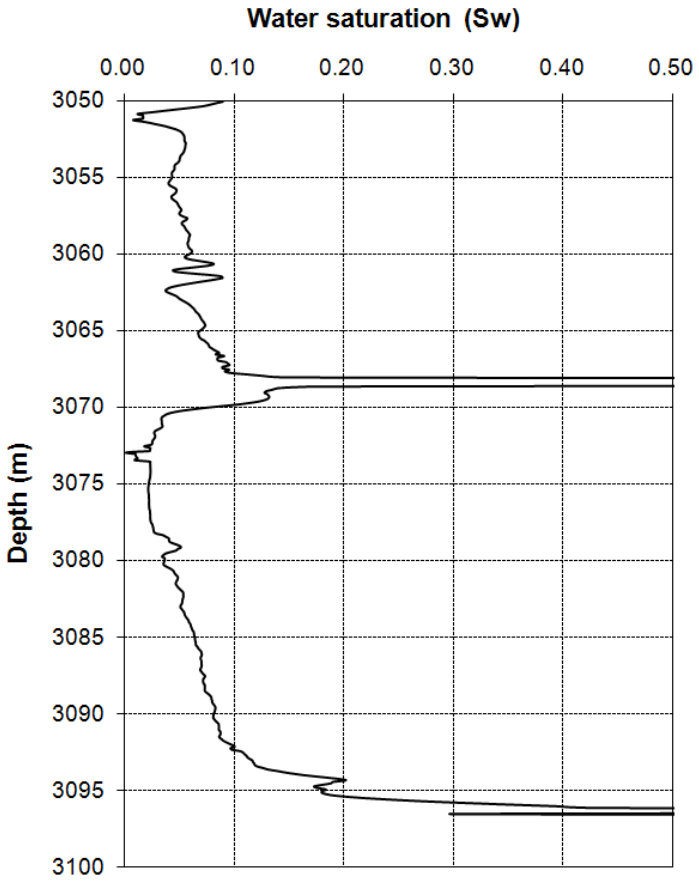

Figure 2.4: Water saturation log showing the water content in this interval, predominantly lower than 10% (the other phase is oil).

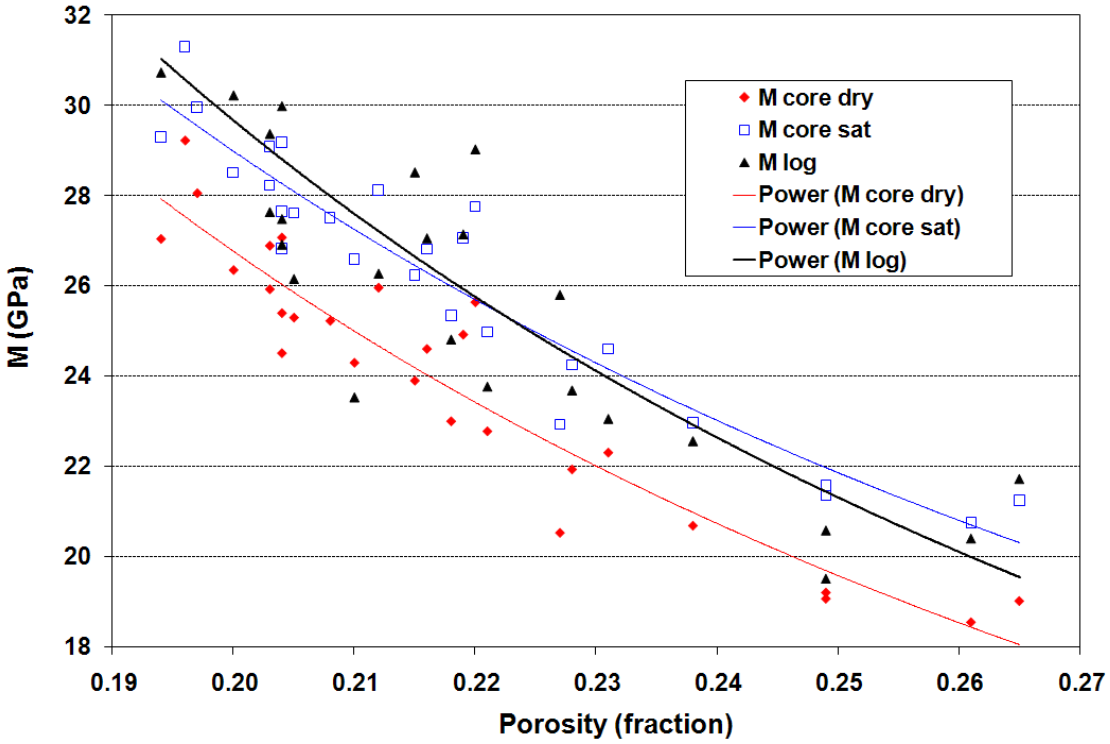

Figure 2.5: P-wave modulus computed from ultrasonic dry measurements (red symbols); the saturated modulus computed from dry core measurements using Gassmann equation (blue symbols); and obtained from sonic and density logs (black symbols). Lines are power-law regressions for each dataset.

However when we look at the regression trends of modulus vs. porosity, we can see that there is a systematic difference between dry laboratory moduli (magenta line) and sonic log moduli (black line), which is almost completely eliminated by Gassmann fluid substitution (blue line).

To perform a more quantitative statistical analysis Figure 2.6 shows the histograms of the difference between computed P-wave moduli from log and dry measurements (brown) and from logs and Gassmann saturated moduli (blue). The average difference between sonic log and dry lab moduli is 2.47 GPa, but reduces to 0.23 after fluid substitution. We also see that this shift is of the same order of magnitude as the standard deviation (width of each distribution), but the difference $M_{\log} - M_{dry}$ is centred around 2.47 GPa while $M_{\log} - M_{sat}$ is centred very close to zero (0.23 GPa).

We observe a very good match between P-wave moduli numerically saturated from cores and from logs. The results suggest the adequacy of Gassmann theory (despite all assumptions and limitations) in this particular reservoir interval.

2.3 Discussion and Conclusions

In this research I have developed a workflow to test Gassmann fluid substitution by comparing saturated P-wave moduli computed from dry core measurements against those obtained from sonic and density logs. The workflow has been tested on 43 samples taken from a 45 m turbidite reservoir in the Campos Basin, offshore Brazil. The results show good statistical agreement between the P-wave elastic moduli computed from cores using Gassmann equation with the corresponding moduli computed from log data. This confirms that all the assumptions of the Gassmann equations are adequate within the measurement error and natural variability of elastic properties.

These results provide further justification for using the Gassmann theory to interpret time-lapse effects in this sandstone reservoir and in similar geological formations.

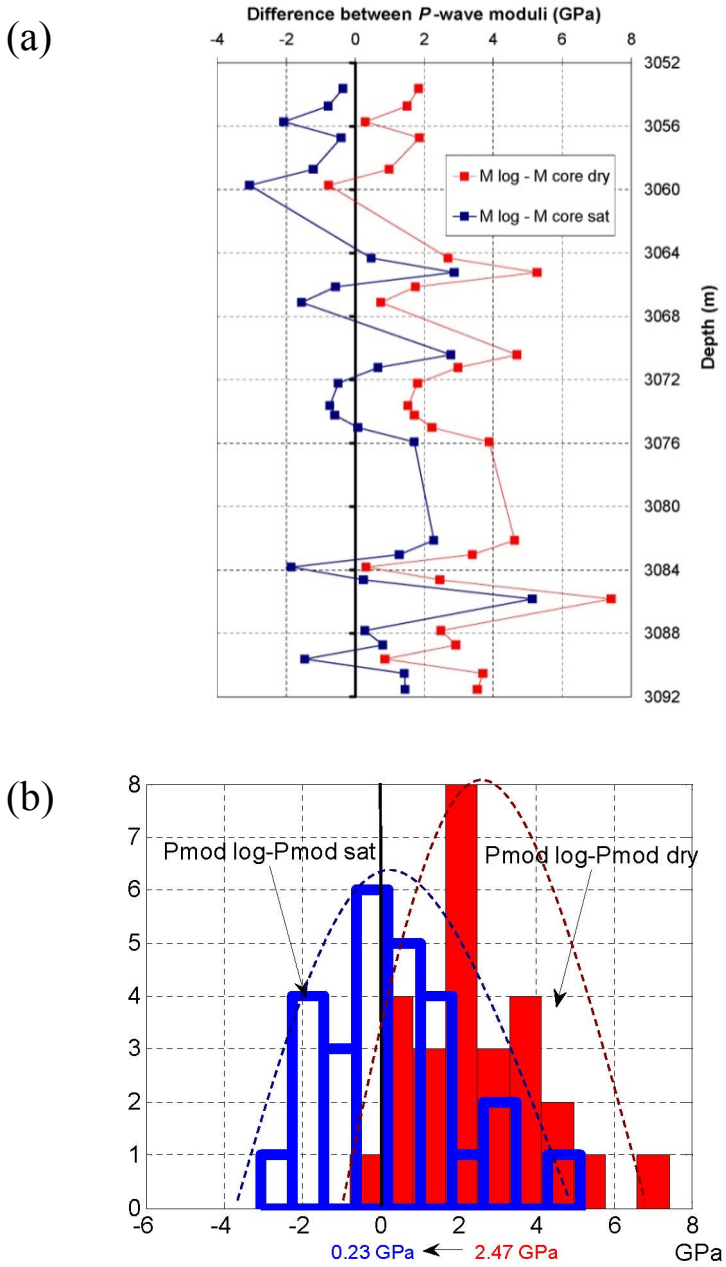

Figure 2.6: Differences between P-wave elastic moduli computed from logs and ultrasonic dry core measurements (red) and between logs and saturated cores (computed from dry cores using Gassmann equation) (blue). In (a) both curves are plotted against depth whereas in (b) the histograms of differences are plotted.

Chapter 3

PRESSURE EFFECTS ON ELASTIC PROPERTIES

In order to develop hydrocarbon fields it is important to understand production effects on repeated seismic data. The main production related effects on seismic properties of rocks are caused by changes in saturation and pore pressure. Saturation effects have been considered in Chapter 2. In this chapter I examine the effects caused by the changes in pore pressure.

It is well known that pore pressure can have a significant impact on the seismic response (Lumley, 1995b). Pressure depletion as a result of oil and gas production causes increase in elastic moduli of the rock, and creates changes in the stress and strain fields of the rock material both inside and outside the reservoir (Hatchell and Bourne, 2005). Pressure increase due to injection is even more pronounced due to asymmetry in the time-lapse response (Sayers, 2007). Therefore, to correctly interpret time-lapse (4D) seismic, the impact of pressure changes on rock physics properties should be studied. Moreover, quantitative interpretation of time-lapse data will require knowledge of quantitative pressure-velocity relationships.

In this chapter the pressure – velocity dependence is analysed from two different perspectives. First, I analyse the reliability of this relationship as obtained from cores. Core damage, under representation and dispersion are issues which may affect stress sensitivity of elastic properties as obtained from ultrasonic measurements. Second, this relationship is investigated using in situ measurements from logs and pressure derived

from repeated formation tester (RFT) data. The advantages and limitations of using each of these approaches are discussed.

3.1 Stress Sensitivity from Ultrasonic Measurements (Cores)

Analysis of pressure changes from time-lapse seismic data requires the knowledge of the effect of pressure on elastic properties of rocks, and this effect is usually studied by ultrasonic measurements on core samples at different pressures. However, laboratory measurements, mainly pressure effect on seismic velocities, may not be representative of the in situ formation and could cause misinterpretation of time-lapse effects. One reason for this is core damage. Cores may be irreversibly damaged during the drilling and extraction processes, inducing the creation of cracks and consequently increasing stress sensitivity.

Several studies have investigated core damage as a result of the stress release during the drill out. Holt et al. (2000), using synthetic rocks manufactured under stress, measured material properties in virgin conditions and compared these to properties of cores that have been unloaded to simulate coring and subsequently reloaded to in situ conditions. Nes et al. (2002) used synthetic sandstones formed under stress to systematically study stress release, which in turn induces core-damage effects.

The validity of acoustic core measurements can be assessed by comparing them to in situ measurements. Perhaps the most reliable in situ measurements of elastic properties of rocks are provided by the sonic log. In this section I assess the adequacy of ultrasonic measurements on core samples by comparing measured ultrasonic velocities at reservoir pressures with sonic-log data from a well in an oil field in Campos Basin, offshore Brazil. The well was chosen because of an unusually large number of core sample measurements; 43 samples of sandstone were available from 45 m of the turbidite reservoir, providing a relatively good representation of reservoir properties.

Measurements of ultrasonic P- and S-wave velocities as functions of confining pressure were performed on these samples under room-dry conditions. The Gassmann equation was then applied to compute the properties of the saturated samples (Mavko et al., 1998), which is expected to give the static limit of the elastic properties. By using dry measurements, we can reduce the effects associated with the dispersion between sonic and ultrasonic frequencies; such dispersion can be large for fluid-saturated samples (Mavko and Jizba, 1991; Batzle et al., 2006). Still, a difference may occur because of dispersion between low-frequency (Gassmann) velocities and sonic-log velocities measured at the kilohertz frequency range.

By mitigating the effect of dispersion, we can focus on the effect of core damage. To assess the magnitude of this effect, I compare the saturated low-frequency elastic-wave velocities at reservoir conditions (computed from the laboratory measurements) with sonic log data recorded in the well.

3.1.1 Description of field data

The dataset analysed was obtained from a hydrocarbon field in the Campos Basin, Brazil. The reservoir pressure has undergone changes during the life of the field. Close to the water injection wells, pore pressure can increase significantly; in other wells, it could decrease because of depletion, resulting in higher effective pressure. Considering the vast range of reservoir properties and the lateral variation of effective pressure within the reservoir (3000 to 6000 psi), local and specific petrophysical studies should be done to guide 4D interpretations.

The reservoir is made up of gravel-to-sand-rich lobes from confined turbidites related to a Santonian / Campanian marine transgressive megasequence. The reservoir is composed of an amalgamation of six turbidite events with thickness ranging between 2.5 – 14.5 m each, and with grain size ranging from sand conglomerate at the base to medium/coarse sandstone at the top.

Figure 3.1 shows logs over this interval and representative rock and thin section with its mineral composition; the reservoir rock can be classified as arkosic sandstone.

After the discovery in 1984, oil production started in 1985, and the reservoir has been depleted by natural water aquifer and water injection. Twenty-five wells produce 29°API (American Petroleum Institute) gravity oil; permeability is 1500 mD, and temperature is 89 °C. The current and forecast recovery factors are 38% and 55%, respectively, and reservoir monitoring is important to locate unswept areas. The reservoir pressure (pore pressure), overburden pressure and effective pressure were initially close to 25.51 MPa (3700 psi), 53.74 MPa (7800 psi) and 28.25 MPa (4100 psi), respectively, and the average oil saturation in the interval under investigation is 90%.

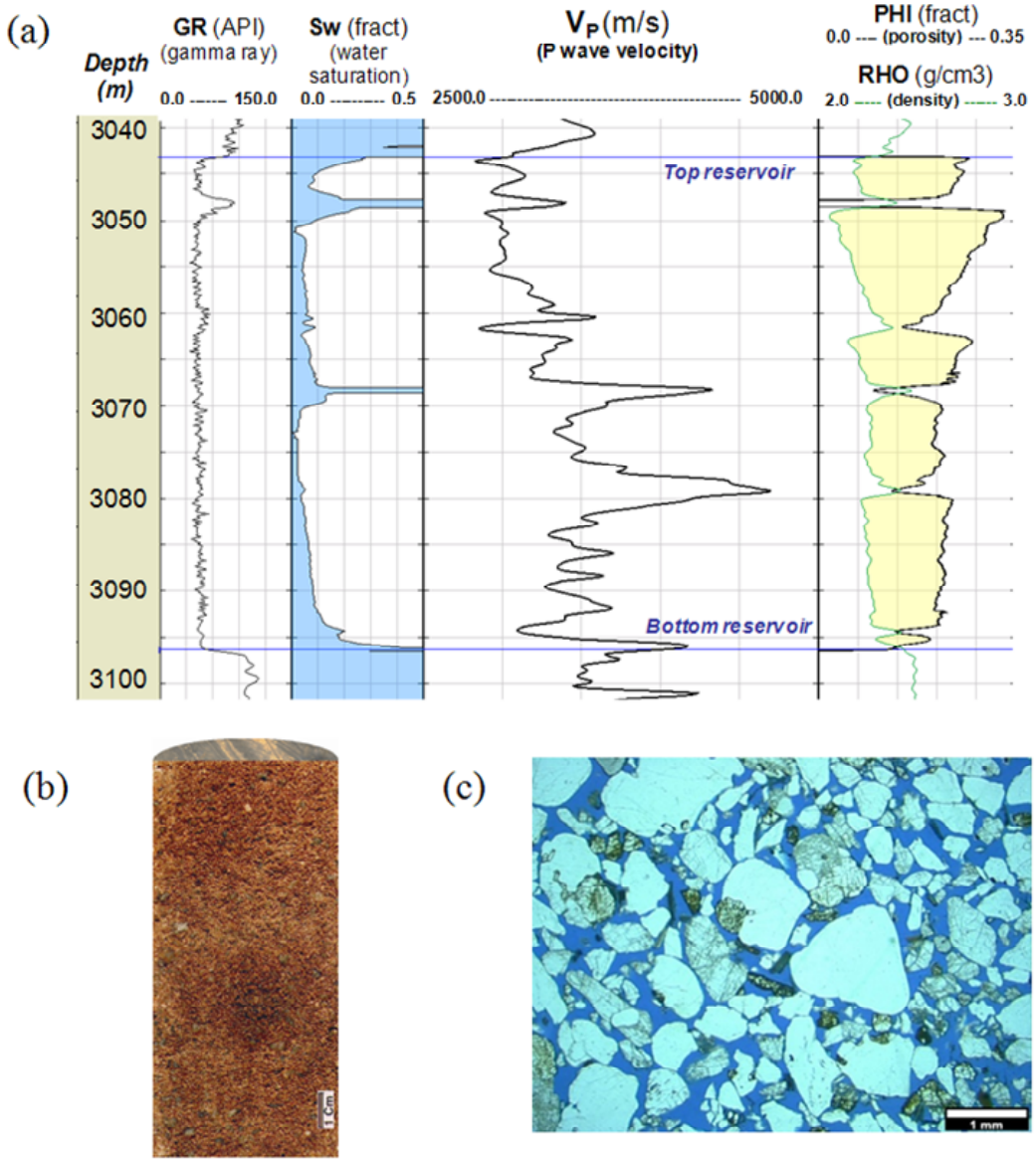

Figure 3.1: (a) Gamma-ray, water saturation, P-wave velocity, porosity and density from the studied well; (b) coarse sandstone representative of confined turbidites present in this field in Campos Basin; (c) representative thin section from the analysed reservoir with mineralogic composition (quartz, 39.5%; feldspar, 25.5%; rock fragments, 10.5%; other minerals (biotite/grenade), 1.5%; cement, 0.5%; and porosity, 22.5%).

3.1.2 Methodology

The main objective of this study is to test the adequacy of using ultrasonic measurements on core samples for quantitative interpretation of time-lapse seismic data. This strategy can be compromised by the following factors.

Under-representation

Core samples are small, and core extraction is usually extremely sparse compared to the volume of rock sampled by seismic waves. Furthermore, cores are more easily taken from well-consolidated intervals, whereas more friable samples may fall apart. Thus, core samples may not be representative of the entire formation interval.

Dispersion

Core measurements are usually performed at ultrasonic frequencies (0.25 – 1 MHz) and may not be representative of the properties at seismic frequencies (10 – 100 Hz) or at log frequencies (10 – 20 KHz) because of dispersion (variation of elastic-wave velocity with frequency).

Core damage

Cores may be irreversibly damaged during the drilling and extraction processes. Specifically, these processes can create cracks and damage cement and grain contacts, that increase the stress sensitivity of the cores as compared to the intact formation (Holt et al., 2000; Holt et al., 2005).

Figures 3.2 and 3.3 illustrates these three factors.

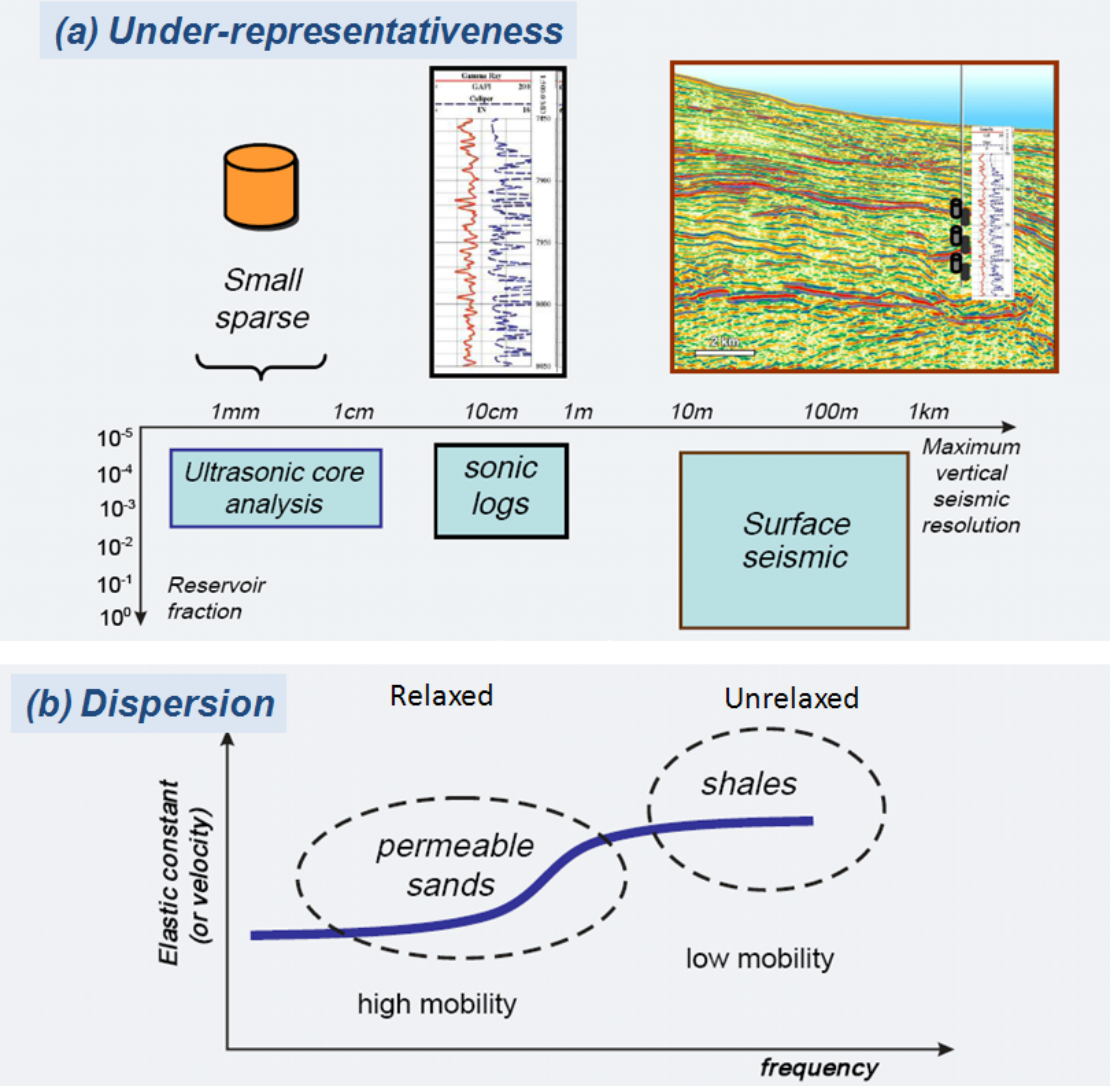

Figure 3.2: (a) Under-representativeness: cores are small and sparse compared with rock sampled by logs and by seismic; (b) dispersion: schematic relation among elastic moduli (or velocity) and frequency and fluid mobility. At low mobility, pore pressure remains unrelaxed, even at seismic frequencies. Hence, for low-permeability shales, even seismic frequencies are unrelaxed or ultrasonic. Only the more permeable rocks can be unrelaxed and remain in the low-frequency domain. (Batzle, 2006).

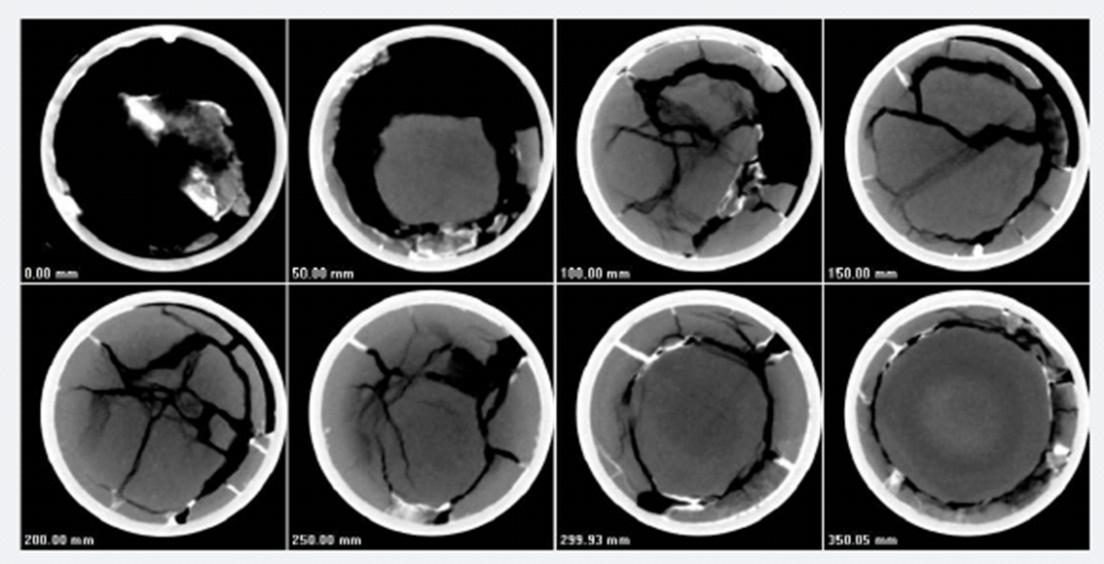

Figure 3.3: X-Ray CT images show cracks that typify core damage in plugs.

The proposed methodology to assess the adequacy of ultrasonic measurements to the properties of the intact rock and to test the significance of these factors consists of seven steps:

1) Extract as many cores as possible along the reservoir interval;

2) Perform ultrasonic measurements on dry cores, obtaining the relationship between stress and velocities;

3) Estimate effective pressure at the reservoir level, taking into account pore pressure and overburden pressure;

4) Estimate properties of fluid and dry rock at the reservoir conditions;

5) Apply Gassmann equation to compute saturated velocities from the dry ultrasonic measurements at the reservoir effective pressure;

6) Perform quality control to discard some samples where the vertical variations in rock properties could not be sampled adequately by either logs or cores (resolution problems);

7) Compare the calculated saturated velocities with sonic-log measurements.

Key elements of this approach are discussed below.

Log and core measurements

Gamma-ray, saturation, sonic (velocity), porosity, and density logs were available in the reservoir zone (Figure 3.1). Cores were extracted continuously from 49.5 m of rocks in and close to the reservoir zone. Core measurements were performed by positioning dry cylindrical samples (3.8 cm in diameter) between two pairs of piezoelectric transducers (for P- and S-waves). Cores were oriented vertically within the core holder, and all were immersed together in a pressure chamber with hydraulic oil (Figure 3.4). The confining pressure was increased up to 41.37 MPa (6000 psi) in 3.45 MPa steps (500 psi) from

3.45 up to 20.68 MPa (3000 psi), then with 6.89 MPa steps (1000 psi). A period of a sinusoidal pulse with 500 kHz central frequency was propagated through the sample. For each step of pressure increment, velocities were determined from the traveltime and length of each sample (J. E. Lira, A. Sobrinho, and J. Pinheiro, personal communication, 2007). I focus on P-wave velocities, but S-wave velocities were also used to compute dry bulk modulus. The measured data are given in Table 3.1.

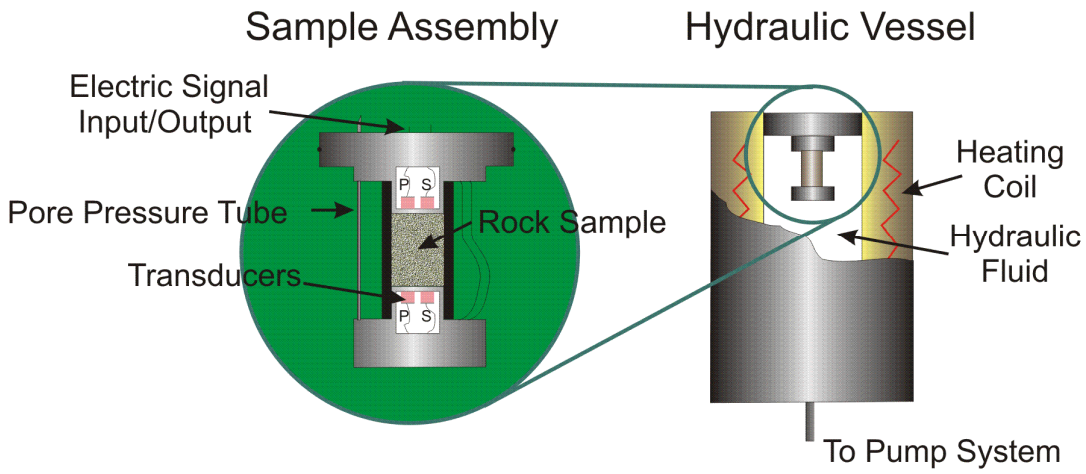

Figure 3.4: Measurement system device.

Table 3.1: Laboratory measurements at reservoir effective pressure (5000 psi) of 43 samples extracted over the reservoir interval**.**

Sample	Depth (m)	*Vp* (m/s)	*Vs* (m/s)	Density mineral (kg/m^3)	Porosity (fraction)
1	3053.65	3060	1818	2680	0.261
2	3054.70	3084	1861	2670	0.249
3	3055.70	3089	1923	2080	0.249
4	3056.70	3182	1924	2680	0.238
5	3058.70	3297	1936	2690	0.221
6	3059.70	3381	2050	2690	0.210
7	3062.25	5974	3334	2710	0.031
8	3063.30	3854	2075	2700	0.191
9	3064.30	3095	1892	2700	0.265
10	3065.25	3136	1886	2700	0.227
11	3066.15	3250	1964	2690	0.228
12	3067.10	3277	1991	2700	0.231
13	3068.20	3196	1966	2700	0.232
14	3069.25	3331	1982	2690	0.201
15	3070.45	3603	2085	2690	0.197
16	3071.20	3377	2057	2700	0.204
17	3072.25	3306	2057	2690	0.218
18	3073.60	3444	2113	2690	0.204
19	3074.25	3477	2175	2690	0.203
20	3075.05	3437	2110	2700	0.219
21	3075.90	3492	2114	2700	0.200
22	3076.80	3355	2047	2700	0.224
23	3077.70	3469	1949	2630	0.198
24	3078.80	4159	2176	2650	0.195
25	3079.45	5268	3276	2720	0.010
26	3080.35	3905	2131	2780	0.199
27	3081.25	3742	2164	2680	0.194
28	3082.10	3364	2085	2690	0.215
29	3083.00	3482	2134	2710	0.220
30	3083.85	3499	2139	2690	0.212
31	3084.65	3409	2072	2700	0.216
32	3085.90	3441	2108	2690	0.208
33	3086.80	2783	1551	2690	0.200

Table 3.1 (continued): Laboratory measurements at reservoir effective pressure (5000 psi) of 43 samples extracted over the reservoir interval**.**

Sample	Depth (m)	*Vp* (m/s)	*Vs* (m/s)	Density mineral (kg/m^3)	Porosity (fraction)
34	3087.80	3534	2162	2700	0.203
35	3088.75	3555	2136	2690	0.204
36	3089.65	3439	2098	2690	0.205
37	3090.55	3531	2139	2690	0.194
38	3091.50	3668	2230	2700	0.196
39	3093.45	3803	2195	2700	0.192
40	3094.70	3640	2106	2690	0.206
41	3095.80	3666	2065	2690	0.190
42	3097.00	4070	2248	2680	0.183
43	3098.30	4040	2339	2670	0.136

Estimating the reservoir's effective pressure

To estimate the effective pressure P_{effec} affecting elastic-wave velocities in the reservoir, I use the equation (2.10) from Chapter 2. Pore pressure was obtained from well (RFT) measurements. The resulting value of effective pressure was 34.47 MPa for this interval. Considering the large number of cores available, it was possible to discard some samples deemed to be nonrepresentative of the reservoir properties. As discussed in Section 2.2.4, a few samples were excluded due to strongly heterogeneous intervals.

Calculation of elastic modulus and sensitivity analyses

Once the laboratory measurements were made on dry cores, the saturated bulk modulus K_{sat} was computed using Gassmann's equation (equation (2.1)).

The petrologic description of the reservoir sands suggests some heterogeneity of the mineral composition of the reservoir. This may lead to a depth-dependent composite mineral modulus. Since the mineral composition was not available for all samples, I used a single representative bulk mineral modulus ($K_{\min}$) value of 41188 MPa. I also performed a sensitivity analysis to evaluate the impact of variations of $K_{\min}$ (and K_{fluid}) on fluid substitution (Figure 3.5). This analysis shows that 10% variations in mineral and fluid modulus have small (less than 0.4%) effect on velocities (8 m/s to -11 m/s and 14 m/s to -13 m/s, respectively), which are insignificant for this study.

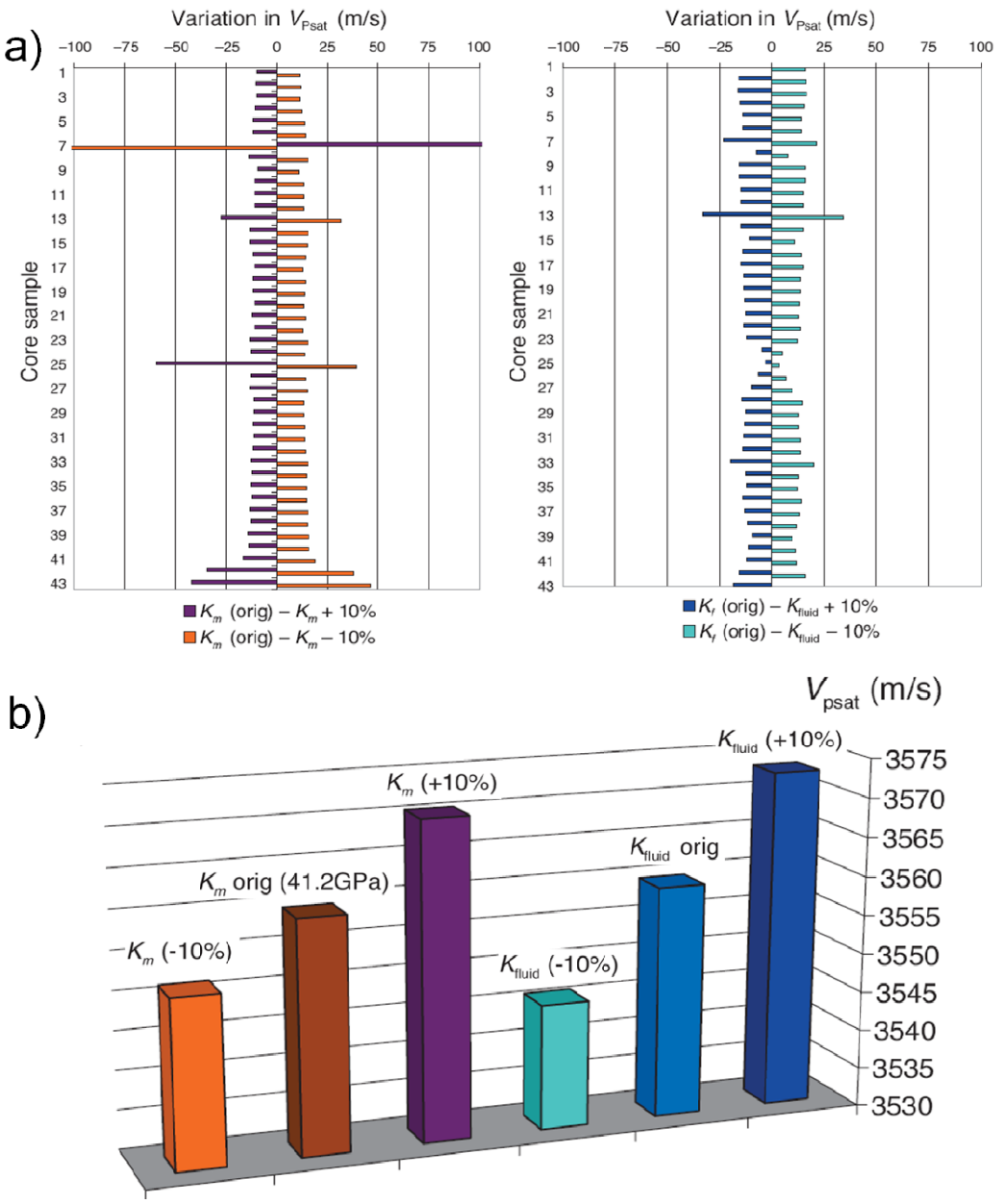

Figure 3.5: The effect of 10% variation in bulk mineral (K_m) and fluid moduli (K_{fluid}) on saturated P wave velocities (V_{Psat}): (a) sample-by-sample; (b) average over the reservoir interval. A variation in bulk mineral modulus of ± 10% will result in V_{Psat} changes of 8 m/s and -11 m/s, and the same percentage of change in fluid modulus will cause 14 m/s and -13 m/s changes, respectively.

As a saturation log was available, the variation of saturation with depth was taken into account to calculate the fluid bulk modulus as a function of depth using Wood's equation (equation (2.11)). Finally, the saturated compressional velocity V_{Psat} was obtained using the standard equation

$$V_{Psat} = \left(\frac{K_{sat} + \frac{4}{3} G}{\rho_{sat}} \right)^{1/2}, \tag{3.1}$$

where $G = V_S{}^2 \rho_{dry}$ is the shear modulus of the rock, $\rho_{fluid} = S_w \rho_w + (1 - S_w) \rho_o$ is the composite fluid density, and $\rho_{sat} = \rho_{fluid} \phi + \rho_{dry}$ is the density of the saturated rock.

Dry rocks are usually assumed to have little or no velocity dispersion, at least relative to the large dispersion that occurs when pore liquids are introduced (Mavko and Jizba, 1991; Winkler, 1986). Therefore, the velocities computed from dry measurements using Gassmann's equation can be considered as measured in the low-frequency (quasi-static) limit.

As a result of this calculation, elastic moduli and saturated velocities were obtained for each sample and for each effective pressure step (3.45 – 41.37 MPa). Figure 3.6 shows the dependency of velocities on effective pressure for six samples extracted from different depths. To compare with log measurements, I selected velocities corresponding to the estimated effective pressure present in situ (34.47 MPa).

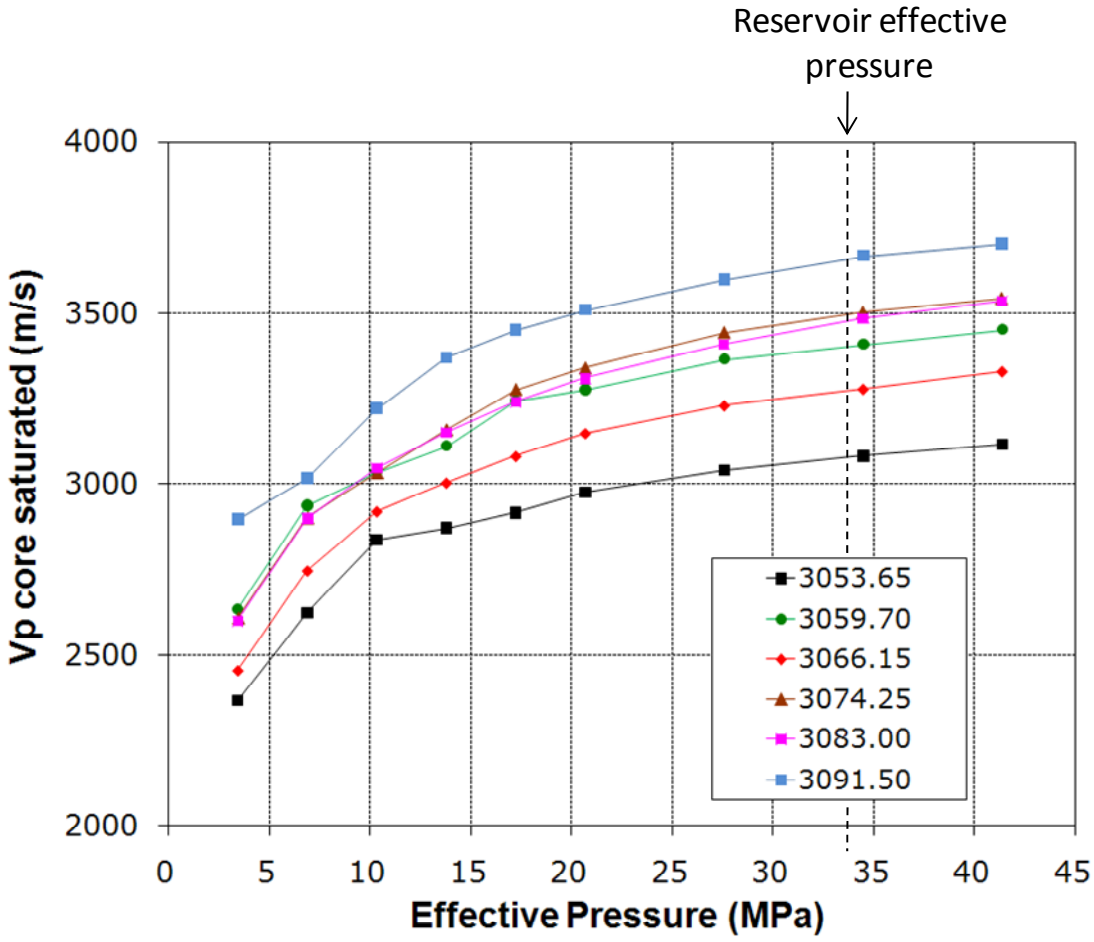

Figure 3.6: Velocity versus effective pressure for a selection of core samples at different depths (from 3053.65 m to 3091.50 m).

3.1.3 Results

In Figure 3.7, Figure 3.8 and Figure 3. 9, I compare the saturated velocities computed from cores (blue dots) against corresponding sonic-log data. We see very good agreement between the two sets of data. The average difference (systematic error) between the two sets is -32 m/s (0.93%), which is within the core measurement error range (up to 3%). The root mean square (rms) of the differences between the sonic log and the computed core velocities is 110 m/s. The fact that random errors are larger than systematic ones suggests that the effect of core damage is insignificant because this effect is expected to result in a systematic weakening of the samples. A similar result was observed in Schiehallion field by Meadows et al. (2005).

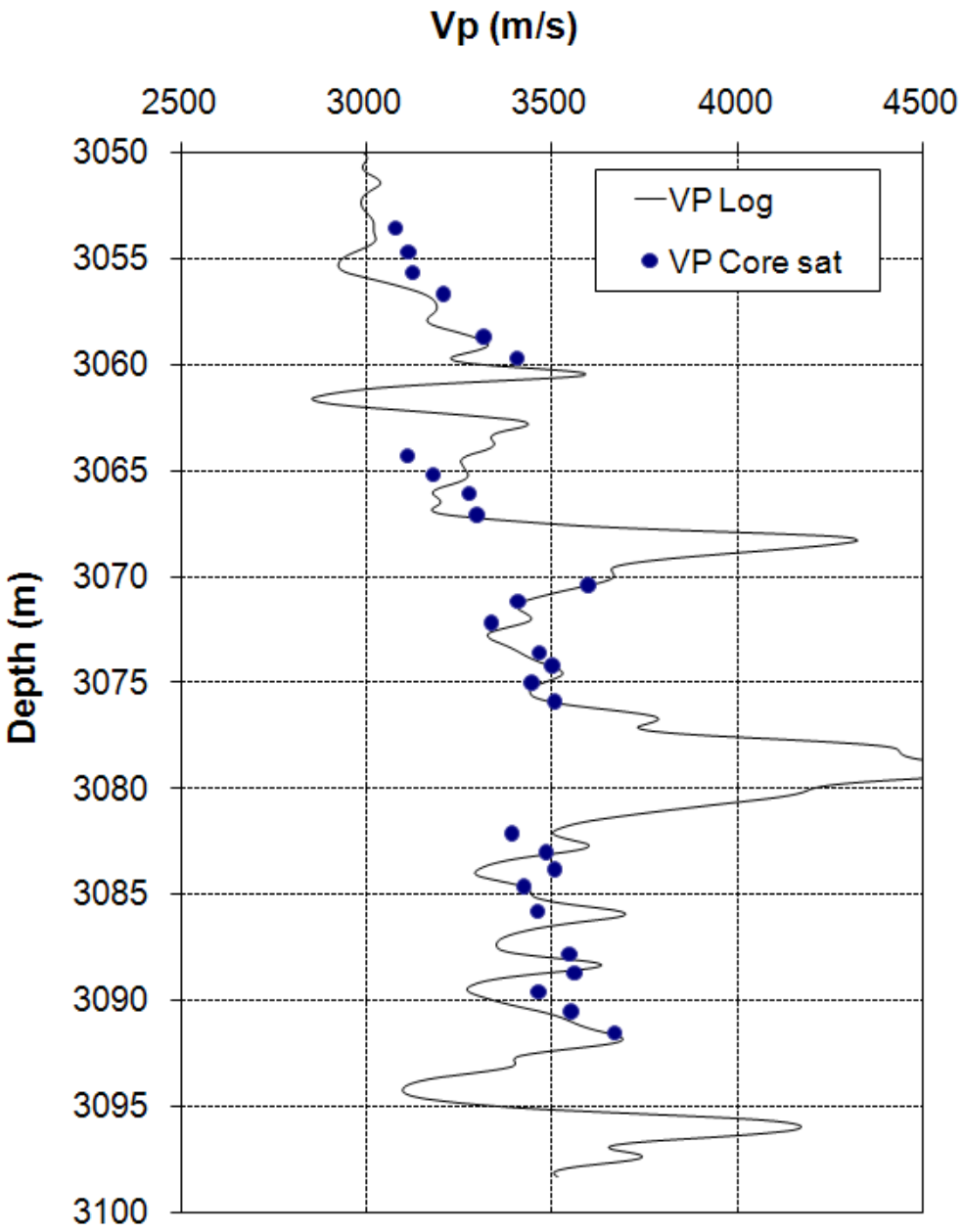

Figure 3.7: Comparison of saturated P-wave velocities computed using Gassmann equations from dry core measurements (dots) against a sonic log (line).

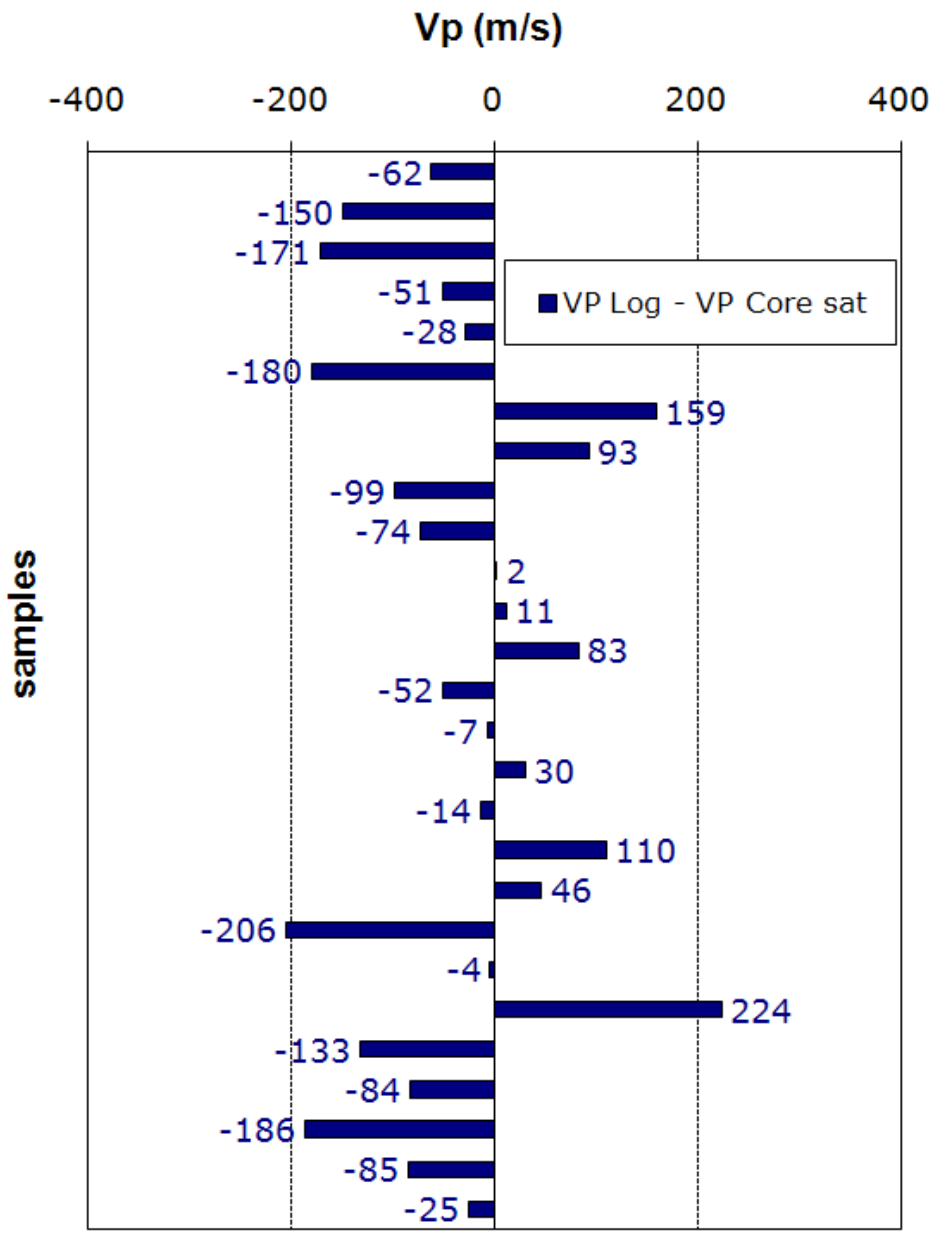

Figure 3.8: Differences between saturated P-wave velocities computed using Gassmann equations from dry core measurements and the sonic log. We can see that differences are usually smaller than 200 m/s.

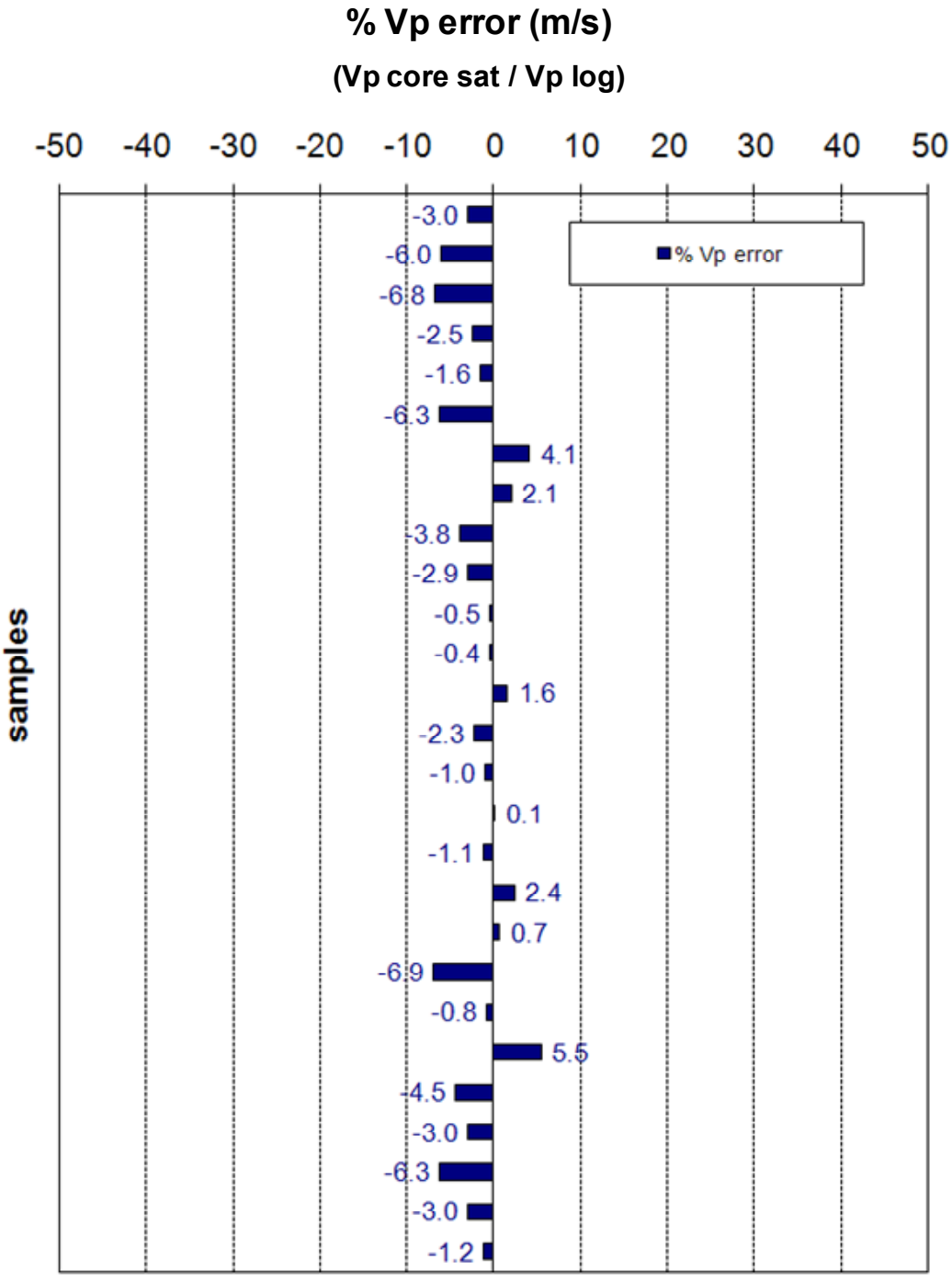

Figure 3. 9: Differences in percentage between saturated P-wave velocities computed using Gassmann equations from dry core measurements and the sonic log.

3.1.4 Conclusions

I have described a methodology to assess the adequacy of ultrasonic velocities measured in the laboratory for use in sonic and seismic modelling (with potential use in time-lapse interpretation), focusing on the effect of core damage. Dispersion effects have been minimized by using dry cores and then computing saturated velocities (Gassmann); under-representing cores are reduced by extracting several cores over the reservoir interval.

The main conclusion is that the saturated velocities computed from core measurements on dry samples match the sonic-log velocities quite well. This is encouraging because it implies that core damages that may occur while bringing the core samples to the surface are small and do not adversely affect the measurement of elastic properties on these core samples. Should core damage have affected our measurements, we would have expected a systematic difference between properties measured in situ and on the recovered. Consequently, stress sensitivity of elastic parameters, as obtained from ultrasonic measurements, is adequate for quantitative interpretation of time-lapse seismic data. These results also suggest the usefulness of laboratory measurements on cores, including core preservation during extraction.

The results of the study relate to a particular reservoir in the Campos Basin, offshore Brazil. Other studies in the same basin and other parts of the world are needed to verify the generality of this conclusion. It is expected that the match between core and log data may be worse at lower effective pressures. Therefore it would be useful to perform similar comparisons for reservoirs with lower effective pressures, particularly in overpressured regimes.

3.2 Stress Sensitivity using an In Situ Approach (Well Logs)

As shown in Section 3.1, velocity-pressure relationship for reservoir rocks can be obtained from ultrasonic measurements on core samples. However, this approach has its limitations. Cores may be affected by damage, bias in the plugging process, scale effects and may not be representative of the in situ properties. Effects of dispersion can be minimised by measuring cores dry, and then applying Gassmann's equation; however drying may sometimes alter the rock fabric, especially for clay-rich rocks (Batzle et al., 2006). Another limitation of using core measurements is the high extraction cost.

Considering the importance of knowing the pressure effect on elastic rock properties for time-lapse studies and the limitations of using cores, it is desirable to obtain this relationship from some in situ measurements. Few methods can sample the in situ rock. Seismic, for instance, provides in situ information, but lacks sufficient vertical resolution. Well logs, on the other hand, can provide high vertical resolution information, but usually are not available in the same well before and after production.

In this section I develop a method to infer the in situ pressure – velocity relationship using log data from wells drilled and logged at different stages of field development, thus providing rock and fluid properties at different pressures. For each well logged at a specific time, pore pressure P_p, P-wave velocity V_p and porosity ϕ, among others properties, are assumed known. Pore pressure is obtained from repeat formation tester (RFT). As the field depletes over time and new wells are drilled and logged, similar datasets related to different pressures become available.

The idea of obtaining the relationship between acoustic impedance versus pore pressure from multiple wells was proposed by Hansen et al. (2006). Furre et al. (2009) proposed a similar approach for predicting the effect on seismic data of pressure depletion within the reservoir, utilizing sonic logs acquired in different wells drilled during varying depletion stages. To avoid pressure dependent fluid effects, Furre et al.

(2009) focused on the stress dependence of the framework (or dry) elastic moduli of the rock and applied it to slightly tilted fault blocks of fluvial deposits in the North Sea. This approach can only be applied to very homogeneous reservoirs, otherwise spatial heterogeneity may cause bigger variations of elastic properties between wells than changes in pressure do. To mitigate this effect, Furre et al. (2009) classified rocks into a few porosity ranges.

In this study I expand and broaden the approach of Furre et al. (2009) by analysing variation of velocity as a function of both pressure and porosity. The idea of including porosity and obtaining a three-dimensional relationship with velocity and pressure helps account for rock properties variability (Meadows et al., 2005).

I apply this approach to a reasonably continuous deposit made up of sandstone turbidites in Campos Basin, Brazil. I obtain the velocity–pressure-porosity relationship in two neighbouring areas with distinct hydraulic compartmentalization, and compare them with the laboratory measurements. The final goal is to increase our understanding of velocity dependence on pressure to support further quantitative time-lapse analyses.

3.2.1 Description of data

An overview of the oil field is provided in Section 3.1.1. There are 24 wells drilled since the start of production. Considering the strong depletion (around 2000 psi) in the main reservoir, there is an opportunity to use pore pressure information from RFT and associate it with rock properties sampled by logs. Twenty three wells penetrated the reservoir with original oil saturation, have borehole logs (including sonic, porosity, gamma-ray and density) and RFT measurements.

It is a challenge to get 4D quantitative information from this field using conventional seismic, probably due to low repeatability. Seismic data were acquired in 1984 and 1999 using streamers, and in 2005 using ocean bottom cable (OBC). This last survey was designed to provide a better image of the reservoir rather than maximise

repeatability with the previous surveys. Considering low seismic repeatability, an additional effort using both well (in situ) and core (laboratory measurements) approaches is explored to understand production effects (pressure) on elastic properties.

3.2.2 Objectives and methodology

The main objective of this study is to assess in situ velocity dependence on pressure to calibrate time-lapse (4D) interpretation. Another aim is to compare the in situ relationship to the one obtained using ultrasonic measurements.

To estimate the pressure-velocity-porosity relationship, I propose the following workflow:

1. *Select all wells that fulfil the following conditions: they drain the main reservoir in this field, were logged at original oil saturation and have RFT measurements.* I select log velocities and porosities into a specific stratigraphic interval from 23 wells.
2. *Load all data (logs, markers, RFT and core measurements) in a software (Rokdoc from Ikon Science).*
3. *Analyse pore pressure depletion over time.* In Figure 3.10 I plot pore pressure obtained by RFT measurements at each well against production time. There are two distinct hydraulic compartments (black line and red ellipse) and the in situ stress sensitivity of elastic properties should be analysed separately for each area. The importance of analysing pressure variation in this time scale is to restrict effects due to production. Changes induced during geological time should not be considered; in this case other effects (e.g. plasticity, the propensity of a material to undergo permanent deformation under load) should be acting.
4. *Analyse pore pressure depletion in space*. The well location shown in Figure 3.11 helps to confirm the existence of two distinct hydraulic compartments, as suggested in Figure 3.10. Each group of wells that belongs to a particular

depletion trend is located in one particular area (named Area 1 and Area 2).

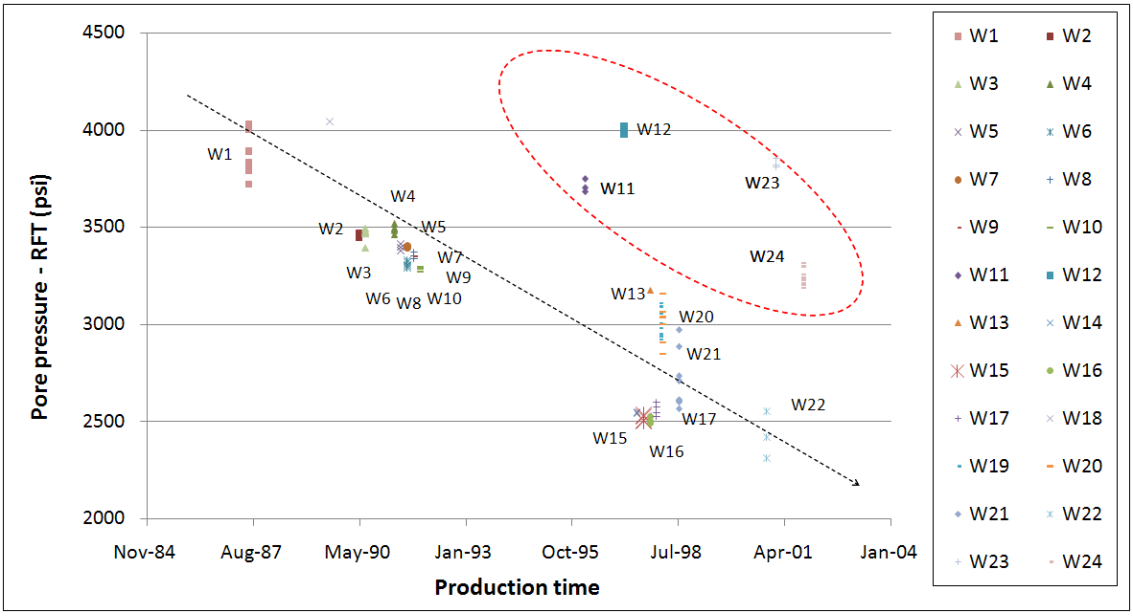

Figure 3.10: Pore pressure variation with time (depletion) from the main reservoir. There are two different compartments with almost no communication between them (black line and red ellipse).

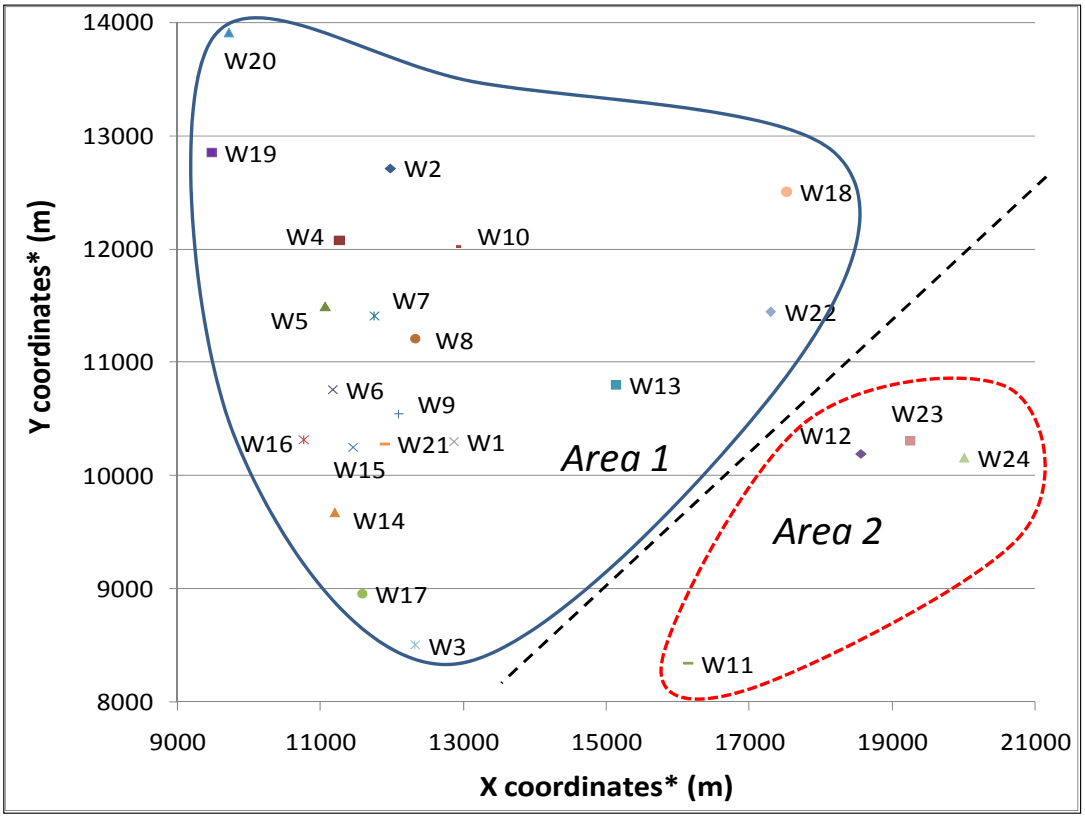

Figure 3.11: Map showing wells drilled through the main reservoir. The wells located at southeast from the dashed line (Area 2) are hydraulically isolated from the other wells (Area 1). All these wells were drilled in the original oil saturation, except W21. The real coordinates have been modified, however the relative distances are preserved (*).

5. *Select all log samples from the main reservoir interval, which have similar lithologic characteristics, by applying gamma-ray and porosity cut-offs*. The reason for this is that despite the reasonable lateral continuity of rock properties of this sandstone, the spatial heterogeneity is still one of the biggest causes of uncertainty (Figure 3.12). Cut-offs also help eliminate outliers in log measurements.

6. *Estimate effective pressure (differential pressure)*. It is done based on sea water and lithostatic pressure gradients, integration of density log and pore pressure measurements (RFT). The water depth for each well is taken into account (equation (2.10)), and it is assumed that effective pressure is constant in the reservoir interval.

7. *Cross-plot V_p, porosity* (logs) and P_{effec} *and fit a plane through these points*. A plane is fitted for each hydraulic compartment using a least-square method in a V_p, ϕ and P_{effec} space.

8. *Compute ultrasonic (core) velocities to compare with the in situ approach.* Core samples are extracted along the reservoir interval and dry ultrasonic velocities are measured for varying confining pressures up to 6000 psi. Saturated velocities are computed from dry core ultrasonic measurements by applying Gassmann equations using in situ fluid properties.

9. *Analyse the results*.

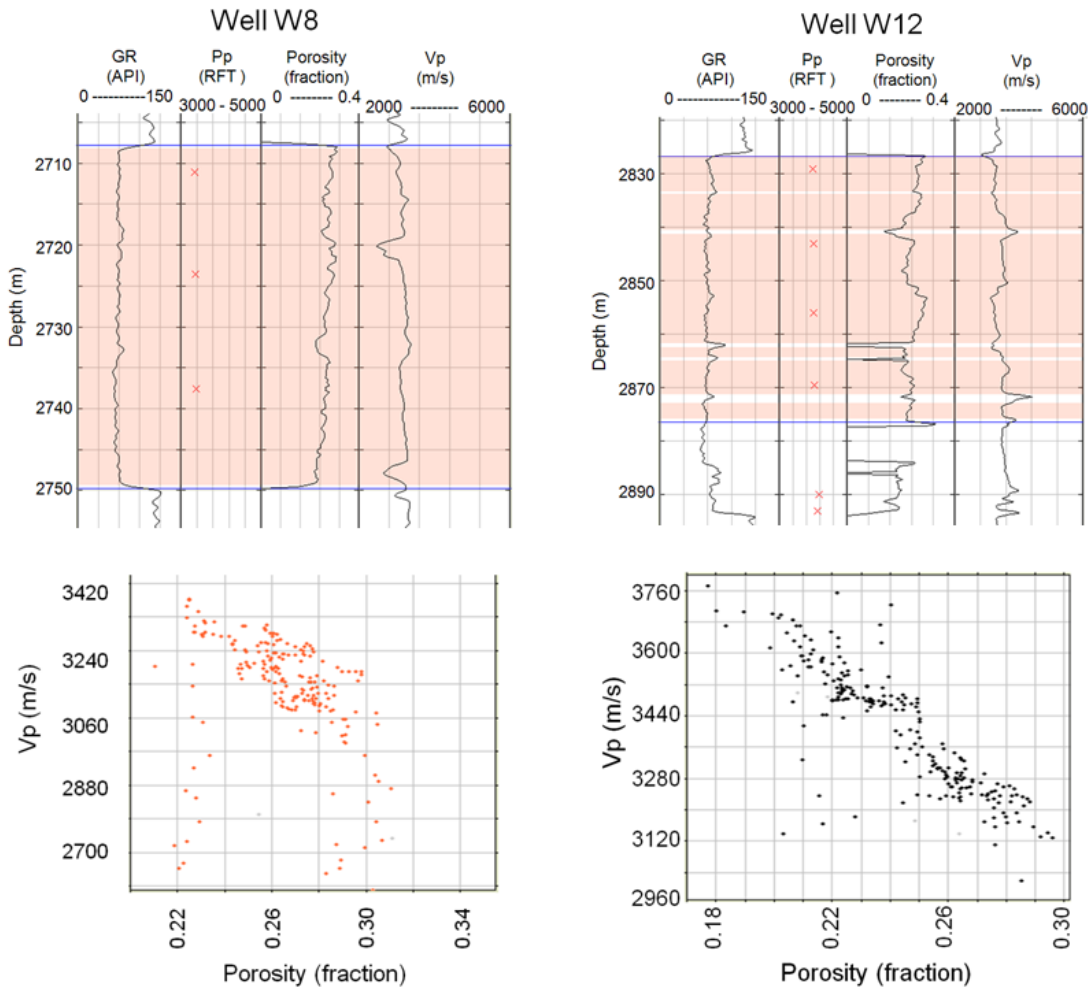

Figure 3.12: Wells W8 and W12 illustrate the characteristics of data used for obtaining in situ velocity dependence on pressure. In the upper part gamma-ray, porosity and velocity from logs and pore pressure discrete measurements (red "x"). In the lower part are shown cross-plots of velocity versus porosity for all values from logs in the reservoir interval which satisfying cut-offs: gamma-ray (GR) < 70 and $\phi > 0.15$.

3.2.3 Results

Pore pressure decay during production time (Figure 3.10) shows clearly the hydraulic compartmentalization in this reservoir. While the majority of wells follow a specific depletion trend, the other four wells are outside of this trend. This other hydraulic compartment is located in the south eastern region of the field (Figure 3.11). The in situ stress sensitivity of elastic properties is analysed separately for each of these two areas.

It is also important to select relatively homogeneous sandstones. Figure 3.12 shows representative wells for Area 1 and Area 2 exemplifying the quality control step. Basically this is done in two steps: by limiting the log data to be used in the same stratigraphic interval; and by applying cut-offs to exclude rocks with different characteristics. Even after applying porosity and gamma-ray cut-offs to exclude intra-reservoir cement and shaly zones, there are still variations of porosity with velocity. These could be related to the rock framework and small changes in mineral composition. For some wells no sample was discarded (i.e. W8), for others (i.e. W12), a few thin intervals with calcite cement and higher shale content were discarded. The remaining log porosities and velocities are then cross-plotted, and the strong influence that porosity has on velocities becomes evident.

Despite appropriate procedures, there are still intrinsic uncertainties like the impact of very small heterogeneities (smaller than 5 cm) that could be smoothed over by log measurements. To mitigate uncertainties and achieve more robust analyses, I used as many points as possible that meet quality control requirements in order to provide statistical robustness. Hundreds of points for which log values fulfil cut-off conditions are selected from this stratigraphic interval.

To capture velocity dependence in both porosity and pore pressure (or corresponding effective pressure), I plot in three dimensions all values (V_p, ϕ and P_{effec}) corresponding to this sandstone. A plane was fitted among these hundreds of points

using a least-square method.

Planes adjusted over datasets for both Area 1 (Figure 3.13) and Area 2 (Figure 3.14) represent the velocity dependence on effective pressure and porosity. Given the uncertainty level, a simple linear function (a plane in 3D) in a relatively narrow range of porosity and pressure is a reasonable approximation.

In Area 1 given the higher number of wells available (19 from 20 fulfil our requirements), the regression coefficients should be more robust, at least in the reservoir effective range used to estimate this plane:

$$V_P = 3707 - 4002\phi + 0.091P_{effec} \tag{3.2}$$

In Area 2 there are only four wells within the same hydraulic compartment. Core samples are available in this area; so saturated velocities have also been computed from dry core ultrasonic measurements by applying Gassmann equations. Then, a plane is fitted for the core dataset (Figure 3.15). The equations for Area 2 from in situ (log) and laboratory (core) approaches are, respectively,

$$V_P = 3787 - 4619\phi + 0.1284P_{effec} \tag{3.3}$$

$$V_P = 3988 - 5774\phi + 0.1306P_{effec} \tag{3.4}$$

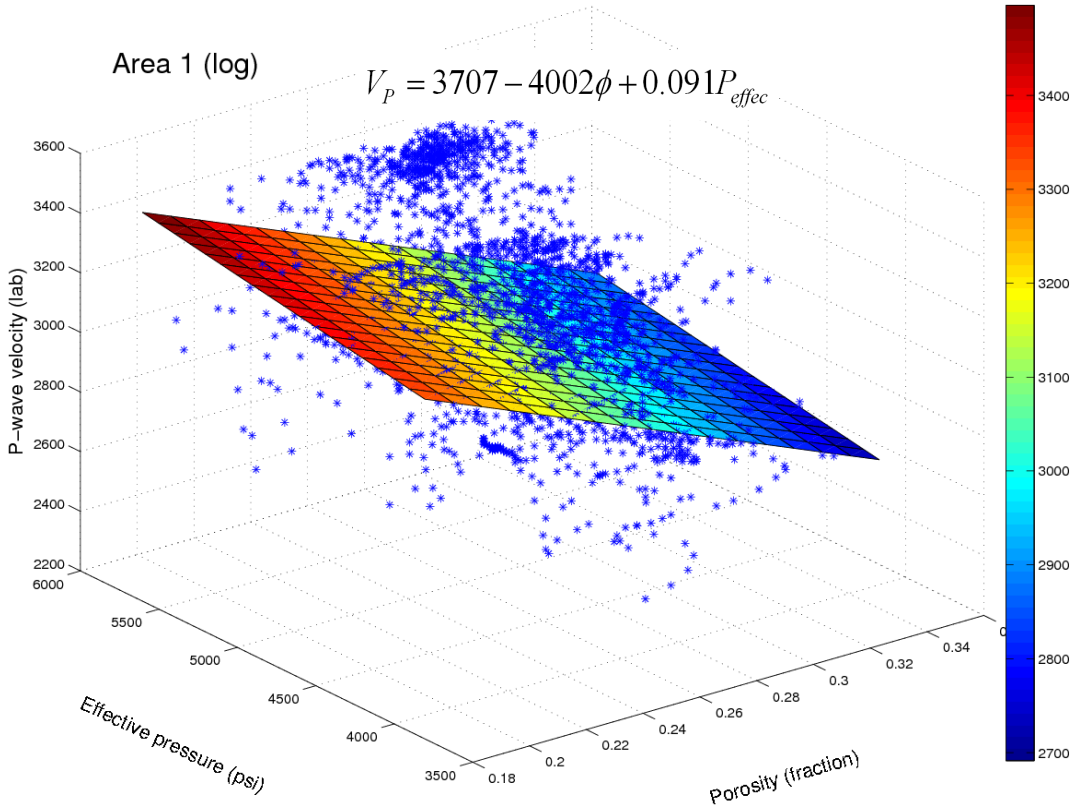

Figure 3.13: In situ P-wave velocity dependence on porosity and effective pressure for Area 1 (19 wells from 20 available). Points are obtained from pressure measurements and from sonic and porosity logs. The plane corresponds to a best fit among all points using a least-square method.

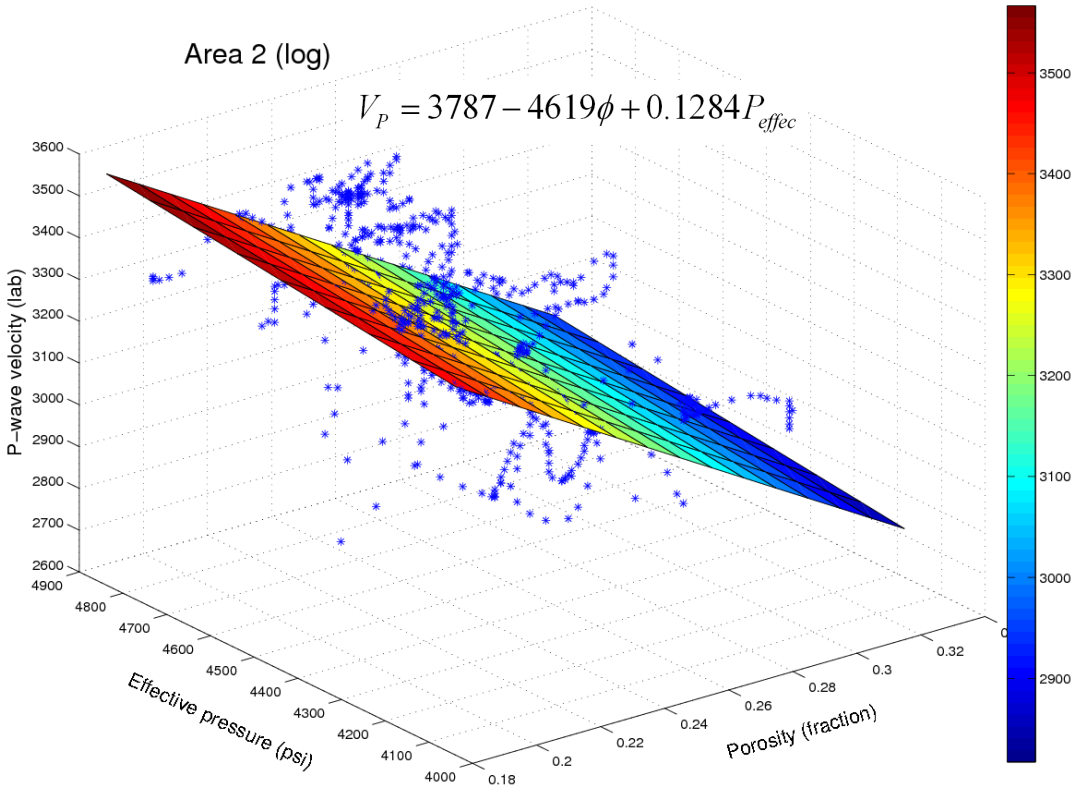

Figure 3.14: In situ P-wave velocity dependence on porosity and effective pressure for Area 2 (all the 4 wells available are used). Points are obtained from pressure measurements and from sonic and porosity logs. The plane corresponds to a best fit among all points using a least-square method.

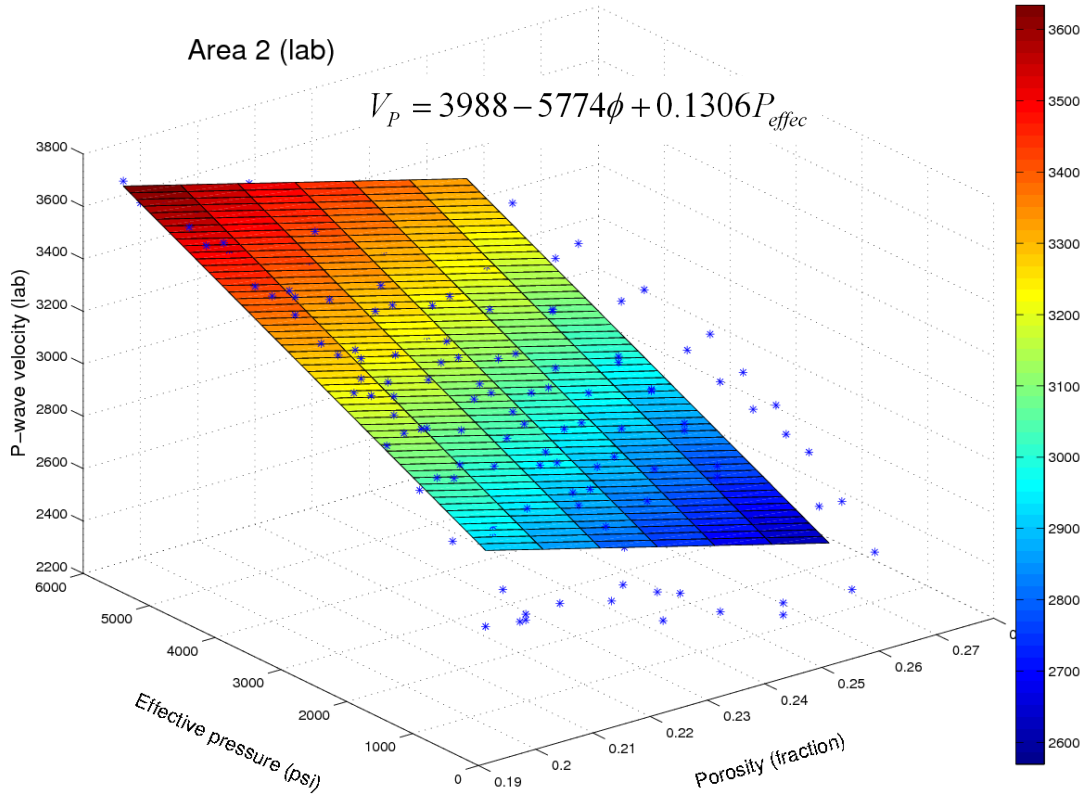

Figure 3.15: P-wave velocity dependence on porosity and effective pressure for Area 2. Points are obtained from ultrasonic measurements in 26 cores (in the laboratory) at different confining pressures. The plane corresponds to a best fit among all points using a least-square method.

3.2.4 Conclusions

I have described a methodology to assess the in situ velocity dependence on both pressure and porosity. Velocity sensitivity to effective pressure is estimated using log data and pore pressure (RFT) measurements. Wells drilled and logged in different stages of depletion allow us to estimate the effect of pressure on elastic parameters.

Due to a lack of lateral stress information, it was assumed confining stress can be approximated by a vertical stress. This approximation appears to be appropriate since there are no significant tectonic forces related to Cretaceous Period in the Campos Basin.

Substituting average porosity and effective pressure (0.25 and 3447 psi, respectively) in regression equations (3.2) - (3.4), the resulting velocities are 3020 m/s (in situ, Area 1), 3075 m/s (in situ, Area 2) and 2995 (lab, Area 2). The difference between Area 1 and Area 2 (in situ approach) is 1.8% and between in situ and laboratory approaches (Area 2) is 2.7%.

Although in situ and lab approaches show similar results for mean properties, uncertainties related to rock and fluid properties are still high. The main intrinsic uncertainties in this methodology are caused by rock heterogeneity and errors in effective pressure estimation. Despite using constraints (same stratigraphic unit, applying gamma-ray and porosity cut-offs), there is a significant porosity variability. Cement and mineral composition may also affect velocity response. Pore pressure derived from repeat formation tester (RFT) measurements is assumed constant within the same stratigraphic unit. The expected magnitude of errors in velocity estimation due to this approximation and effective pressure estimation is up to 1.5%.

Consequently, for this particular dataset from Campos Basin, the results are not conclusive mainly, perhaps, because spatial variations (heterogeneity) mask a relatively small pressure effect. In more favourable conditions (higher rock homogeneity) or

steeper part of the pressure - velocity curve, this methodology may be used as a complementary assessment of rock elastic properties together with the one derived from core measurements.

The possibility of comparing velocity dependence on pressure and porosity relationship using in situ and laboratory approaches is very attractive. It represents a significant increase in spatial coverage of information over an oil field, particularly in mature oil fields, in comparison to the typically sparse samples provided by cores. Considering that the pressure response is much quicker than the saturation response, the understanding of the pressure changes can significantly contribute to the early identification of preferential zones and barriers within the reservoir.

Chapter 4

CHARACTERIZATION OF THIN STRATIFICATION

Quantitative time-lapse studies require precise knowledge of the response of rocks sampled by a seismic wave. Small-scale vertical changes in rock properties, such as those resulting from centimetre scale depositional layering, are usually undetectable in either seismic or standard borehole logs (Murphy et al., 1984).

In the first section of this chapter I present a methodology to assess rock properties by using X-ray computed tomography (CT) images along with laboratory velocity measurements and borehole logs. This methodology is applied to rocks extracted around 2.8 km depth from offshore Brazil. The improved understanding of physical property variations may help to correlate stratigraphy between wells and to calibrate pressure effects on velocities for seismic time-lapse studies.

Small scale intra-reservoir shales have a very different response to fluid injection and depletion from that of sand, and thus may have a strong effect on the equivalent properties of a heterogeneous clastic reservoir. In the second part of this chapter I present a methodology to compute the combined seismic response for depletion and injection scenarios as a function of net to gross (sand – shale fraction). This approach is appropriate for modelling time-lapse effects of thin layers of sandstones and shales in repeated seismic surveys when there is no time for pressure in shale and sand to equilibrate.

4.1 Using X-Ray Computed Tomography to Characterize Finely Layered Sediments

In order to correctly model and interpret time-lapse data, the effect of finely layered sediments should be taken into account. The wavelength of seismic data usually is much bigger than is required to resolve small scale rock property variations. Well logs have higher vertical resolution (or smaller volume of investigation) than seismic. But even when the log sampling interval is small (e.g. frame spacing of 2 inches = 5.08 cm), it may still have a relatively large investigation volume. This presents a problem when we wish to capture the full variation in physical properties for purposes such as rock physics modelling and time-lapse interpretation.

One method that gives useful information in an automated way and at a higher resolution than downhole logs is X-ray computed tomography (CT) of cores (Mees et al., 2003). Marine sediment core samples are the fundamental source of information on seabed character, depositional history and environmental change (Rothwell and Rack, 2006). The CT number encodes a combination of mass density and electron density proportional to mean atomic number (Desrues et al., 2006; Moore and Reynolds, 1997; Wellington and Vinegar, 1987). CT analysis is completely non-destructive, preserving all core material for additional analyses or archiving. CT scanning can be used routinely at slice and pixel resolutions of 1 mm, so that very fine-scale changes in rock properties can be distinguished.

In this section, I present a methodology to assess rock properties by using X-ray computed tomography images combined with ultrasonic measurements. I apply this methodology to a Brazilian offshore deepwater oil field. This analysis demonstrates that these data provide valuable information on centimetre-scale heterogeneity. The analysis also reveals sedimentary cyclicity and potentially can reveal other small scale heterogeneity that may help in 4D studies. Moreover, possible stress changes in this

interval (reservoir's overburden rock) due to production or injection in the subjacent reservoir could further be modelled using this dataset.

4.1.1 Description of data

The data come from a well in Campos Basin, offshore Brazil. The interval is approximately 2800 m below sea floor, in an Oligocene to Miocene hemipelagic sequence of alternating marls and shales that form the overburden to the main sandstone reservoir. The data consist of CT images of the whole core, ultrasonic P-wave measurements on core plugs and electronic borehole logs.

X-ray CT images were taken every 5 cm from cores at the depth of around 2800 m. To acquire these CT images, we used a Picker – PQS scanner with X-ray voltage set to 130 kV and current to 100 mA. The time per scan was 4 seconds and image resolution was 0.5 mm x 0.5 mm. The standard deviation of the X-ray CT value measurements is 0.56%. The slice thickness is 1 cm, meaning that the support volume of the measurements is smaller than the sampling interval. This is an important difference from the high resolution downhole density log, where the sampling interval is similar (2 inches = 5.08 cm), but the support volume is larger (10 cm).

Ultrasonic (500 kHz) P-wave velocities were measured at different pressures on 23 rock samples, providing complementary information about their elastic properties. The measurements were done for horizontally and vertically oriented samples using varying confining pressures from 1000 to 6000 psi.

An extensive suite of borehole logs is also available including high-resolution gamma-ray and density logs with sample interval of 5.08 cm, as well as photoelectric factor and density correction. The sonic P- and S- velocities were measured by a monopole sonic logging tool with a spacing of 20 cm (standard) and 5.08 cm (high resolution).

4.1.2 Methodology

I initially investigated standard borehole logs over the interval to assess the rock physical properties. I found that the resolution was not enough to detect lithology intercalation in the rocks immediately above the sandstone reservoir. However, ultrasonic velocity measurements made at different depths and at different confining pressures show a substantial variation in elastic properties. High resolution logs showed some indications of a cyclic pattern. These logs have a small sampling rate (5.08 cm); but the actual resolution is lower because the volume of investigation of the sensors is 2 to 6 times larger than the frame spacing at which data were collected.

In order to get more insight about the variation of elastic properties, I used the regularly spaced X-ray CT scans performed on the whole core. I computed the mean X-ray CT value for each image by averaging it over a large circular area chosen to remove the outer part of the slices, in order to reduce the impact of beam hardening (Desrues et al., 2006). Beam hardening is the process of selective removal of soft X-rays from the X-ray beam. As these X-rays are removed, the beam becomes progressively harder or more penetrating. The amount of beam hardening depends on the initial X-ray spectrum as well as on the composition of the material traversed. This effect causes so-called beam hardening artefacts in CT images. If uncorrected, beam hardening artefacts appear as cupping, or a reduction of the reconstructed attenuation coefficient toward the centre of a large object.

Though beam hardening is ubiquitous and difficult to correct for, cropping the edge off is a reasonable way to deal with it. Figure 4.1 (a) shows X-ray CT values in Hounsfield units (HU) for different depths. The Hounsfield unit (HU) scale is a linear transformation of the original linear attenuation coefficient measurement in one in which the radio density of distilled water at standard pressure and temperature (STP) is defined as zero Hounsfield units (HU), while the radio density of air at STP is defined as -1000 HU (Mess et al., 2003). Figure 4.1 (b) shows CT values obtained from the HU values by

conversion to an 8-bit gray scale. In the depth interval from 2862 m to 2870 m there is a clear signature of cyclicity. In the sandstone interval (2870 m to 2874.3 m), the X-ray CT values are lower and the cyclicity disappears.

Using a correlation between mass density measured on core samples and X-ray CT value, I computed so-called X-ray densities (or “mean density from CT”). Next, I crossploted ultrasonic P-wave velocity versus mean X-ray density of the corresponding samples (Figure 4.2). I selected velocities corresponding to the estimated in situ confining pressure (3000 psi), by taking into account lithostatic stress. Figure 4.2 shows reasonable good correlation between X-ray density and P-velocity. This correlation is then used to compute the velocities as a function of density for each CT image.

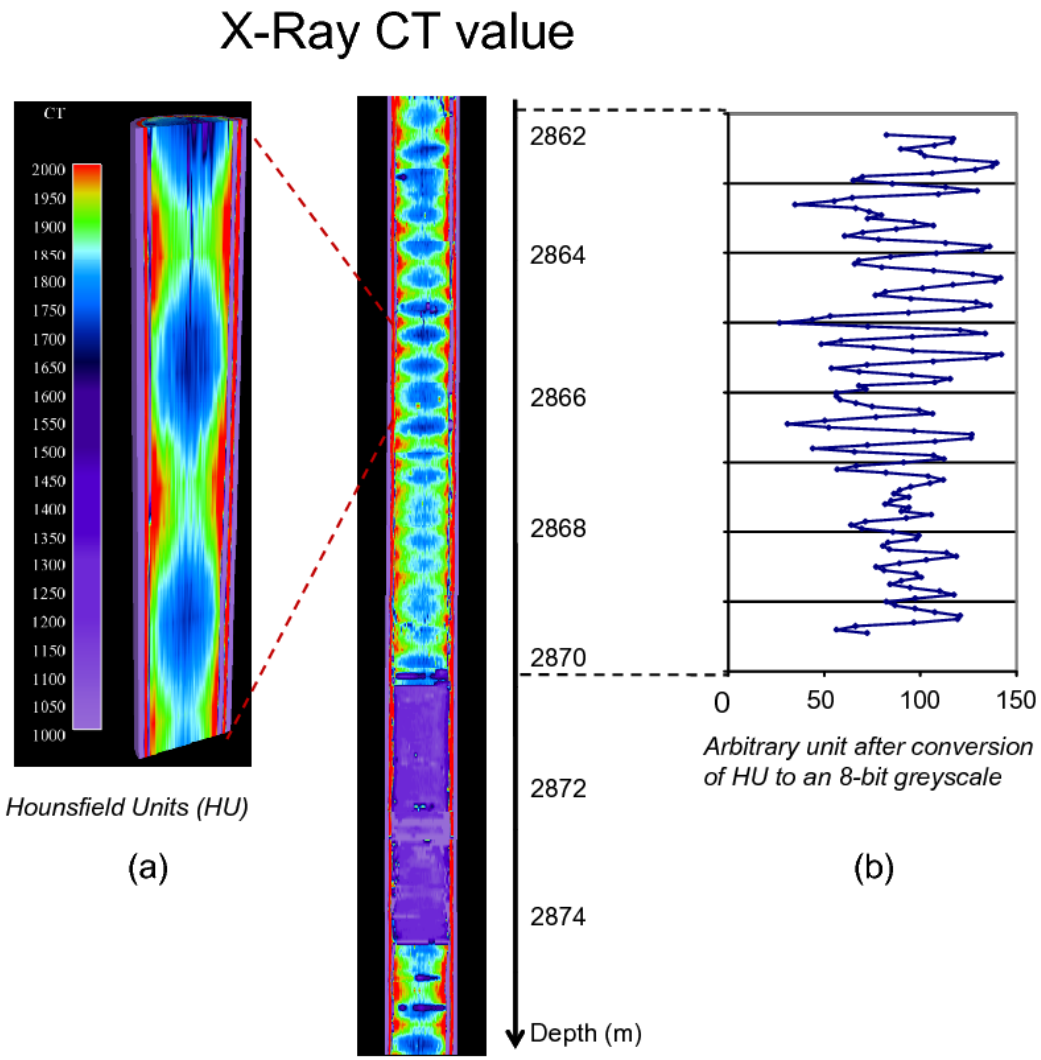

Figure 4.1: X-ray CT values obtained by computing the average value over a circular area for each CT image at every 5 cm. Alternating low and high CT values provide evidence of cyclicity. Hounsfield units (a) and arbitrary unit after conversion to an 8-bit gray scale (b).

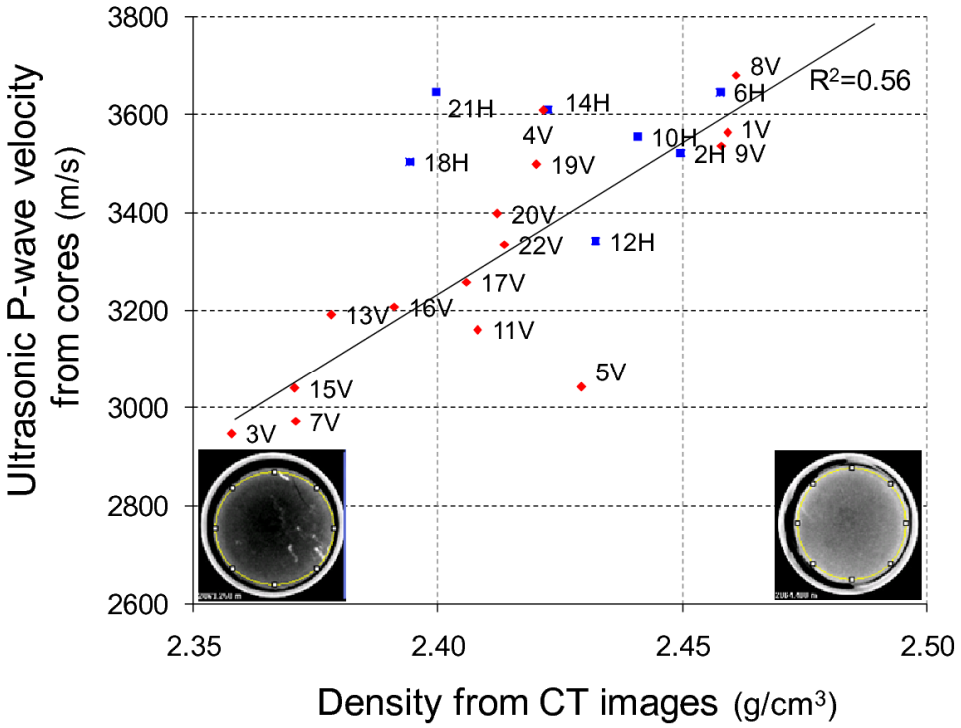

Figure 4.2: Ultrasonic P-wave velocity measured from plugs versus relative X-ray density from CT images, obtained at the same position. The correlation coefficient is 0.56. Red and blue symbols correspond to V_p values for vertically and horizontally oriented samples, respectively. CT images from samples 3 (2863.25 m) and 8 (2864.40 m) are also shown. Bright colours mean higher X-ray CT values (higher mass densities, higher P-wave velocities), whereas dark colours correspond to low CT values.

4.1.3 Quantification of sedimentary cycles on the centimetre scale

The computed X-ray densities reveal well defined cycles. Shales are related to dark images with smaller densities and velocities; marlstones are in the other extreme, and there exist a gradation between the two (Figure 4.2 and Figure 4.3). These changes are caused by the differing amount of calcium carbonate, which is enhanced in CT imagery owing to the relatively high atomic number of calcium. These cycles are not visible in standard resolution logs, and even in high resolution logs they are still aliased or smoothed over.

The computed velocities from CT images (using previously established correlation) show clearly the cyclic behaviour with much higher resolution than the sonic log (Figure 4.3). However, comparison between these velocities and the sonic log shows discrepancy in the upper part of the interval. There is a better agreement in the lower part. The misfit between sonic log and ultrasonic measurements may be related to dispersion effects (500 kHz in the lab; 10 - 20 kHz in the logs) and/or fluid substitution effects. The lab measurements were done on partially dried samples. Correction for frequency, fluids and anisotropy would be needed to adequately upscale this layered sequence to match interval travel times on the log or seismic scale.

Vertical variation of X-ray CT values shows a clear pattern of sedimentary cyclicity with a spatial period of 37.7 cm estimated from the autocorrelation function and the periodogram (Figure 4.4). Given an estimated accumulation rate of 2 cm/ka (G. Albertao, personal communication, 2008) for this interval, it corresponds to a time period of approximately 19 ka. This appears to be related to precessional cycles (23 ka - 19 ka). This interpretation hinges on the accuracy of the accumulation rate which, in general, is difficult to obtain.

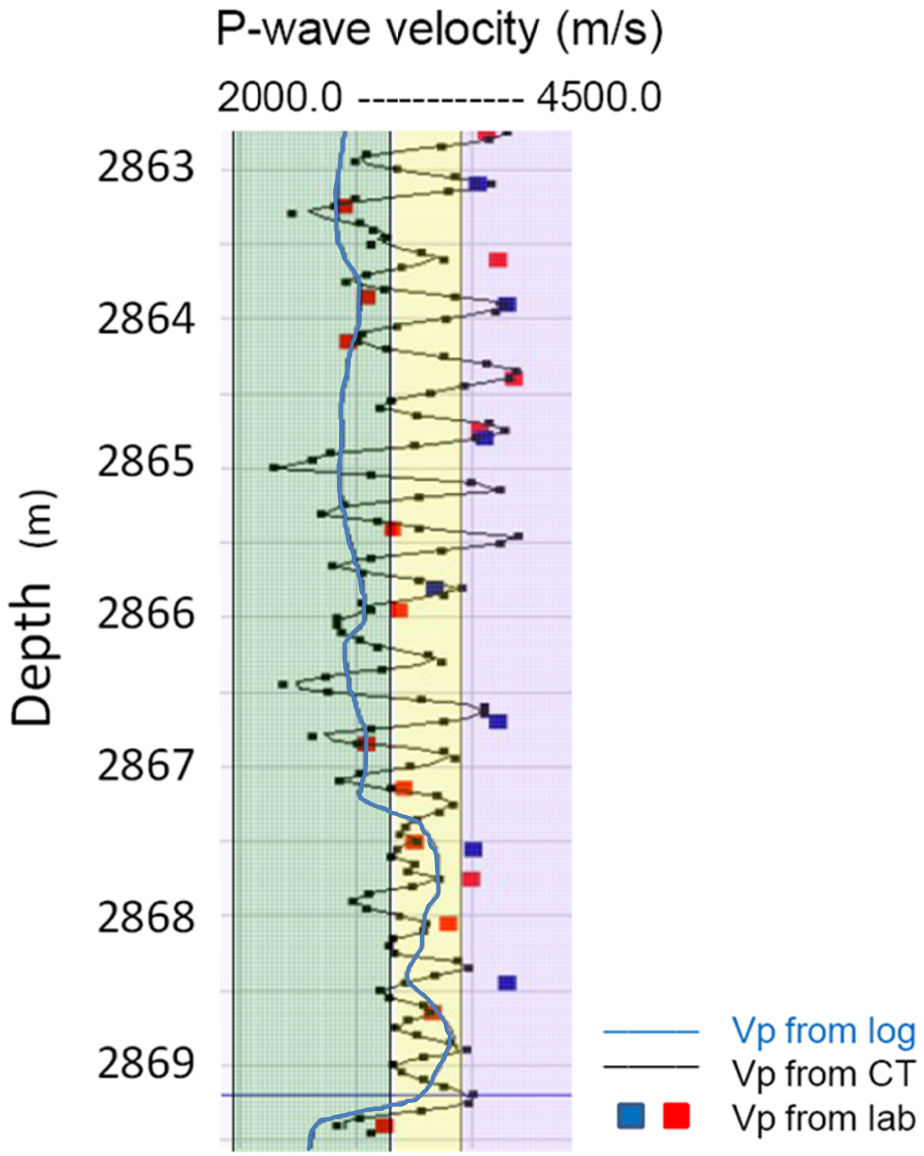

Figure 4.3: Ultrasonic P-wave velocity from plugs at reservoir effective pressure (3000 psi) measured on vertically (red symbols) and horizontally (blue symbols) oriented core plugs; P-wave velocity from high resolution sonic log (blue line) and velocity derived from CT images (black line). Magenta, yellow and green colours are related to higher (contains more $CaCO_3$), medium and lower (contains more shale) velocities computed from CT images.

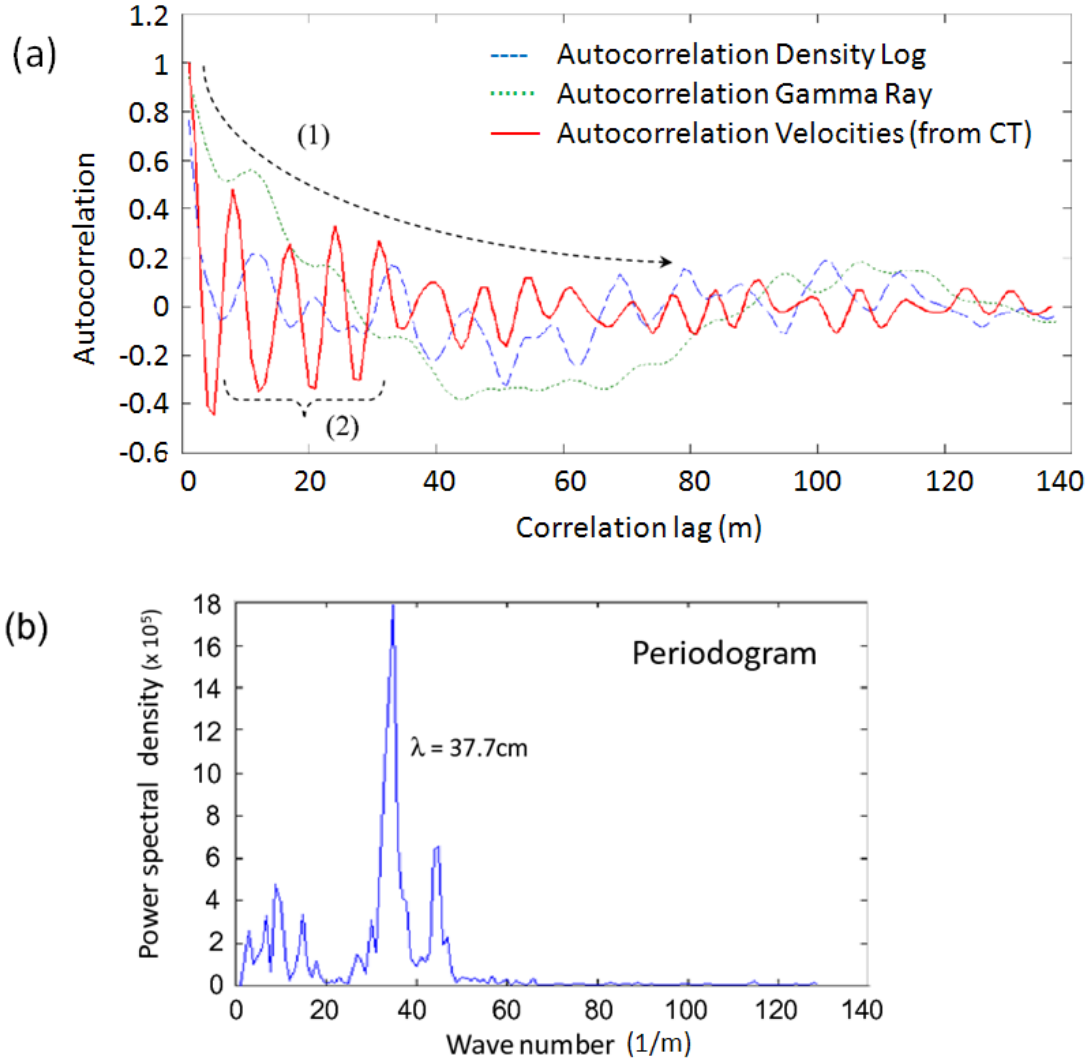

Figure 4.4: (a) Autocorrelation function of gamma-ray log (green dots), density log (blue dashed line) and CT velocities (red line) for the depth interval shown in Figure 4.3. The autocorrelation function of the CT velocities consists of two parts: (1) a signature of a random process showing a decrease of correlation function with correlation lag; and (2) a signature of a periodic (cyclic) process with a period of 37.7 cm. (b) Power spectral density computed from CT images in shale-marl interval showing the dominant period of 37.7 cm.

4.1.4 Discussion

CT images over the reservoir interval, aside from giving extraordinary vertical resolution, also provide lithologic information (Figure 4.1), which is useful for interpretation of petrophysical and rock physics measurements on core plugs.

In principle, the resolution of the CT-derived information could be increased further by reducing the spacing between slices (down to 1 mm so that the slices are adjacent), though for this study the time and expense of this would be unwarranted. The real value of X-ray CT as compared with other observations on core (e.g. colour, texture or mineralogic analysis) is the direct quantitative link to seismically relevant physical properties (velocities and densities) and the parallel assessment of the quality of the core for laboratory testing purposes.

X-ray density obtained from CT images shows a reasonable correlation (correlation coefficient 0.56) with ultrasonic P-wave velocity. This correlation is much better than X-ray density with mass density (correlation coefficient 0.2). This may be explained by the fact that variations in calcium carbonate content have a strong effect on both velocity and X-ray CT, but lesser effect on mass density. Higher content of calcium carbonate causes stiffening and shifts the V_p curve to higher velocities. I classified the velocities computed from CT images into three groups according to their magnitude, and associated to the gradation of shales and marlstones (Figure 4.3). The above observations help understand the relationship between velocity and confining pressure (Figure 4.5). All the ultrasonic measurements are now consistent with this interpretation, and this insight could be useful for future time-lapse studies as these rocks are located in the vicinity of a reservoir which should experience a pressure variation with time.

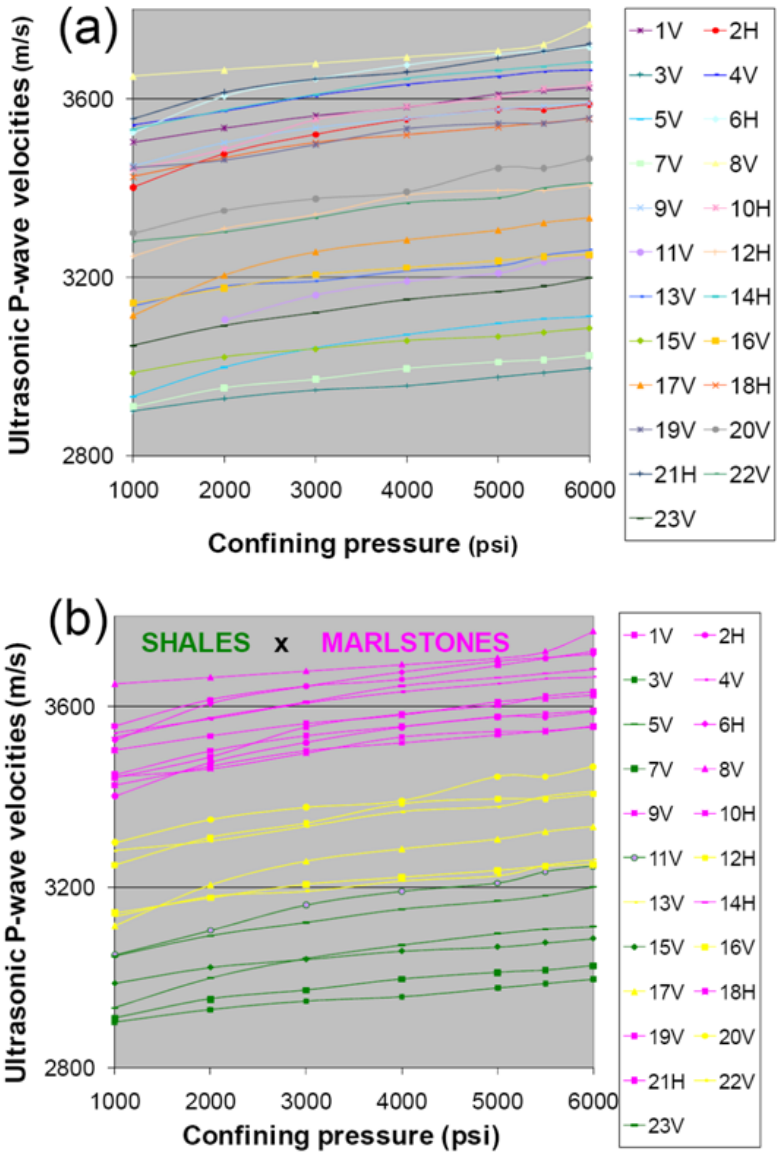

Figure 4.5: Ultrasonic P-wave velocities (23 plugs) versus confining pressure measured in the laboratory. From the meaningless (from a geological point of view) curves (a), I classify and group plugs based on CT X-ray absorption (b), to be used in a further 4D study. Magenta, yellow and green colours are related to higher, middle and smaller ranges of velocity computed from CT images.

4.1.5 Conclusions

I have shown that densely sampled X-ray CT images over a shale/marl interval reveal small scale sedimentary heterogeneity and aid in the interpretation of petrophysical and rock physics measurements. In particular, I demonstrated that there is spatial cyclicity that cannot be revealed even using high resolution logs. The understanding of the cyclicity characteristics in the area under study allowed us to identify Milankovich cycles, which I interpret as precession cycles (19 ka periodicity). There are other evidences of sedimentary cyclicity in this region at larger scales obtained by other methods (Azambuja *et al*., 2007; Barbosa *et al.*, 2007; Cunha and Koutsoukos, 2001). Consequently, there is a potential for X-ray CT studies to assess not only rock physical properties when used in combination with ultrasonic measurements or logs, but to be used for paleo-climate studies.

The good match between measured ultrasonic velocities and those computed from CT shows that the large variations of ultrasonic velocities between different samples are caused by vertical heterogeneity (variation of calcium carbonate content) and not by strong anisotropy. The cyclic variations in X-ray CT values disappear completely in the sand reservoir (turbidite).

The understanding of cyclicity characteristics and the presence of velocity variability with confining pressure in the study interval (which lies over a hydrocarbon reservoir), could be further used for detailed modelling of time-lapse effects.

4.2 Effect of Net to Gross (Thin Layers) on Pressure Sensitivity in Hydrocarbons Reservoirs

Time-lapse studies consider changes of elastic properties in the vicinity of a reservoir interval according to changes in pressure due to production or injection. Considering clastic reservoirs, it is usual to have sub-seismic low permeability shales intercalated with sandstone reservoir. During depletion, sandstone compacts and shales may expand. On the other hand, during fluid injection, sandstones may soften. This phenomenon may induce hardening of the surrounding shales. The combined seismic response depends on the net to gross, permeability of both shales and sands, and on the required time for the layers to reach the equilibrium pressure. Hatchell and Bourne (2005) studied time-shifts taking into account intra-reservoir shales during reservoir depletion. Because shales have very low permeability, the pore pressure in shales may not have enough time between seismic surveys to equilibrate with the pressure in surrounding sands MacBeth et al. (2008). In such cases shales may be considered as impermeable. This is an approach that I have investigated in this research.

The evaluation of the magnitude of thin shale layers on the reservoir stress sensitivity response may help to correct this effect for quantitatively modelling 4D seismic. The impact of this study in hydrocarbon reservoirs which have varying net to gross (turbidites, deltas) may be significant. In Brazil, for instance, the majority of known Campos Basin mature reservoirs undergoing development are comprised of sandstone turbidites containing thin intra-shale layers (Bruhn et al., 2003).

In this study I propose a workflow to compute the combined seismic response of a reservoir undergoing pressure changes as a function of net to gross. To evaluate the magnitude of thin shale layers on the reservoir stress sensitivity response, I apply the developed workflow to a typical clastic reservoir located in Campos Basin, offshore Brazil.

4.2.1 Effect of thin intra-reservoir shale layers during production

Consider a reservoir interval composed of a sequence of hydraulically communicating sands and nearly impermeable shales. During production, fluid pore pressure in the sandstone is reduced, increasing the effective pressure. Consider that there is no fluid communication among shales and sands during a period of time between repeated 3D surveys. As there is no time for fluids to move between shales and sands in order to equilibrate pressure, the stress conditions will change only due to the mechanical pull caused by neighbouring depleting sands. Consequently, during depletion the pore pressure will decrease in sandstones and stiffen these rocks (hardening), whereas the surrounding shales will mechanically expand (softening) (MacBeth et al., 2008). Fluid injection into sand will cause the opposite effect: pore pressure in sand will increase causing its softening and consequently the hardening of the shales.

4.2.2 Computing elastic parameters of an equivalent medium

To quantify the effect of the extension and contraction induced by stress changes, I consider the vertical P-wave propagation through the stack of shales and sands for different NTG (net to gross or sand-shale ratio) in the reservoir interval. In this study I assume that the induced stress change in the shales has the same magnitude as, and the opposite sign to, the stress change in the sandstone: $\delta P_{shale} = -\delta P_{sand}$.

To estimate velocity dependence on pressure I use the equation (Eberhart-Phillips et al., 1989; Shapiro, 2003):

$$V(P) = A + KP - B\exp(-PD), \tag{4.1}$$

where V is the P-wave velocity (in m/s), P is the effective stress (in MPa), A, K, B and D are fitting parameters for the set of measurements.

The elastic moduli of the sand/shale package are computed using Backus averaging (Backus, 1962; Mavko et al., 1998). The long-wave equivalent P-wave modulus M_{av}^{0} and density ρ_{av}^{0} of the package before production can be written as

$$\frac{1}{M_{av}^{0}} = \frac{N}{M_{sand}(P)} + \frac{1-N}{M_{shale}(P)}\ , \tag{4.2}$$

and

$$\rho_{av}^{0} = N\rho_{sand}(P) + (1-N)\rho_{shale}(P)\ . \tag{4.3}$$

After depletion or production we have

$$\frac{1}{M_{av}^{1}} = \frac{N}{M_{sand}(P+\Delta P)} + \frac{1-N}{M_{shale}(P-\Delta P)}\ , \tag{4.4}$$

and

$$\rho_{av}^{1} = N\rho_{sand}(P+\Delta P) + (1-N)\rho_{shale}(P-\Delta P)\,, \tag{4.5}$$

where $M_{sand}(P)$, $M_{shale}(P)$, $\rho_{sand}(P)$ and $\rho_{shale}(P)$ are P-wave moduli and densities of sand and shales, respectively, at effective pressure *P, N* is the net to gross (sand-shale ratio). The superscripts 0 and 1 refer to times before and after production and $\Delta P = P^{1} - P^{0}$ is effective pressure change between the two surveys.

4.2.3 A case study for a clastic reservoir in Campos Basin

In this subsection I analyse the seismic combined response (1D) using real data from a clastic reservoir in Campos Basin. In this basin there are more than 40 oil fields from different ages, representing a variety of reservoir properties. Each field and each reservoir has its own characteristics in terms of lithology, grain size, and cementation. I analyse rock properties from a clastic reservoir located in the south portion of Campos

Basin, around 100 km off the coast of Rio de Janeiro (south eastern Brazil), in a water depth of approximately 700 m.

In deep and ultra-deep water projects, it is important to avoid costly workovers; therefore programs of pressure maintenance are frequently used (Bruhn et al., 2003). Close to the water injector wells, pore pressure can significantly increase, whereas in other positions it could decrease due to depletion, resulting in higher effective pressure. The sub seismic intra-reservoir shale layers can vary in thickness and content (NTG) (Figure 4.6). Considering the variation of NTG and the possible lateral variation of effective pressure within the reservoir, the understanding of the combined seismic response of small scale intra-reservoir shales may be essential for quantitative 4D interpretations.

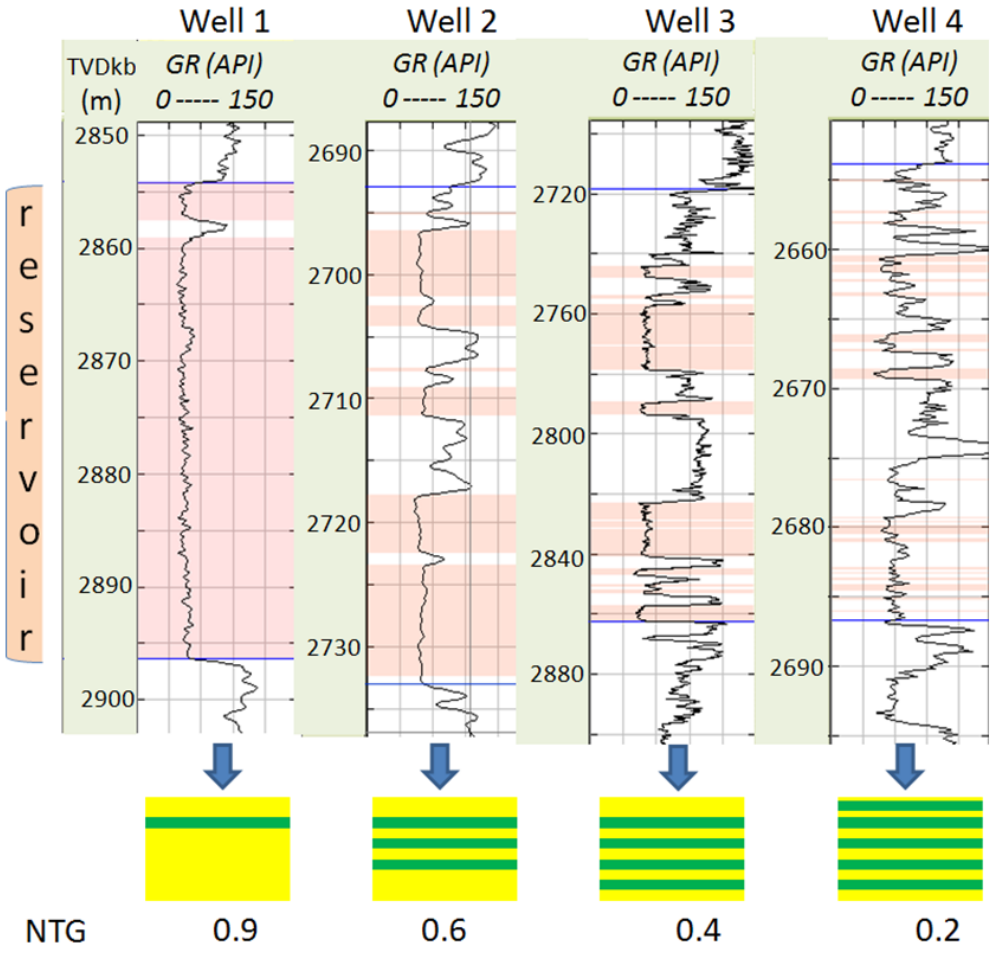

Figure 4.6: Gamma-ray logs over the reservoir interval for 4 wells located in an oil field in Campos Basin. The reservoir is comprised of sandstones (orange) and shales (white, GR > 55) with composition (NTG) varying laterally.

The reservoir is comprised of gravel to sand rich lobes - mainly arkosic sandstone - from confined turbidities related to Santonian / Campanian Stage. This 45 m thick reservoir is comprised of an amalgamation of turbidites intercalated by shale layers with thickness ranging from centimetres to several meters. After the discovery in 1984, oil production started in 1985 and the reservoir (hydraulically interconnected) has been depleted by natural water aquifer and water injection. There are 25 wells producing 29°API oil, permeability is 1500 mD and temperature 89ºC. The current and forecast recovery factors are 38% and 55%, respectively, and reservoir monitoring is important to locate unswept areas and map pressure variations.

Ultrasonic measurements were routinely done on sandstones and, in some cases, on shales to calibrate velocity sensitivity to pressure. A sinusoidal pulse with the central frequency 500 kHz was propagated through the sample and for each step of pressure increment velocities were determined from the travel time and the length of each sample.

The velocity-pressure dependence is obtained by fitting equation (4.1) to ultrasonic data using a nonlinear least-squares regression (Figure 4.7). The fitting parameters A, K, B and D for the set of measurements are, respectively, $A = 2.86 \cdot 10^3$, $K = 6.40$, $B = 1.04 \cdot 10^3$, $D = 0.205$ for sand; and $A = 3.43 \cdot 10^3$, $K = 0.0$, $B = 0.27 \cdot 10^3$, $D = 0.0585$ for shale.

I consider two production scenarios: injection and depletion. During injection, the pore pressure in the sand increases by $\Delta P = 10$ MPa, causing a decrease of effective pressure for shales by the same amount. During the depletion the opposite happens: pore pressure decreases: $\Delta P = -10$ MPa (Figure 4.7), causing corresponding increase of effective pressure on shale layers.

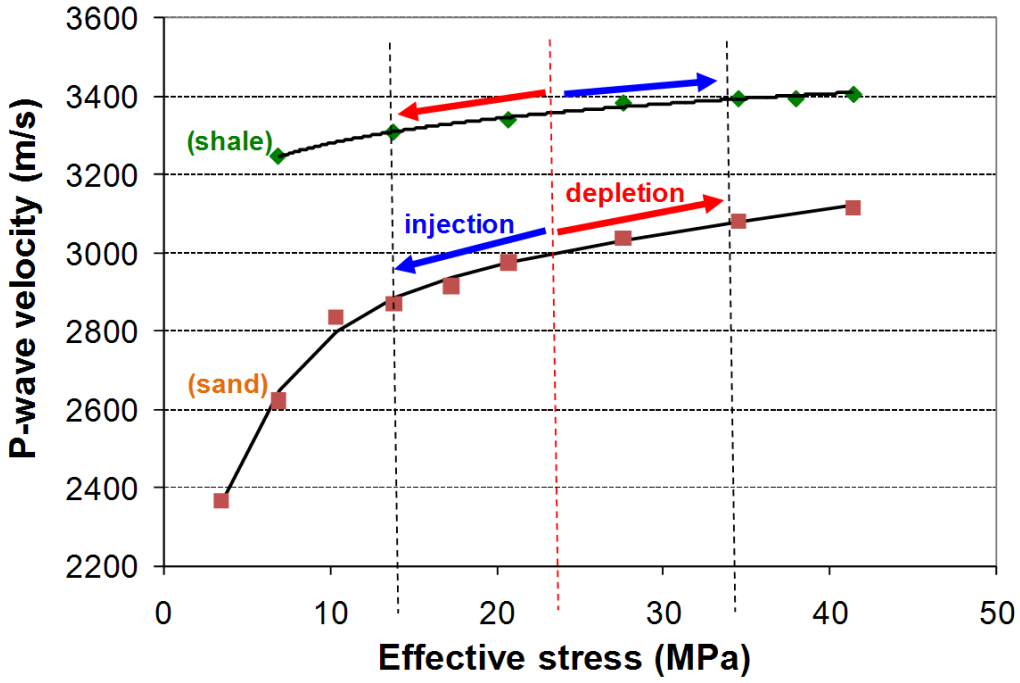

Figure 4.7: Velocity dependency on effective pressure from ultrasonic measurements for sand (brown) and shales (green). During depletion (red arrow) sand increases velocity (hardening) whereas shale decreases (softening). During injection (blue arrow) the opposite occurs.

From the original pressure condition, using equation (4.1) I compute new velocities for sandstone and shale for both scenarios: pressure increase (10 MPa) and decrease (-10 MPa). Using these velocities, I calculate average P-wave moduli (M_{av}) and average density (ρ_{av}) as a function of net to gross (equations (4.2) and (4.4)). In the range of stress considered, density is expected to vary by no more than 0.1% (Mavko and Jizba, 1991; Gurevich, 2004); thus it is assumed to be independent of pressure ($\rho_{av}^0 = \rho_{av}^1$). Finally, impedances and reflection coefficients are obtained from P-wave moduli and densities for each net to gross increment.

4.2.4 Results

Figure 4.8 shows the expected P-wave impedance of a sand/shale package as a function of NTG for undisturbed conditions (black), and after depletion (red) and injection (blue) corresponding to change of pressure by ±10MPa. Impedances of this package increase for higher shale content since shale has higher impedance than sand. The rate of increase is higher for injection than depletion due to the shape of the stress sensitivity curves.

The variation of impedance relative to the initial pressure condition as a function of net to gross is shown in Figure 4.9. In a depletion scenario (red line), hardening occurs in a reservoir made up only by sand (NTG = 1). This is easily predictable since pore pressure is reduced, thus hardening the rock. When shale content increases (reducing NTG), the combined sand/shale impedance response decreases due to shale expansion, reacting to sand contraction. For NTG smaller than 0.3 the composite reservoir package changes the expected behaviour: instead of hardening, softening happens even in a reservoir depletion scenario. For an injection scenario (blue line) the opposite occurs. These unexpected combined pressure responses could happen even for higher NTG for shales which are more sensitive to pressure.

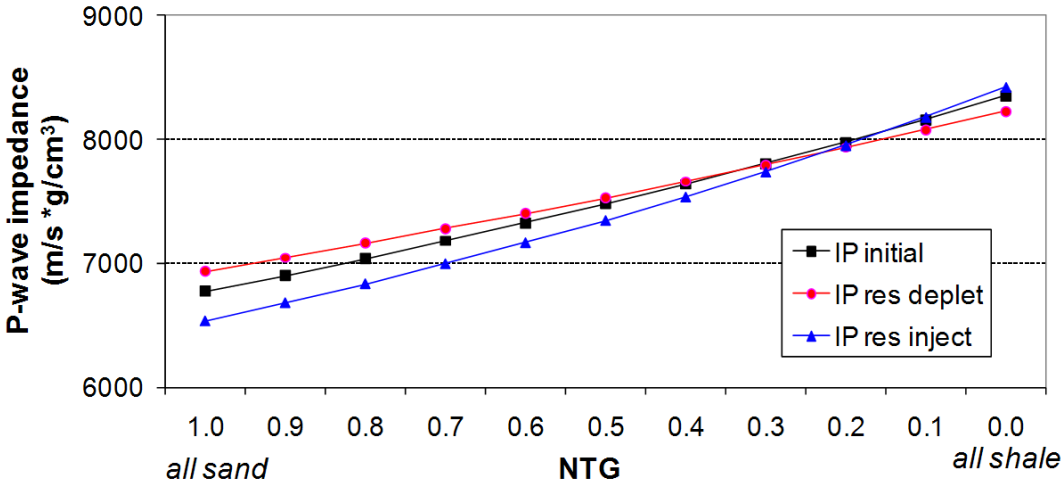

Figure 4.8: P-wave impedance of a heterogeneous (shales and sands) reservoir computed using Backus average. Depletion (red) and injection (blue) of 10 MPa from the initial (black) conditions are modelled as a function of net to gross.

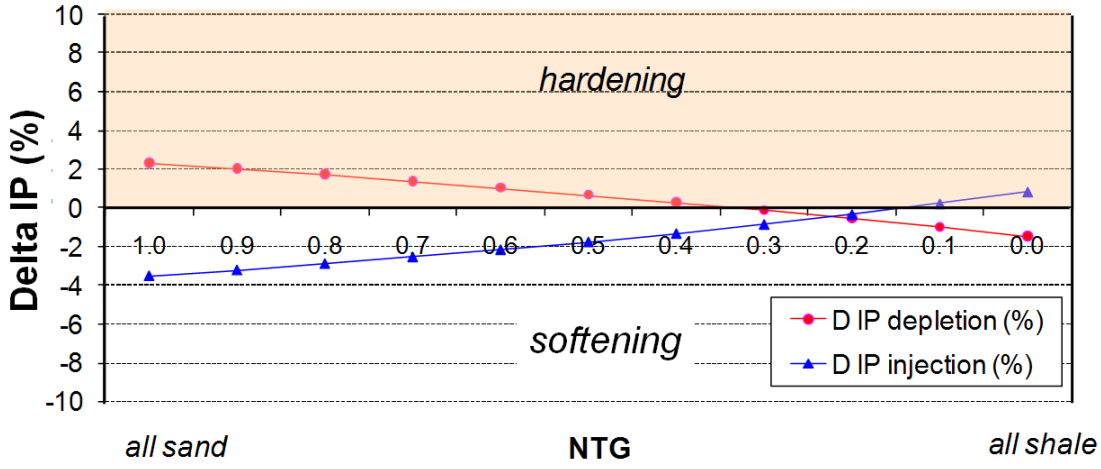

Figure 4.9: Relative changes in P-wave impedance (Delta *IP*) relative to the initial pressure condition as a function of net to gross. Depletion (red) and injection (blue) of 10 MPa are modelled.

Figure 4.9 also shows asymmetry in the impedance response during depletion and injection as pointed out by Sayers (2007). For a homogeneous sandstone reservoir (NTG=1) undergoing depletion, the impedance increases by 2.3%, whereas during injection it decreases by 3.5%.

The impact of intra-reservoir shales on seismic data can be better understood by looking at reflection coefficients. Figure 4.10 shows P-wave reflection coefficients related to the top of the heterogeneous reservoir as a function of net to gross. Reflection coefficients become smaller (by absolute value) with the increase of shale content in the reservoir. The anticipated dimming effect on 4D data will be more prominent for a depletion scenario once the composite reservoir impedance is more similar to that of the overburden rock. When we analyse changes in reflection coefficients due to shale/sand expansion and contraction, their correct magnitude (as shown in Figure 4.10 for stress sensitivities in this study) should be taken into account for quantitative time-lapse interpretation.

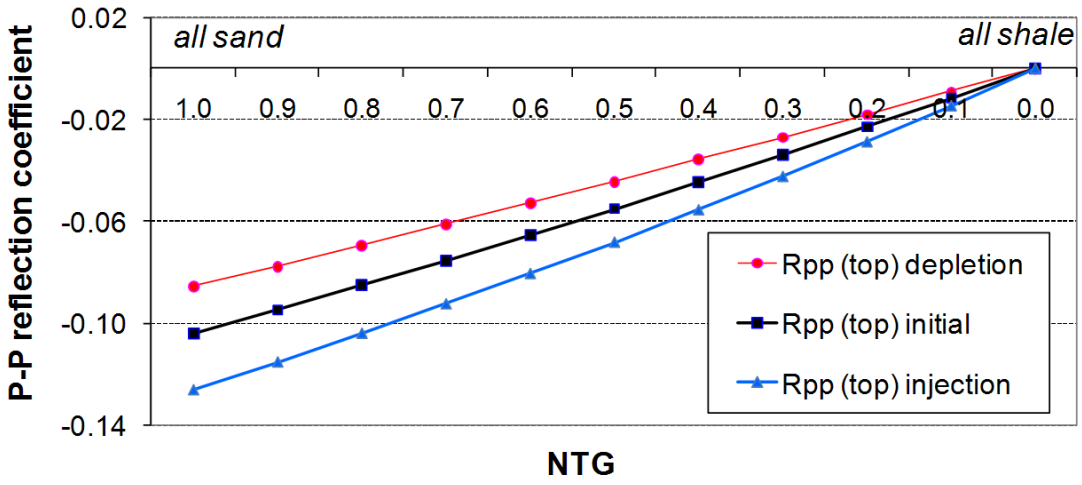

Figure 4.10: P-P reflection coefficients corresponding to the interface between the overburden shale and the heterogeneous reservoir. Depletion (red) and injection (blue) of 10 MPa from the initial (black) conditions are modelled as a function of net to gross.

4.2.5 Discussion and conclusions

Small scale intra-reservoir shales have a very different response to fluid injection and depletion from that of sand, and thus may have a strong effect on the equivalent properties of a heterogeneous sandstone reservoir. I proposed a methodology using Backus average to compute the combined seismic response for depletion and injection scenarios as a function of net to gross. This approach is appropriate for modelling time-lapse effects in repeated seismic surveys when there is no time for pressure in shale and sand to equilibrate.

I apply this methodology using typical Campos Basin elastic properties. I conclude that impedances and reflection coefficients may be wrongly estimated without considering the presence of small scale intra-reservoir shales. The magnitude of the error in impedance estimation can vary from 3.5% to 0.8% (injection) and 2.3% to -1.5% (depletion), the same magnitude as many expected changes in real time-lapse effects. Similarly, reflection coefficients could be largely misestimated if the presence of small scale intra-reservoir shales is ignored. Considering net to gross of 0.6, for example, the correct value of the reflection coefficient is -0.053 instead of -0.086 (depletion scenario), and -0.080 instead of -0.126 (injection scenario). The differences are 38% and 36%, respectively.

Disregarding the net to gross effect may bias results for frequently repeated surveys. The time-lapse response from the combined sand-shale reservoir can be even the opposite of the expected response. Instead of hardening during depletion, softening could occur. This unexpected behaviour is more likely to happen for low net to gross or in places where shales have higher sensitivity to pressure, as shallow layers.

Based on presented evidence of net to gross effect on time-lapse response, I suggest this methodology to be taken into account for quantitative time-lapse studies. I also suggest expanding analyses to 3D models to incorporate other geomechanical effects (like stress arching effects).

Chapter 5

CONCLUSIONS AND FUTURE RESEARCH

Time-lapse (4D) seismic is a modern geophysical technology for monitoring producing hydrocarbon fields. This technology can be used to detect changes related to fluid movements and pressure variations during reservoir depletion or injection. Time-lapse seismic has evolved during the past decade and become a widespread monitor tool utilised in petroleum industry. Time-lapse seismic technology has proven extremely useful in identifying compartments, barriers to flow, unswept zones and improved characterisation of the reservoir geometry. However time-lapse monitoring has also potential to optimize production strategy using quantitative mapping of pressure, stress and saturation in and around the reservoir. To this end, knowledge of the quantitative dependency of elastic properties on pressure and saturation is required.

In this Chapter I present the main conclusions of the thesis and directions for future work. The broadness of time-lapse seismic subject means that this thesis cannot cover all the related problems. However, a number of important challenges have been addressed and several conclusions are presented. These challenges are related to the investigation of production induced changes in time-lapse seismic data. Both saturation and pressure effects on elastic parameters have been investigated. I have analysed pressure effects using information from laboratory and in situ measurements. I have also integrated seismic, logs, cores, and X-ray CT in order to analyse and predict time-lapse effects on various scales.

5.1 Conclusions

Changes in elastic properties due to changes in saturation are usually calculated using Gassmann equations. Gassmann theory is based on a number of assumptions. In this research I have proposed a workflow to test the validity of Gassmann theory in a real geologic environment (Grochau and Gurevich, 2008b, 2009a). To this end, I compared saturated P-wave moduli computed from dry core measurements against those obtained from sonic and density logs. The workflow was tested with a dataset from Campos Basin, Brazil. The results show good statistical agreement between the P-wave elastic moduli computed from cores using Gassmann equation and the corresponding moduli computed from log data. This confirms that all the assumptions of the Gassmann equations are adequate within the measurement error and natural variability of elastic properties. The proposed workflow and the results obtained provide further justification for using the Gassmann theory to interpret time-lapse effects in similar geological formations.

In this thesis I have also analysed the pressure – velocity dependence of rocks. It was done from two different perspectives: as obtained from ultrasonic measurements and from in situ measurements (logs). The pressure effect on seismic velocities is usually obtained from core samples, and they may not be representative of the in situ formation due to core damage. One of the achievements of this thesis is to present a methodology to assess the adequacy of ultrasonic measurements to the in situ properties from core samples (Grochau and Gurevich, 2007a, b, 2008a). Dispersion effects have been minimized by using dry cores and then computing saturated velocities using Gassmann equations. To mitigate under-representation, cores were extracted over all reservoir interval. Then I compared measured ultrasonic velocities at reservoir pressure with sonic-log data, and the saturated velocities computed from core measurements on dry samples match the sonic-log velocities quite well. The core damages that may occur while bringing the core samples to the surface are small and do not adversely affect the measurement of elastic properties on these core samples. Should core damage have

affected our measurements, we would have expected a systematic difference between properties measured in situ and on the recovered. Consequently, stress sensitivity of elastic parameters, as obtained from ultrasonic measurements (including core preservation during extraction), is adequate for quantitative interpretation of time-lapse seismic data.

Another achievement of this research is to present a method to infer the in situ pressure – velocity relationship using log data from wells drilled and logged during field development. I have analysed velocity variations as a function of both pressure and porosity. The three dimensional regression proposed in this thesis aims to help account for rock property variability. The proposed methodology was applied to a reservoir with heavy depletion. The in situ stress sensitivity of elastic properties was analysed from twenty three well logs and from repeated formation tester. The pore pressure changes in time and space suggest two distinct hydraulic compartments. I plotted, in three dimensions, all values (V_p, ϕ and P_{effec}) corresponding to this sandstone and a plane was fitted among these hundreds of points using a least-square method for each compartment. I also compared the relationship between V_p, $-\phi$ - P_{effec}, from in situ approach and the laboratory measurements, which showed similar results for the reservoir's mean properties. Despite using constraints (same stratigraphic unit, gamma-ray and porosity cut-offs), there was still significant porosity variability. Therefore, I concluded that the uncertainties related to rock and fluid properties remain high. The main intrinsic uncertainties in this methodology are caused by rock heterogeneity and errors in effective pressure estimation. Consequently, for this particular dataset from Campos Basin, the results are not completely reliable to assure the true in situ pressure – velocity – porosity relationship. Spatial variations (heterogeneity), perhaps, mask a relatively small pressure effect. In more favourable conditions (higher rock homogeneity) or steeper part of pressure-velocity curve, this methodology may be used as a complementary assessment of rock elastic properties together with the ones derived from core measurements.

Production induced effects in time-lapse seismic data often occur in small scale layers, below seismic resolution. Ideally, in order to model or interpret these effects, those layers should be identified and taken into account. In this thesis I have demonstrated that even high resolution logs may not identify very thin layers. Thus I have proposed a methodology to assess rock properties and to overcome log (and seismic) resolution limitation by using X-ray computed tomography (CT) together with ultrasonic measurements (Grochau et al., 2009). This methodology was applied to rocks extracted from a deepwater oil field, offshore Brazil at 2.8 km depth. Densely sampled X-ray CT images over a shale/marl interval revealed small scale sedimentary heterogeneity and thereby aided the interpretation of petrophysical and rock physics measurements. Sedimentary cyclicity was revealed and interpreted as precession cycles (19 ka periodicity), related to Milankovich cycles. This could potentially reveal other small scale heterogeneity that could help 4D studies. Possible stress changes in this interval (reservoir's overburden rock) due to production or injection in the subjacent reservoir could further be modelled using this dataset. Moreover, the improved understanding of physical property variations may help to correlate stratigraphy between wells and to calibrate pressure effects on velocities for seismic time-lapse studies.

Another achievement of this thesis was the development of a methodology to compute the combined seismic response of a reservoir undergoing pressure changes as a function of net to gross (NTG or sand – shale fraction). Considering clastic reservoirs, it is usual to have sub-seismic low permeability shales intercalated within a sandstone reservoir. During depletion, the sandstone compacts and the shales may expand. During injection, the opposite occurs. To evaluate the effect of thin shale layers on the reservoir stress sensitivity response, I have applied the methodology using Backus average to a typical clastic reservoir located in Campos Basin, offshore Brazil. I concluded that impedances and reflection coefficients may be erroneously estimated without considering the presence of small scale intra-reservoir shales (Grochau and Gurevich, 2009b). The magnitude of the error in impedance estimation can vary from 3.5% to

0.8% (injection) and 2.3% to -1.5% (depletion), i. e., the same magnitude of generally expected changes in real 4D effects. The reflection coefficients could be poorly estimated if the presence of small scale intra-reservoir shales is ignored. Disregarding the net to gross effect may bias results for frequently repeated surveys. The 4D response from the combined sand-shale reservoir can even be the opposite of the expected response. Instead of hardening during depletion, softening could occur for low NTG or in places where shales have higher sensitivity to pressure, as shallow layers.

5.2 Future Research

I found that Gassmann equations are adequate within the measurement error and natural variability of elastic properties in the area under study (Section 2.3). Tests in other geological environments with different rocks (e. g. carbonates), fluid content and pressure ranges may affect more significantly Gassmann predictions. Similar tests of Gassmann assumptions should be done in different parts of the world to verify how generic the conclusions obtained in this research are.

Regarding the evaluation of pressure – velocity relationship from core measurements (Section 3.1), I also suggest applying the methodology proposed in this research (to test core integrity by comparing with measured sonic logs) in other regions and petrophysical conditions. Obtaining a good match between computed saturated velocities from measurements in dry cores and sonic logs may indicate the adequacy of core extraction and preservation processes. On the other hand, mismatch between both datasets may indicate those processes should be reviewed. This could be a standard quality control step for 4D studies because it indicates the reliability of pressure - velocity –relationship obtained from cores.

Concerning the velocity dependence on pressure from the in situ approach (Section 3.2), it is necessary to investigate other factors that may affect velocities. I suggest for future works including more physical quantities than those investigated here

(V_p, ϕ and P_{effec}), e. g., cementation. Another suggestion for further work is to take into account lateral stresses in order to have a better representation of the effective pressure. I recommend to further explore the in situ approach, particularly in mature oil fields, where many wells with logs are usually available. The use of well logs can give a significant increase in spatial coverage of information in comparison to the typically sparse sampling provided by cores. Furthermore, the joint comparison of in situ and laboratory approaches may provide robustness for determining the pressure – velocity relationship. Considering that the pressure response is much quicker than the saturation response, the understanding of the pressure changes can significantly contribute to the early identification of preferential zones and barriers within the reservoir.

In order to identify time-lapse effects in thin layers (Section 4.1), I suggest routinely analysing X-ray computed tomography images from all core samples extracted from drilled wells. Based on the correlation of X-ray absorption, logs and ultrasonic measurements, petrophysical properties may be derived. A natural improvement from this research is to compute X-ray absorption from a three dimensional volume rather than using a two dimensional image. A three dimensional visualization of X-ray absorption could guide the selection process of plug extraction from cores to perform ultrasonic measurements. Otherwise a bias may be introduced caused by performing ultrasonic measurements only in the most preserved regions of the extracted cores. I suggest for future work, the use of high resolution information derived from CT images to improve correlation between wells and to model time-lapse response in details.

In relation to thin intra-reservoir shale layers (net to gross) behaviour during depletion and injection (Section 4.2), I suggest expanding the approach presented in this research to a three dimensional investigation. This could be done using both numerical and physical models to incorporate other geomechanical effects (like stress arching effects). The physical models to be created, could mimic real depositional environments and applying simulated production effects (pressure and saturation changes) on these models it may be possible to obtain useful insights. I also suggest evaluating the time

scale which should affect pressure equilibration between sands and low permeable shales.

REFERENCES

Al-Naijjar, N., P. Doyen, I. Brevik, L. Kvamme, and D. Psaila, 1999, Statfjord field – time-lapse seismic interpretation using a 4D earth model: Presented at SEG Annual International Meeting, Expanded Abstracts.

Amundsen, L., and M. Landro, 2007, 4D seismic – status and future challenges, Recent Advances in Technology: GEO ExPro, 66-68.

Anderson, R. N., A. Boulanger, W. He, L. Xu, P. B. Flemings, T. D. Burkhart, and A. R. Hoover, 1997, 4-D time-lapse seismic monitoring in the south Timbalier 295 field, Gulf of Mexico: 67th Ann. Internat. Mtg., Soc. Expl. Geophys., Expanded Abstracts, 868–871.

Artola, F. A. V., and V. Alvarado, 2006, Sensitivity analysis of Gassmann's fluid substitution equations: some implications in feasibility studies of time-lapse seismic reservoir monitoring: Applied Geophysics, **59**, 47-62.

Azambuja, N. C., A. H. A. Castro, A. A. S. Cunha, C. R. Becker, C. F. Santos, J. G. R. Silva, J. M. C. Mendes, M. C. G. Severino, P. R. C. Cunha, and R. L. M. Azevedo, 2007, Application of Climatic Changes to Understand Sedimentary Processes and a Tool to Refine the Stratigraphy in Brazilian Sedimentary Basins - An Overview: AAPG Annual Conference.

Backus, G. E., 1962, Long-wave elastic anisotropy produced by horizontal layering: Journal of Geophysical Research, **67**, 4427-4440.

Barbosa, V., A. Cunha, S. Shimabukuro, and L. Gamboa, 2007, Relative sea level variations driven by short-term orbital-climatic cycles in Campos Basin during the Oligocene: a palaeoecological, biostratigraphic and cyclostratigraphic approach. Geological Society Bicentenary Conference, Expanded Abstracts, 145-148.

Batzle, M., D.-h. Han, and R. Hofmann, 2006, Fluid mobility and frequency-dependent seismic velocity — Direct measurements: Geophysics, **71**, no. 1, N1-N9.

Berryman, J. G., 1999, Origin of Gassmann's equations: Geophysics, **64**, 1627-1629.

Biot, M., 1956a, Theory of propagation of elastic waves in a fluid saturated porous solid; I-Low frequency range: Journal of the Acoustical Society of America, **28**, 168-178.

—, 1956b, Theory of propagation of elastic waves in a fluid saturated porous solid; II-High frequency range: Journal of the Acoustical Society of America, **28**, 179-191.

Brown, R.J.S., J. Korringa, 1975. On the dependence of the elastic properties of a porous rock on compressibility of a pore fluid. Geophysics, **40**, 608– 616.

Brown, L., and B. Gurevich, 2004, Frequency-dependent seismic anisotropy of porous rocks with penny-shaped cracks: Exploration Geophysics, **35**, 111-115.

Bruhn, C. H. L., C. D. Lucchese, J. A. T. Gomes, and P. R. S. Johann, 2003, Campos Basin: Reservoir characterization and management — Historical overview and future challenges: Presented at Offshore Technology Conference, OTC - Expanded Abstracts.

Burkhart, T., A. Hoover, and P. B. Flemings, 2000, Time-lapse (4-D) seismic monitoring of primary production of turbidite reservoirs at South Timbalier Block 295, offshore Louisiana, Gulf of Mexico: Geophysics, **65**, 351-367.

Calvert, R., 2005, Insights and methods for 4D reservoir monitoring and characterization: Society of Exploration Geophysicists.

Cunha, A. A., and E. A. M. Koutsoukos, 2001, Orbital cyclicity in a Turonian sequency of the Cotinguiba Formatio, Sergipe Basin, NE Brazil: Cretaceous Research, **22**, 529-548.

Desrues, J., G. Viggiani, and P. Besuelle, 2006, Advances in X-ray tomography for geomaterials: Presented at International Workshop on X-ray CT for Geomaterials.

Eberhart-Phillips, D., D.-H. Han, and M. D. Zoback, 1989, Empirical relationships among seismic velocity, effective pressure, porosity and clay content in sandstone: Geophysics, **54**, 82-89.

Eiken, O., and R. Tøndel, 2005, Sensitivity of time-lapse seismic data to pore pressure changes: Is quantification possible?: The Leading Edge, **24**, 1250-1254.

Eastwood, J., P. Lebel, A. Dilay, and S. Blakeslee, 1994, Seismic monitoring of steam-based recovery of bitumen: The Leading Edge, **13**, 242–251.

Furre, A. K., A. S. Anderson, A. S. Moen, and R. K. Tonnessen, 2009, Deriving effects of pressure depletion on elastic framework moduli from sonic logs: Geophysical Prospecting, **58**, 1-11.

Gabriels, P. W., N. A. Horvei, J. K. Koster, A. Onstein, A. Geo, and R. Staples, 1999, Time lapse seismic monitoring of the Draugen Field: Presented at SEG Annual International Meeting, Expanded Abstracts.

Gassmann, F., 1951, Uber die Elastizitat poroser Medien: Verteljahrsschrift der Naturforschenden Gesellschaft in Zurich, **96**, 1-23.

Gommesen, L., I. L. Fabricius, T. Mukerji, G. Mavko, and J. M. Pedersen, 2007, Elastic behaviour of North Sea chalk: A well-log study: Geophysical Prospecting, **55**, 307-322.

Greaves, R. J., and T. J. Fulp, 1987, Three-dimensional seismic monitoring of an enhanced oil recovery process: Geophysics, **52**, 1175–1187.

Grochau, M., and B. Gurevich, 2007a, Effect of core damage on elastic properties for time-lapse interpretation, offshore Brazil: Presented at Annual Rock Physics Workshop.

—, 2007b, Investigation of core data reliability to support time-lapse interpretation in Campos Basin, Brazil: Presented at SEG Annual International Meeting ***(Award of Merit: Best student paper in 2007)***.

—, 2008a, Investigation of core data reliability to support time-lapse interpretation in Campos Basin, Brazil: Geophysics, **73**, E59-E65.

—, 2008b, Testing Gassmann fluid substitution using sonic logs and core measurements in a sandstone reservoir: Presented at EAGE Conference & Exhibition.

—, 2009a, Testing Gassmann fluid substitution: sonic logs versus ultrasonic core measurements: Geophysical Prospecting, **57**, 75-79.

—, 2009b, Effect of net to gross on time-lapse seismic response in Campos Basin, Brazil: Accepted for SBGf International Conference.

Grochau, M., E. Campos, T. Muller, B. Clennell, and B. Gurevich, 2009, Using CT images to improve rock physics calibrations and stratigraphic analysis: an example from Campos Basin, Brazil: Accepted for EGU International Conference.

Gurevich, B., 2004, A simple derivation of the effective stress coefficient for seismic velocities in porous rocks: Geophysics, **69**, 393-397.

Hannah, T., L. R. Bentley, and E. S. Krebes, 2005, Monitoring fluid injection in a carbonate pool using time-lapse analysis: Rainbow Lake case study: The Leading Edge, **24**, 530-534.

Hansen, H. J., L. Gommesen, and Y. El Ouair, 2006, Using RFT data for elastic rock properties' dependency on pore pressure in 4D quantitative analysis: Presented at EAGE meeting, Expanded Abstracts.

Harris, J. M., R. T. Langan, T. Fasnacht, D. Melton, B. Smith, J. Sinton, and H. Tan, 1996, Experimental verification of seismic monitoring of CO2 injection in carbonate reservoirs: Presented at SEG Annual International Meeting, Expanded Abstracts. 1870–1872.

Hatchell, P., and S. Bourne, 2005, Rocks under strain: Strain-induced time-lapse time shifts are observed for depleting reservoirs: The Leading Edge, **24**, 1222-1225.

Holt, R. M., M. Brignoli, and C. J. Kenter, 2000, Core quality: Quantification of coring-induced rock alteration: International Journal of Rock Mechanics and Mining Sciences, **37**, 889-907.

Holt, R. M., O. M. Nes, and E. Fjaer, 2005, In-situ stress dependence of wave velocities in reservoir and overburden rocks: The Leading Edge, **24**, 1268-1274.

Jenkins, S. D., M. W. Waite, and M. F. Bee, 1997, Time-lapse monitoring of the Duri steamflood: A pilot and case study: The Leading Edge, **16**, 1267–1273.

Johnstad, S. E., R. H. Seymour, and P. J. Smith, 1995, Seismic reservoir monitoring over the Oseberg field during the period 1989–1992: First Break, **13**, 169-183.

Johnston, D., J. Shyeh, and J. Eastwood, 1999, Interpretation and modeling of time-lapse seismic data: Lena Field, Gulf of Mexico: Presented at SEG Annual International Meeting, Expanded Abstracts.

Kahraman, S., 2007, The correlations between the saturated and dry P-wave velocity of rocks: Ultrasonics, **46**, 341-348.

Landro, M., 2001, Discrimination between pressure and fluid saturation changes from time-lapse seismic data: Geophysics, **66**, 836-844.

Landro, M., 2008, Source strength variations and 4D seismic: Presented at SEG Annual International Meeting, Expanded Abstract.

Lumley, D., 1995a, 4-D seismic monitoring of an active steamflood: Presented at SEG Annual International Meeting, Expanded Abstract, 203–206.

—, 1995b, Seismic time-lapse monitoring of subsurface fluid flow: Ph.D. Thesis, Stanford University.

Lumley, D., 2001, Time-lapse seismic reservoir monitoring: Geophysics, **66**, 50-53.

—, 2004, Business and technology challenges for 4D seismic reservoir monitoring: The Leading Edge, **23**, 1166-1168.

Lumley, D., R.A. Behrens, and Z. Wang, 1997, Assessing the technical risk of a 4D seismic project: The Leading Edge, **16**, 1287-1291.

Lumley, D., S. Cole, M. Meadows, A. Tura, B. Hottman, B. Cornish, M. Curtis, and N. Maerefat, 2000, A risk analysis spreadsheet for both time-lapse VSP and 4D seismic reservoir monitoring: Presented at SEG Annual International Meeting, Expanded Abstracts.

MacBeth, C., K. Stephen, and A. Gardiner, 2008, The impact of sub-seismic shale layers on the reservoir's stress sensitivity: Presented at SEG Annual International Meeting, Expanded Abstracts.

Mavko, G., and D. Jizba, 1991, Estimating grain-scale fluid effects on velocity dispersion in rocks: Geophysics, **56**, 1940-1949.

Mavko, G., and T. Mukerji, 1998, Bounds on low-frequency seismic velocities in partially saturated rocks: Geophysics, **63**, no. 3, 918-924.

Mavko, G., T. Mukerji, and J. Dvorkin, 1998, The rock physics handbook - tools for seismic analysis in porous media: Cambridge University Press.

Meadows, M., D. Adams, R. Wright, A. Tura, S. Cole, and D. Lumley, 2005, Rock physics analysis for time-lapse seismic at Schiehallion field, North Sea: Geophysical Prospecting, **53**, 205-213.

Mees, F., R. Swennen, M. Van Geet, and P. Jacobs, 2003, Applications of X-ray computed tomography in the geosciences: Geological Society London Special Publications, **215**, 1-6.

Meunier, J., and F. Huguet, 1998, Cere-la-Ronde: A laboratory for time-lapse seismic monitoring in the Paris Basin: The Leading Edge, **17**, 1388, 1390, 1392–1394.

Moore, D. M., and R. C. J. Reynolds, 1997, X-Ray diffraction and the identification and analysis of clay mineral: Oxford University Press.

Murphy, W. F. I., J. N. Roberts, D. Yale, and K. W. Winkler, 1984, Centimeter scale heterogeneities and microstratification in sedimentary rocks: Geophysical Research Letters, **11**, 697-700.

Nes, O. M., M. H. Holtz, and E. Fjaer, 2002, The reliability of core data as input to seismic reservoir monitoring studies: Presented at SPE Annual International Meeting.

Nur, A., 1989, Four-dimensional seismology and (true) direct detection of hydrocarbons: The petrophysical basis: The Leading Edge, **8**, 30-36.

Nur, A., C. Tosaya, and D. Thanh, 1984, Seismic monitoring of thermal enhanced oil recovery processes: Presented at SEG Annual International Meeting, Expanded Abstracts.

Oldenziel, T., 2003, Time-lapse seismic within reservoir engineering: Delft University of Technology.

Pickering, S., 2006, Time-lapse seismic technology - Past, Present and Future: E&P Magazine, Hart Energy Publishing.

Pullin, N., L. Matthews, and K. Hirsche, 1987, Techniques applied to obtain very high resolution three-dimensional seismic imaging at an Athabasca tar sands thermal pilot: The Leading Edge, **6**, 10–15.

Rothwell, R. G., and F. R. Rack, 2006, New techniques in sediment core analysis: an introduction: Geological Society London Special Publications, **267**, 1-29.

Rutledal, H., J. Helgesen, and H. Buran, 2003, 4D elastic inversion helps locate in-fill wells at Oseberg field: First Break, **21**, 39-43.

Sayers, C. M., 2007, Asymmetry in the time-lapse seismic response to injection and depletion: Geophysical Prospecting, **55**, 699-705.

Shapiro, S. A., 2003, Elastic piezosensitivity of porous and fractured rocks: Geophysics, **68**, 482-486.

Sheriff, R. E., and L.P. Geldart, 1995, Exploration seismology: Cambridge University Press.

Smith, M., A. Gerhardt, L. Bourdon, and B. Mee, 2007, Using 4D seismic data to understand production-related changes in Enfield, NWS Australia: Presented at ASEG, Expanded Abstracts.

Smith, M., A. Gerhardt, B. Mee, T. Ridsdill-Smith, A. Wulff, and L. Bourdon, 2008, The Benefits of Early 4D Seismic Monitoring to Understand Production Related Effects at Enfield, North West Shelf, Australia: Presented at SEG Expanded Abstracts, Expanded Abstracts.

Smith, P. J., J. I. Berg, F. Verhelst, and J. Helgesen, 2001, 4-D seismic in a complex fluvial reservoir: The Snorre feasibility study: The Leading Edge, **20**, 270-276.

Sonneland, L., H. H. Veire, B. Raymond, C. Signer, L. Pedersen, S. Ryan, and C. Sayers, 1997, Seismic reservoir monitoring on Gullfaks: The Leading Edge, **16**, 1247-1252.

Staples, R., J. Ita, R. Burrell, and R. Nash, 2007, Monitoring pressure depletion and improving geomechanical models of the Shearwater Field using 4D seismic: The Leading Edge, **26**, 636-642.

Staples, R., J. Stammeijer, S. Jones, J. Brain, F. Smith, and P. Hatchell, 2006, Time-Lapse (4D) Seismic Monitoring - Expanding Applications: Presented at CSPG - CSEG - CWLS Convention.

Tura, A., T. Barker, P. Cattermole, C. Collins, J. Davis, and P. Hatchell, 2005, Monitoring primary depletion reservoirs using amplitudes and time shifts from high-repeat seismic survey: The Leading Edge, **24**, 1214-1221.

Veire, H. H., S. B. Reymond, C. Signer, P. O. Tennebo, and L. Sonneland, 1998, Estimation of reservoir fluid volumes through 4D seismic analysis on Gullfaks: Presented at SEG Expanded Abstracts, Expanded Abstracts.

Waal, H., and R. Calvert, 2003, Overview of global 4D seismic implementation strategy: Petroleum Geoscience, **9**, 1-6.

Walls, J. D., and M. B. Carr, 2001, The use of fluid substitution modeling for correction of mud filtrate invasion in sandstone reservoirs: Presented at SEG Annual International Meeting, Expanded Abstract, 385-387.

Wang, Z., 2000, The Gassmann equation revisited: Comparing laboratory data with Gassmann's predictions: Seismic and Acoustic Velocities in Reservoir Rocks - SEG - Recent Developments.

Wang, Z., M.L. Batzle, and A.M. Nur, 1990, Effect of different pore fluids on seismic velocities in rocks: Canadian Journal of Exploration Geophysics, **26**, no. 1, 2, 104-112.

Watts, G., D. Jizba, D. Gawith, and P. Gutteridge, 1996, Reservoir monitoring of the Magnus field through 4-D time-lapse seismic analysis: Petroleum Geoscience, **2**, 361-372.

Weisenborn, T., and P. Hague, 2005, Time-lapse seismic in Gannet A: One more lead firmly integrated: The Leading Edge, **24**, 80-85.

Wellington, S. L., and H. J. Vinegar, 1987, X-ray computerized tomography: Journal of Petroleum Technology: Journal of Petroleum Technology, **39**, 885-898.

Winkler, K. W., 1986, Estimates of velocity dispersion between seismic and ultrasonic frequencies: Geophysics, **51**, 183-189.

APPENDIX A – Papers related with time-lapse (4D) studies

Author	Publication	Year	Title
Aanonsen	SPE International	2003	Effect of Scale Dependent Data Correlations in an Integrated History Matching Loop Combining Production Data and 4D Seismic Data
Abubakar, A.	SEG Expanded Abstracts	2001	A feasibility study on nonlinear inversion of time-lapse seismic data
Acuna, Catalina	SEG Expanded Abstracts	2001	Time-lapse multicomponent seismic characterization of Glorieta-Paddock carbonate reservoir at Vacuum Field -New Mexico
Akintunde, Olusoga M.	SEG Expanded Abstracts	2004	Cross-well seismic monitoring of Coal Bed Methane (CBM) production: A case study from the Powder River Basin of Wyoming
Al-Ismaili, I	SEG Expanded Abstracts	2004	Matching time-lapse seismic data using neural networks
Almaskeri, Y.	SEG Expanded Abstracts	2005	Location and evaluation of flow barriers using 4D seismic
Al-Mazroey, M.	SEG Expanded Abstracts	2002	Identifying non-linear time-lapse wavefield perturbations using predictability and spectral coherency
Al-Mazroey, M.	SEG Expanded Abstracts	2002	Identifying production zones using time-lapse coherency
Al-Naamani, A.	SEG Expanded Abstracts	2003	Constraining the reservoir model of a turbidite reservoir using production and 4D seismic
Al-Naamani, A.	SEG Expanded Abstracts	2002	Joint interpretation of the time-lapse P-P and P-S response of a thin-bed reservoir
Al-Najjar, Nazih	SPE International	1999	4D Seismic Modelling of the Statfjord Field: Initial Results
Al-Najjar, Nazih	SEG Expanded Abstracts	1999	Statfjord field — Time lapse seismic interpretation using a 4-D earth model
Altan, Suat	SEG Expanded Abstracts	1997	Time-lapse seismic monitoring: Repeatability processing tests
Altan, Suat	SEG Expanded Abstracts	2001	Schiehallion 4D: From time-lapse repeatability study to reservoir monitoring
Altan, Suat	SEG Expanded Abstracts	1999	Schiehallion: A 3-D time - lapse processing case history
Anderson, Roger N.	The Leading Edge	1998	4-D seismic reservoir simulation in a South Timbalier 295 turbidite reservoir
Anderson, Roger N.	SEG Expanded Abstracts	1997	4D time-lapse seismic monitoring in the South Timbalier 295 field, Gulf of Mexico
Angerer, Erika	SEG Expanded Abstracts	2000	Time-lapse seismic changes in a CO2 injection process in a fractured reservoir
Artola, Fredy A.V.	Journal of Applied Geophysics	2005	Sensitivity analysis of Gassmann's fluid substitution equations: Some implications in feasibility studies of time-lapse seismic reservoir monitoring
Arts, R.	Energy, Volume 29	2004	Monitoring of CO2 injected at Sleipner using time-lapse seismic data
Ashbaugh, James P.	SEG Expanded Abstracts	1999	Dynamic reservoir characterization of the ST295 field (offshore Louisiana): Reservoir simulation, acoustic modeling, and time-lapse seismic refines geologic model and illuminates dynamic behavior

Bachrach, Ran	SEG Expanded Abstracts	2004	Joint estimation of porosity and saturation and of effective stress and saturation for 3D and 4D seismic reservoir characterization using stochastic rock physics modeling and Bayesian inversion
Bair, J. F.	SEG Expanded Abstracts	1999	Time-lapse imaging of steam and heat movement in the Cymric 36W Cyclic Steam Pilot using crosswell seismology
Bard, Karen C.	SPE International	1999	Tracking Miscible Processes in the Subsurface Utilizing Time Lapse Shear Wave Seismic Data
Barker, Ron	The Leading Edge	1998	The application of time-lapse electrical tomography in groundwater studies
Barkved, Olav I.	SEG Expanded Abstracts	2004	Continuous seismic monitoring
Beasley, Craig J.	The Leading Edge	1997	Repeatability of 3-D ocean-bottom cable seismic surveys
Behrens, Ronald	SPE International	2001	4D Seismic Monitoring of Water Influx at Bay Marchand: The Practical Use of 4D in an Imperfect World
Behrens, Ronald	SPE International	2002	4D Seismic Monitoring of Water Influx at Bay Marchand: The Practical Use of 4D in an Imperfect World
Benson	SPE International	2000	Time-Lapse Seismic Monitoring and Dynamic Reservoir Characterization, Central Vacuum Unit, Lea County, New Mexico
Benson	SPE International	1998	Time-Lapse Seismic Monitoring and Dynamic Reservoir Characterization, Central Vacuum Unit, Lea County, New Mexico
Berkhout, A. J.	Geophysics	2001	Seismic imaging beyond depth migration
Bertrand, A.	SEG Expanded Abstracts	2002	Seawater velocity variations and their impact in permanent installations for reservoir monitoring
Bertrand, A.	SEG Expanded Abstracts	2004	Uncertainties in the 4D seismic signature due to seawater velocity variations
Bianchi, T.	SEG Expanded Abstracts	2004	Acquisition and processing challenges in continuous active reservoir monitoring
Birken, Ralf	Journal of Applied Geophysics	2000	Use of four-dimensional ground penetrating radar and advanced visualization methods to determine subsurface fluid migration
Bogan, Catherine	SPE International	2003	Building Reservoir Models Based on 4D Seismic & Well Data in Gulf of Mexico Oil Fields
Boyd-Gorst, John	The Leading Edge	2001	4-D time lapse reservoir monitoring of Nelson Field, Central North Sea: Successful use of an integrated rock physics model to predict and track reservoir production
Brevik, Ivar	SEG Expanded Abstracts	1999	Rock model based inversion of saturation and pressure changes from time lapse seismic data
Brinks, John	SPE - Colorado School of Mines	2001	Geologic Sequestration: Modeling and Monitoring Injected CO2
Brown, Leo T.	SEG Expanded Abstracts	2002	Integration of rock physics, reservoir simulation, and time-lapse seismic data for reservoir characterization at Weyburn Field, Saskatchewan

Burkhart, Tucker	Geophysics	2000	Time-lapse (4-D) seismic monitoring of primary production of turbidite reservoirs at South Timbalier Block 295, offshore Louisiana, Gulf of Mexico
Burkhart, Tucker	SEG Expanded Abstracts	1997	Time-lapse seismic monitoring of the South Timbalier 295 field, offshore Louisiana
Burns, Scott	SPE International	2002	Facts from Fiction : 4D Seismic Model-Based Interpretation
Burtz, Olivier	SEG Expanded Abstracts	2002	Model-based calibration of band-limited impedance data: Hoover Field
Cabrera-Garzón, Raúl	SEG Expanded Abstracts	2000	Time lapse shear wave anisotropy: A tool for dynamic reservoir characterization at Vacuum Field, New Mexico
Cambois,	SEG Expanded Abstracts	2000	AVO inversion and elastic impedance
Capello de P., Maria Angela	The Leading Edge	1997	Rock physics in seismic monitoring
Castagna, John	SEG Expanded Abstracts	1999	Rock physics basis for time lapse seismic monitoring
Chazy, A.	SPE International	2005	4D Seismic and Through Tubing Drilling and Completion Wells Extend Life on the Gullfaks Field
Chen, Sandy	SEG Expanded Abstracts	2003	Cold production footprints of heavy oil on time-lapse seismology: Lloydminster field, Alberta
Chen, Sandy	SEG Expanded Abstracts	2004	Do wormholes play a role in heavy oil cold production?
Christie, Philip A. F.	The Leading Edge	2000	An Introduction to this Special Section: Development and Production
Christie, Philip A. F.	SEG Expanded Abstracts	1999	Time-lapse measurements in reservoir management: A summary of the 1999 SEG D&P Forum
Christie, Philip A. F.	The Leading Edge	2000	Research and development for reservoir monitoring: A contractor's viewpoint
Christie, Philip A. F.	SEG Expanded Abstracts	1999	Research and development for reservoir monitoring: A contractor's viewpoint
Clifford, Peter J.	SPE International	2003	Integration of 4D Seismic Data into the Management of Oil Reservoirs with Horizontal Wells between Fluid Contacts
Cole, Steve	SEG Expanded Abstracts	2002	Pressure and saturation inversion of 4D seismic data by rock physics forward modeling
Coléou, Thierry	SEG Expanded Abstracts	2002	Multivariate geostatistical filtering of time-lapse seismic data for an improved 4-D signature
Cooper, Mike	SEG Expanded Abstracts	1999	Foinaven active reservoir management : Towed streamer and buried sea-bed detectors in deep water for 4D seismic
Crampin, Stuart	The Leading Edge	2003	Round Table—The new geophysics: Shear-wave splitting provides a window into the crack-critical rock mass
Crampin, Stuart	SEG Expanded Abstracts	2000	The potential of shear-wave splittng in a stress-sensitive compliant crust: A new understanding of pre-fracturing deformation from time-lapse studies
Cursino, Delson F.	SPE - Petrobras	2002	An Example of a Steam Drive Pilot Project Management With 3D Seismic Survey in Northeast Brazil

S.			
Dasgupta, Shiv N.	SEG Expanded Abstracts	2004	Reservoir monitoring with permanent borehole seismic sensors: Ghawar field arab-D reservoir
Davies, Paul	SEG Expanded Abstracts	1999	Non-linear cross-equalisaton of seismic surveys acquired with different bandwidths
Davis, Thomas L.	The Leading Edge	2003	Multicomponent seismic characterization and monitoring of the CO2 flood at Weyburn Filed, Saskatchewan
Davis, Thomas L.	SEG Expanded Abstracts	2003	The future of reservoir characterization
Davis, Thomas L.	SEG Expanded Abstracts	2001	Monitoring production processes by 4-D multicomponent seismic surveys at Vacuum Field, New Mexico
Davis, Thomas L.	SEG Expanded Abstracts	2004	Weyburn field seismic monitoring project
Day-Lewis, Frederick D.	Geophysics	2002	Time-lapse inversion of crosswell radar data
DeVault, Bryan	Geophysics	2002	Multicomponent AVO analysis, Vacuum field, New Mexico
Dewhurst, David N.	SEG Expanded Abstracts	2004	Impact of stress and sedimentary anisotropies on velocity anisotropy in shale
Dey, A.	SEG Expanded Abstracts	2004	A convolutional earth: Modeling, inversion and time-lapse considerations
DiFrancesco, Daniel J.	SEG Expanded Abstracts	2002	Time lapse gravity gradiometry for reservoir monitoring
Dillen, Menno	SEG Expanded Abstracts	2000	Convolution type interaction of time-lapse acoustic wave fields
Dong, Yannong	SPE - Society of Petroleum Engineers	2005	Quantitative Use of 4D Seismic Data for Reservoir Description
Dorrington, Kevin P.	SEG Expanded Abstracts	2002	A genetic algorithm/neural network approach to seismic attribute selection for well log prediction
Druzhinin, A.	SEG Expanded Abstracts	2001	Factorized ray tracing for time-lapse seismic reservoir monitoring
Dubucq, Dominique	SEG Expanded Abstracts	2003	Deep offshore seismic monitoring: The Girassol field, a West Africa textbook example
Duranti, Luca	SEG Expanded Abstracts	2000	Time-lapse analysis and detection of fluid changes at Vacuum field, New Mexico
Eastwood, John	SEG Expanded Abstracts	1998	Processing for robust time-lapse seismic analysis: Gulf of Mexico example, Lena Field
Ebrom, Dan	SEG Expanded Abstracts	2002	Numerical modeling of PS moveout as a function of pore pressure
Ebrom, Dan	SEG Expanded Abstracts	1999	Offshore multicomponent seismics for time-lapse observations
Ecker, Christine	SEG Expanded Abstracts	1999	Estimating separate steam thickness and temperature maps from 4D seismic data: An example from San Joaquin Valley, California
Eiken, Ola	The Leading Edge	2005	Sensitivity of time-lapse seismic data to pore pressure changes: Is quantification possible?

Eiken, Ola	SEG Expanded Abstracts	2002	Repeated seismic surveys from the Norwegian Sea using new streamer technology
Eiken, Ola	SEG Expanded Abstracts	2004	Gravimetric monitoring of gas production from the Troll field
Elde, Rigmor M.	SEG Expanded Abstracts	2000	Troll West — Time lapse processing and analysis
Elde, Rigmor M.	SPE International	2000	Troll West - Reservoir Monitoring by 4D Seismic
Ellison, Shelley J.	Geophysics	2004	Modeling offset-dependent reflectivity for time-lapse monitoring of water-flood production in thin-layered reservoirs
Ellison, Shelley J.	SEG Expanded Abstracts	2001	Modeling offset-dependent reflectivity for time-lapse monitoring of water flood production in thin-layered reservoirs
Erdemir, Cemal	SEG Expanded Abstracts	2002	Multi-mode, multi-component time-lapse imaging at Lost Hills
Fagervik, K.	SEG Expanded Abstracts	2001	A method for performing history matching of reservoir flow models using 4D seismic
Falcone, Gioia	SPE International	2004	Petroelastic Modelling as Key Element of 4D History Matching: A Field Example
Fanchi, John R.	The Leading Edge	2001	Time-lapse seismic monitoring in reservoir management
Fanchi, John R.	Journal of Petroleum Science and Engineering	2001	Integrating forward modeling into reservoir simulation
Fanchi, John R.	SPE - Colorado School of Mines	2001	Feasibility of Monitoring CO2 Sequestration in a Mature Oil Field Using Time-Lapse Seismic Analysis
Floricich, Mariano	SEG Expanded Abstracts	2005	An engineering approach for separating pressure and saturation using 4D seismic: Application to a Jurassic reservoir in the UK North Sea
Floricich, Mariano	SEG Expanded Abstracts	2006	Determination of a seismic and engineering consistent petro-elastic model for time-lapse seismic studies: Application to the Schiehallion Field
Floricich, Mariano	EAGE Expanded Abstracts	2006	A new technique for pressure - saturation separation from time-lapse seismic: Schiehallion Case Study
Fuh, Shi-Chie	SEG Expanded Abstracts	2004	Comprehensive analysis of hydrocarbon entrapment of the Hsinying gas field and its application to hydrocarbon exploration
Gabriels, Pieter W.	SEG Expanded Abstracts	1999	Time lapse seismic monitoring of the Draugen field
Gaiser, James E.	SEG Expanded Abstracts	2004	Vector-fidelity benefits of buried OBC detectors at Teal South
Gaiser, James E.	The Leading Edge	2001	Multicomponent technology: the players, problems, applications, and trends: Summary of the workshop sessions
Gaiser, James E.	SEG Expanded Abstracts	2002	PS-wave azimuthal anisotropy: benefits for fractured-reservoir management
Galikeev, Tagir	SEG Expanded Abstracts	2003	Reservoir modeling of a thin carbonate reservoir using geostatistics and 4-D seismic attributes,

			Weyburn field, Saskatchewan, Canada
Galikeev, Tagir	SEG Expanded Abstracts	2002	Reservoir-scale velocity modelling — An integrated part of reservoir characterization
Gan, Lideng	SEG Expanded Abstracts	2004	Applying 4D seismic to monitoring water drive reservoir
Gasperikova, Erika	SEG Expanded Abstracts	2004	A feasibility study of geophysical methods for monitoring geologic CO2 sequestration
Geo, A. O. A.	SEG Expanded Abstracts	1999	Time-lapse seismic - A reservoir engineer's perspective
Gesbert, Stéphane	Geophysics	2002	From acquisition footprints to true amplitude
Gibson, Garth	The Leading Edge	2004	Business Bottom Line—Optimizing performance: Object storage for seismic applications
Gilbert, Fabien	SEG Expanded Abstracts	2002	Downscaling a seismic scale acoustic impedance model with stochastic modeling for uncertainty analysis
Gluck, S.	SEG Expanded Abstracts	2000	Time-lapse impedance inversion of post-stack seismic data
Gonzalez, Ezequiel F.	SEG Expanded Abstracts	1999	Discriminating seismic signatures of steam injection from lithology variations: Feasibility study in a Venezuela heavy oil reservoir
Gosselin	SPE International	2003	History matching Using Time-lapse Seismic (HUTS)
Goto, Richard	SEG Expanded Abstracts	2004	Steered-streamer 4D case study over the Norne field
Gouveia, Wences P.	The Leading Edge	2004	Jotun 4D: Characterization of fluid contact movement from time-lapse seismic and production logging tool data
Gouveia, Wences P.	SEG Expanded Abstracts	2004	Remarks on the estimation of time-lapse elastic properties: The case for the Jotun Field, Norway
Grannemann, W. W.	Geophysics	1995	FIELD TESTING SEISMIC INSTRUMENTS
Grechka, Vladimir	SEG Expanded Abstracts	2002	Feasibility of seismic characterization of multiple fracture sets
Grêt, A.	SEG Expanded Abstracts	2002	Time lapse monitoring of acoustic emissions with Coda Wave interferometry
Groenenboom, Jeroen	Geophysics	1998	Monitoring the width of hydraulic fractures with acoustic waves
Groenenboom, Jeroen	Geophysics	2000	Monitoring hydraulic fracture growth: Laboratory experiments
Hall, Stephen A.	SEG Expanded Abstracts	2003	Time-lapse seismic analysis of pressure depletion in the Southern Gas Basin
Hall, Stephen A.	SEG Expanded Abstracts	2001	AVOA attribute analysis and cross-plotting for time-lapse monitoring of stress and saturation changes: Application to the Teal South 4D-4C dataset
Hall, Stephen A.	SEG Expanded Abstracts	2002	Time-lapse seismic monitoring of compaction and subsidence at Valhall through cross-matching and interpreted warping of 3D streamer and OBC data

Hannah T. Ng	The Leading Edge	2005	Monitoring fluid injection in a carbonate pool using time-lapse analysis: Rainbow Lake case study
Hanson, R.	SEG Expanded Abstracts	2000	4C seismic data and reservoir modeling at Alba Field, North Sea
Hare, Jennifer L.	Geophysics	1999	The 4-D microgravity method for waterflood surveillance: A model study for the Prudhoe Bay reservoir, Alaska
Harris, Jerry M.	Geophysics	1995	High-resolution crosswell imaging of a west Texas carbonate reservoir: Part 1—Project summary and interpretation
Harris, P. E.	SEG Expanded Abstracts	1998	Time-lapse processing: A North Sea case study
Harris, P. E.	SEG Expanded Abstracts	1999	Seismic resolution and uncertainty in time-lapse studies
Hatchell, P. J.	SEG Expanded Abstracts	2003	Whole earth 4D: Reservoir monitoring geomechanics
Haverl, M. C.	SPE International	2005	Integrated workflow for quantitative use of time-lapse seismic data in history matching: A North Sea field case
He, Bingshou	SEG Expanded Abstracts	2001	Theoretical analyse of time-lapse explosion method
He, Wei	SEG Expanded Abstracts	1998	Constructing 3-D reservoir model of a complex turbidite sand using time-lapse seismic and well data in the ST295 Field, Gulf of Mexico
Herawati, Ida	SEG Expanded Abstracts	2003	The use of time-lapse P-wave impedance inversion to monitor CO2 flood at Weyburn Field, Saskatchewan, Canada
Herron, Don	The Leading Edge	2004	An introduction—Gulf of Mexico
Hicks, Paul J. Jr.	SEG Expanded Abstracts	1997	Reservoir simulation in time-lapse (4D) seismic analysis
Hirsche, Keith	SEG Expanded Abstracts	1998	Time-lapse seismic monitoring of a SE Asian field — A case history
Hofmann, Ronny	SEG Expanded Abstracts	2004	Which effective pressure coefficient do you mean?
Hoover, A. R.	SEG Expanded Abstracts	1997	Reservoir and production analysis of the K40 sand, South Timbalier 295, offshore Louisiana, with comparison to time-lapse (4-D) seismic results
Houston, Louis M.	The Leading Edge	1998	Minimal-effort time-lapse seismic monitoring: Exploiting the relationship between acquisition and imaging in time-lapse data
Hoversten, G. Michael	SEG Expanded Abstracts	2002	Fluid saturation and pressure prediction in a multi-component reservoir by combined seismic and electromagnetic imaging
Howie, John M.	The Leading Edge	2005	Developing the long-term seismic strategy for Azeri-Chirag-Gunashli, South Caspian Sea, Azerbaijan
Howie, John M.	SEG Expanded Abstracts	2004	Long-term seismic strategy for a major asset: Azeri-Chirag-Gunashli, South Caspian Sea, Azerbaijan
Huang, Xuri	The Leading Edge	2001	Integration of time-lapse seismic and production data in a Gulf of Mexico gas field

Huang, Xuri	The Leading Edge	2001	Integrating time-lapse seismic with production data: A tool for reservoir engineering
Huang, Xuri	SEG Expanded Abstracts	1997	Production history matching with time lapse seismic data
Huang, Xuri	SEG Expanded Abstracts	2000	Constraining time-lapse seismic analysis with production data
Huang, Xuri	SEG Expanded Abstracts	1999	Reprocessing of time-lapse seismic data improves seismic history matching
Huang, Xuri	SEG Expanded Abstracts	1999	Integration of production and time-lapse seismic data
Huang, Xuri	The Leading Edge	1998	Improving production history matching using time-lapse seismic data
Jenkins, S. D.	The Leading Edge	1997	Time-lapse monitoring of the Duri steamflood: A pilot and case study
Jin, Long	SEG Expanded Abstracts	2004	New quality control method for time-lapse seismic processing
Johnston, David H.	The Leading Edge	2000	Using legacy seismic data in an integrated time-lapse study: Lena Field, Gulf of Mexico
Johnston, David H.	The Leading Edge	1998	Time-lapse seismic analysis of Fulmar Field
Johnston, David H.	SEG Expanded Abstracts	1997	Time-lapse seismic analysis of the North Sea Fulmar Field
Johnston, David H.	SEG Expanded Abstracts	1999	Interpretation and modeling of time-lapse seismic data: Lena Field, Gulf of Mexico
Johnston, David H.	SEG Expanded Abstracts	2003	Integration of time-lapse seismic and production logging data: Jotun Field, Norway
Johnston, David H.	SEG Expanded Abstracts	2002	Time-lapse seismic analysis at Irong Barat: Malay Basin
Jones, Ian F.	SEG Expanded Abstracts	2002	4D illumination and elastic modeling
Jones, Ian F.	SEG Expanded Abstracts	2002	Continuous high resolution velocity as a 4D attribute
Julien, P.	SEG Expanded Abstracts	2002	The importance of pre-stack massive seismic modeling for AVO calibration and seismic reservoir characterization
Kaldy, W. John	SEG Expanded Abstracts	2004	Amberjack 4D seismic processing — A Gulf of Mexico case history
Kelly, Michael C.	SEG Expanded Abstracts	2002	Prediction of bed geometry, net and gross reservoir thickness
Kendall, Robert R.	SEG Expanded Abstracts	2003	9C, 4D seismic processing for the weyburn CO2 flood, Saskatchewan, Canada
Key, Scott C.	The Leading Edge	1998	Adding value to reservoir management with seismic monitoring technologies
Khazanehdari, J.	SEG Expanded Abstracts	2005	Quantitative time-lapse seismic analysis through prestack inversion and rock physics
Khoshood, A.	The Leading Edge	2005	Effect of reservoir properties changes on time-lapse synthetics for well 31 in Gachsaran Field, Iran
King, Michael S.	Geophysics	2005	Rock-physics developments in seismic exploration: A personal 50-year perspective
Kjelstadli	SPE International	2005	Quantitative History Match of 4D Seismic Response and Production Data in the Valhall Field
Korneev, Valeri A.	Geophysics	2004	Seismic low-frequency effects in monitoring fluid-saturated reservoirs
Koster, Klaas	The Leading Edge	2000	Time-lapse seismic surveys in the North Sea and their business impact
Kragh, Ed	The Leading Edge	2002	Seismic repeatability, normalized rms, and predictability

Kragh, Ed	SEG Expanded Abstracts	2001	Seismic Repeatability, Normalized RMS and Predictability
Kretz, Vicent	SPE International	2004	Fluid Front History Matching Using 4D Seismic and Streamline Simulation
Kretz, Vicent	SPE International	2002	An Integrated Reservoir Characterization Study Matching Production Data and 4D Seismic
Kretz, Vicent	SPE International	2004	An Integrated Reservoir Characterization Study Matching Production Data and 4D Seismic
Kristiansen, Pål	SEG Expanded Abstracts	2000	Foinaven 4D: Processing and analysis of two designer 4Ds
Kvam, Øyvind	Geophysics	2005	Pore-pressure detection sensitivities tested with time-lapse seismic data
Kvam, Øyvind	SEG Expanded Abstracts	2003	Lithological inversion of time-lapse seismic data using reflectivity ratios
Landa, Jorge L.	SEG Expanded Abstracts	1999	Integration of 4D seismic and production data for reservoir parameter estimation
Landa, Jorge L.	SPE International	1997	A Procedure to Integrate Well Test Data, Reservoir Performance History and 4-D Seismic Information into a Reservoir Description
Landrø, Martin	Journal of Petroleum Science and Engineering	2001	Time-lapse seismic as a complementary tool for in-fill drilling
Landrø, Martin	Geophysics	2001	Discrimination between pressure and fluid saturation changes from time-lapse seismic data
Landrø, Martin	Geophysics	2004	Quantitative estimation of compaction and velocity changes using 4D impedance and traveltime changes
Landrø, Martin	Geophysics	2003	Discrimination between pressure and fluid saturation changes from marine multicomponent time-lapse seismic data
Landrø, Martin	Geophysics	1999	Repeatability issues of 3-D VSP data
Landrø, Martin	SEG Expanded Abstracts	2004	Vp-Vs ratio versus effective pressure and rock consolidation — a comparison between rock models and time-lapse AVO studies
Landrø, Martin	SEG Expanded Abstracts	1999	Discrimination between pressure and fluid saturation changes from time lapse seismic data
Landrø, Martin	SEG Expanded Abstracts	2004	Time lapse refraction seismic - a tool for monitoring carbonate fields?
Langan, R. T.	SEG Expanded Abstracts	2000	Time-lapse reflection and velocity imaging in the Lost Hills Steam Pilot using crosswell seismology
Langlais	SPE International	2005	4D Monitoring of an Underground Gas Storage Case Using an Integrated History-Matching Technique
Lankston, Robert W.	SEG Expanded Abstracts	1998	Propagating uncertainty in fluid replacement modeling: A tool for time lapse seismic survey planning and amplitude variation with angle (ava) analysis
Lazaratos, Spyros K.	The Leading Edge	1997	Crosswell seismic imaging of reservoir changes caused by CO2 injection
Leary, P. C.	SEG Expanded Abstracts	1998	Wide-angle scattering detection of a thermal event in time-lapse borehole seismics
Lecerf, D.	SEG Expanded Abstracts	2004	High resolution processing for time-lapse seismic

Lecomte, Isabelle	SEG Expanded Abstracts	2003	Simulated prestack local imaging: A robust and efficient interpretation tool to control illumination, resolution, and time-lapse properties of reservoirs
Lee, Doo Sung	Geophysics	1995	Time-lapse crosswell seismic tomography to characterize flow structure in the reservoir during the thermal stimulation
Lefeuvre, Frédéric	SEG Expanded Abstracts	2003	Improved reservoir understanding through rapid and effective 4D: Girassol field, Angola, West Africa
Leggott, Richard J.	SEG Expanded Abstracts	1999	Co-location of 4D seismic data in the presence of navigational and timing errors
Leggott, Richard J.	SEG Expanded Abstracts	1999	Accurate positioning of seismic surveys in space and time for improved 4-D sensitivity
Leslie, Damian M.	SEG Expanded Abstracts	2001	Focusing time-lapse seismic data using time-reversed acoustics
Li, Guoping	The Leading Edge	2001	Effective processing of nonrepeatable 4-D seismic data to monitor heavy oil SAGD steam flood at East Senlac, Saskatchewan, Canada
Li, Guoping	The Leading Edge	2003	4D seismic monitoring of CO2 flood in a thin fractured carbonate reservoir
Li, Jingye	SEG Expanded Abstracts	2004	Study on time-lapse seismic AVO of fine layering porous unconsolidated reservoir
Li, X.-P.	SEG Expanded Abstracts	2004	Oseberg 4D re-processing — a case history of seismic repeatability analysis
Liner, Christopher L.	The Leading Edge	1997	On the history and culture of geophysics, and science in general
Lines, Laurence R.	SEG Expanded Abstracts	2002	Seismic monitoring of "hot" and "cold" heavy oil Production
Litvak	SPE International	2005	Uncertainty Estimation in Production Predictions Constrained by Production History and Time-Lapse Seismic in a GOM Oil Field
Liu, Enru	The Leading Edge	2004	Modeling seismic wave propagation during fluid injection in a fractured network: Effects of pore fluid pressure on time-lapse seismic signatures
Liu, Enru	SEG Expanded Abstracts	2000	Seismic detection of fluid saturation in aligned fractures
Liu, Wei	SEG Expanded Abstracts	1998	Time-lapse crosswell seismic imaging of the Athabasca Tar Sands at Steepbank
Lou, Min	SEG Expanded Abstracts	2000	Modeling study of marine multi-component seismic data in anisotropic fractured media by a Fourier method
Lucet, Nathalie	SEG Expanded Abstracts	2001	4D data interpretation through seismic facies analysis
Lumley, David E.	The Leading Edge	2004	Business and technology challenges for 4D seismic reservoir monitoring
Lumley, David E.	Geophysics	2001	Time-lapse seismic reservoir monitoring
Lumley, David E.	The Leading Edge	2002	Synergies in time-lapse seismic, medical, and space imaging
Lumley, David E.	SEG Expanded Abstracts	1997	Assessing the technical risk of a 4D seismic project
Lumley, David E.	SEG Expanded Abstracts	1999	Meren Field, Nigeria: A 4D seismic case study

Lumley, David E.	SEG Expanded Abstracts	2000	A risk analysis spreadsheet for both time-lapse VSP and 4D seismic reservoir monitoring
Lumley, David E.	SEG Expanded Abstracts	1997	Practical geophysical issues of 4D seismic reservoir monitoring
Lumley, David E.	SEG Expanded Abstracts	2003	4D seismic data processing issues and examples
Lumley, David E.	SEG Expanded Abstracts	2003	Estimation of reservoir pressure and saturations by crossplot inversion of 4D seismic attributes
Lumley, David E.	SPE International	1998	Practical Issues of 4D Seismic Reservoir Monitoring: What an Engineer Needs to Know
Lygren, M.	SEG Expanded Abstracts	2002	History matching of CO2 flow models using seismic modeling and time-lapse data
Maaø, Frank	SEG Expanded Abstracts	2000	Prestack calibration of time-lapse seismic data
MacBeth, Colin	SEG Expanded Abstracts	2002	4D seismic signatures of OWC movement on the Nelson field — Modeling and interpretation
MacBeth, Colin	SEG Expanded Abstracts	2004	Going quantitative with 4D seismic analysis
MacBeth, Colin	SEG Expanded Abstracts	2004	Deconvolving permeability from time-lapsed seismic data
MacKay, Scott	The Leading Edge	2003	The impact of water-velocity variations on deepwater seismic data
Magesan, Mag	The Leading Edge	2005	Seismic processing for time-lapse study: Genesis Field, Gulf of Mexico
Malaver, Cristian	SEG Expanded Abstracts	2004	Statistical applications for quantitative reservoir characterization and monitoring at West Pearl Queen field, Lea County, New Mexico
Marschall	SPE International	2002	Some Aspects of 4-D Seismics for Reservoir Monitoring
Mathisen, Mark E.	Geophysics	1995	Time-lapse crosswell seismic tomogram interpretation: Implications for heavy oil reservoir characterization, thermal recovery process monitoring, and tomographic imaging technology
Matsushima, Jun	Journal of Volcanology and Geothermal Research	2004	Repeated seismic reflection measurements in the Kakkonda geothermal field
Maxwell, Shawn C.	The Leading Edge	2001	The role of passive microseismic monitoring in the instrumented oil field
McGillivray, Peter R.	SEG Expanded Abstracts	2004	Microseismic and time-lapse monitoring of a heavy oil extraction process at Peace River
McKenna, Jason	Journal of Contaminant Hydrology	2001	Time-lapse 3-D seismic imaging of shallow subsurface contaminant flow
McKenna, Jason	SEG Expanded Abstracts	2000	Repeatability of physical modelling time-lapse 3-D seismic data
Meadows, Mark A.	SEG Expanded Abstracts	2001	Enhancements to Landro's method for separating time-lapse pressure and saturation changes
Meadows, Mark A.	SEG Expanded Abstracts	2002	Rock physics analysis for time-lapse seismic at Schiehallion Field, North Sea
Meunier, Julien	The Leading Edge	1998	Céré-la-Ronde: A laboratory for time-lapse seismic monitoring in the Paris Basin
Meunier, Julien	SEG Expanded Abstracts	2003	Evaluation and handling of positioning differences in 4D seismic

Mezghani	SPE International	2004	History Matching and Quantitative Use of 4D Seismic Data for an Improved Reservoir Characterization
Michaud, Gwénola	SEG Expanded Abstracts	2001	Time-lapse borehole case study in vacuum field, New Mexico
Michaud, Gwénola	SEG Expanded Abstracts	2000	Time-lapse vertical seismic profile study in Vacuum Field, New Mexico
Mikkelsen	SPE International	2005	IMPROVED RESERVOIR MANAGEMENT THROUGH INTEGRATION OF 4D SEISMIC INTERPRETATION
Miller, Richard D.	SEG Expanded Abstracts	2004	4-D high-resolution seismic reflection monitoring of miscible CO2 injected into a carbonate reservoir in the Hall-Gurney Field, Russell County, Kansas
Minkoff, Susan E.	Geophysics	2004	Coupled geomechanics and flow simulation for time-lapse seismic modeling
Minkoff, Susan E.	SEG Expanded Abstracts	1999	Coupled geomechanics and flow simulation for time-lapse seismic modeling
Minkoff, Susan E.	SEG Expanded Abstracts	1998	Reservoir characterization via time-lapse prestack seismic in version
Mitra, Partha P.	SPE International	2003	4D Seismic in Mapping the Change in Fluid Phase in Carbonate: A Case Study
Moldoveanu, N.	SEG Expanded Abstracts	1996	Repeatability of the seismic experiments for 4D seismic in transition zone surveys
Nakagawa, Seiji	SEG Expanded Abstracts	2000	Effect of static shear stress on the scattering of elastic waves across fractures
Navarro, J.B.	SPE - Delta Are & Capillary Services Ltd	2005	Key High-Quality Technologies as Pilot for Hydrocarbon-Reserves Expansion
Nickel, M.	SEG Expanded Abstracts	1999	Non-rigid matching of migrated time-lapse seismic
Nickel, M.	SEG Expanded Abstracts	2001	New tools for 4D seismic analysis in carbonate reservoirs
Nivlet, Philippe	SEG Expanded Abstracts	2001	A new methodology to account for uncertainties in 4D seismic interpretation
Nolen-Hoeksema, Richard C.	Geophysics	1995	High-resolution crosswell imaging of a west Texas carbonate reservoir: Part 5—Core analysis
Nur, A.	SEG Expanded Abstracts	1997	Rock physics and 4D seismic for improved oil recovery
O'Brien, John	The Leading Edge	2004	Time-lapse VSP reservoir monitoring
O'Brien, John	SEG Expanded Abstracts	2004	Time-lapse 3-D VSP monitoring of a CO2 EOR Flood
O'Donovan, A. R.	SPE International	2000	Foinaven 4D Seismic - Dynamic Reservoir Parameters and Reservoir Management
Olden, Peter	The Leading Edge	2001	Modeling combined fluid and stress change effects in the seismic response of a producing hydrocarbon reservoir
P. L. A. Winthaegen	SEG Expanded Abstracts	2001	CFP-approach to time-lapse angle-dependent reflectivity analysis
Pacheco, Carlos	SEG Expanded Abstracts	2003	Time-lapse monitoring with multiply scattered waves
Pannett, Stephen	SPE International	2004	Constraining a Complex Gas-Water Dynamic Model Using 4D Seismic

Parr, R. S.	SEG Expanded Abstracts	2003	Andrew 4D reservoir surveillance
Parr, R. S.	SEG Expanded Abstracts	2000	Interpretation and integration of 4-D results into reservoir management, Schiehallion Field, UKCS
Pennington, Wayne D.	The Leading Edge	2001	Seismic time-lapse surprise at Teal South: That little neighbor reservoir is leaking!
Pennington, Wayne D.	SEG Expanded Abstracts	2000	"Do No Harm!" — Seismic petrophysical aspects of time — Lapse monitoring
Peterson, John E. Jr.	SEG Expanded Abstracts	1998	Moisture migration using high resolution time-lapse radar tomography
Phan, Vinh	SPE - Stanford University	1999	Determining Depth-Dependent Reservoir Properties Using Integrated Data Analysis
Phan, Vinh	SPE International	2002	Fluvial Channel Parameter Estimation Constrained to Static, Production, and 4D Seismic Data
Pisetski, V. B.	SEG Expanded Abstracts	2001	Dynamic fluid method of reservoir characterization. Last step of interpretation — estimation of the current fluid flow: Kogalym (Western Siberia) and Chagodaev (Tatarstan) fields' examples
Poggiagliolmi, Elio	SEG Expanded Abstracts	1998	Time-lapse seismic repeatability — A case study
Porter-Hirsche, Jan	SEG Expanded Abstracts	1998	Repeatability study of land data acquisition and processing for time lapse seismic
Pramanik, A. G.	SEG Expanded Abstracts	2002	Stratigraphic interpretation using post stack seismic inversion: Case histories from Indian basins
Raef, A. E.	The Leading Edge	2005	4D seismic to image a thin carbonate reservoir during a miscible CO2 flood: Hall-Gurney Field, Kansas, USA
Raef, A. E.	The Leading Edge	2004	4D seismic monitoring of the miscible CO2 flood of Hall-Gurney Field, Kansas, U.S.
Ribeiro, Christophe	SEG Expanded Abstracts	2004	A petroelastic-based approach to pressure and saturation estimation using 4D seismic
Ribeiro, Christophe	SEG Expanded Abstracts	2005	Inversion for reservoir pressure and saturation changes in the Foinaven field, UK
Ribeiro, N.	SPE International	2005	Challenges of the 4D Seismic in the Reservoir Management of Marlim Field, Campos Basin
Richardson, Sarah E.	SEG Expanded Abstracts	2002	Time-lapse imaging of CO2 injection into coalbed methane strata; a numerical modeling study
Rickett, James	Geophysics	2001	Cross-equalization data processing for time-lapse seismic reservoir monitoring: A case study from the Gulf of Mexico
Rickett, James	SEG Expanded Abstracts	1998	A cross-equalization processing flow for off-the-shelf 4D seismic data
Rickett, James	SEG Expanded Abstracts	1999	Acoustic daylight imaging via spectral factorization: Helioseismology and reservoir monitoring
Ritchie, Bryan	SEG Expanded Abstracts	2002	The impact of new 4D seismic technology on the magnus field
Robertsson, Johan O. A.	Geophysics	2000	A finite-difference injection approach to modeling seismic fluid flow monitoring
Robertsson, Johan O.	Geophysics	2000	An efficient method for calculating finite-difference seismograms after model alterations

A.			
Robertsson, Johan O. A.	SEG Expanded Abstracts	1999	A finite-difference injection approach to modeling of seismic fluid flow monitoring
Robinson, Nigel	The Leading Edge	2005	4D time-lapse monitoring of Chirag Field
Roche, Steven L.	SEG Expanded Abstracts	1998	An onshore time-lapse (4-D), multicomponent, data processing case history, vacuum field, New Mexico
Ronen, Shuki	SEG Expanded Abstracts	1999	Repeatability of sea bed multi-component data
Ross, Christopher P.	The Leading Edge	1996	Inside the crossequalization black box
Ross, Christopher P.	The Leading Edge	1997	Time-lapse seismic monitoring: Some shortcomings in nonuniform processing
Rossi, D. J.	SPE - Schlumberger	2000	Discussion on Integrating Monitoring Data into the Reservoir Management Process
Rothert, Elmar	SEG Expanded Abstracts	2002	Microseismic monitoring of borehole fluid injections: Data modeling and inversion for hydraulic properties of rocks
Sanches, V.	SEG Expanded Abstracts	2005	Is it statiscally significant anomaly?
Sarkar, Debashish	Geophysics	2003	Anisotropic inversion of seismic data for stressed media: Theory and a physical modeling study on Berea Sandstone
Sarkar, Sudipta	SEG Expanded Abstracts	2003	On the inversion of time-lapse seismic data
Sasagawa, Glenn S.	Geophysics	2003	A new sea-floor gravimeter
Saunders, Mike	SEG Expanded Abstracts	2004	Source signature repeatability and source array directivity — Measurements from the Valhall 4D survey
Schmitt, Douglas R.	SEG Expanded Abstracts	1998	Shallow seismic profiling over heated heavy oils: Directions towards time lapse monitoring
Schonewille, M. A.	Geophysics	2003	A general reconstruction scheme for dominant azimuth 3D seismic data
Schonewille, M. A.	SEG Expanded Abstracts	2003	A modeling study on seismic data regularization for time-lapse applications
Sengupta, Madhumita	Geophysics	2003	Quantifying subresolution saturation scales from time-lapse seismic data: A reservoir monitoring case study
Sengupta, Madhumita	SEG Expanded Abstracts	2000	Integrating time-lapse seismic and flow simulation to map saturation changes: A reservoir monitoring case study
Seymour	SPE International	1996	An Improved Seabed Seismic 4D Data Collection Method for Reservoir Monitoring
Shams, A.	SEG Expanded Abstracts	2002	Robust time-lapse AVOA analysis using OBC: A case study from Teal South
Shen, Feng	SEG Expanded Abstracts	2000	Scattering of P-S converted waves in fractured reservoirs

Sherlock, Donald H.	SEG Expanded Abstracts	2004	Analog reservoir modeling of turbidite channel sands
Sherlock, Donald H.	The Leading Edge	2001	Time-lapse monitoring of immiscible fluid-flow models
Sherlock, Donald H.	SEG Expanded Abstracts	1999	Time-lapse 3-D seismic with analogue sandbox models
Sinartio, Franciscus Boetje	SEG Expanded Abstracts	2002	Predicting fluid composition from seismic data: CO2 detection from seismic
Skidmore, Charles M.	SEG Expanded Abstracts	2002	Visualization of rock property attribute cubes for field analysis
Skjervheim	SPE International	2005	Incorporating 4D Seismic Data in Reservoir Simulation Models Using Ensemble Kalman Filter
Skov, Thorleif	SEG Expanded Abstracts	2002	Monitoring and characterization of a CO2 storage site
Slawinski, Raphael A.	SEG Expanded Abstracts	2000	Non-welded contact: A finite-difference approach
Smit, Dirk	SEG Expanded Abstracts	2004	Tidal-driven constraints for time-lapse reservoir monitoring
Smith, Patrick	The Leading Edge	2001	4-D seismic in a complex fluvial reservoir: The Snorre feasibility study
Sønneland, Lars	The Leading Edge	1997	Seismic reservoir monitoring on Gullfaks
Sønneland, Lars	SEG Expanded Abstracts	2000	Detecting flow-barriers with 4D seismic
Sparkman, Gene W.	The Leading Edge	1998	An introduction to this special section: Time lapse or time elapse?
Sparkman, Gene W.	The Leading Edge	2001	Paving the road to real-time reservoir monitoring—The next step? Summary of an ERCH workshop
Spetzler, Jesper	SEG Expanded Abstracts	2003	Time-lapse seismic monitoring in the prestack domain
Spetzler, Jesper	SEG Expanded Abstracts	2004	On the sensitivity of the NRMS function to non-repeatability causes and production
Staples, Rob	SPE International	2002	Integrating 4D seismic to optimize production
Stephen, K.	First Break	2006	Seismic history matching in the UKCS Schiehallion field
Stephen, Ralph A.	SEG Expanded Abstracts	1999	Ambient noise below the seafloor
Stovas, A.	Geophysics	2005	Fluid-pressure discrimination in anisotropic reservoir rocks — A sensitivity study
Swanston, A. M.	Geophysics	2003	Time-lapse imaging at Bullwinkle field, Green Canyon 65, offshore Gulf of Mexico
Talwani, Manik	SEG Expanded Abstracts	1999	Time lapse gravity gradiometry
Tennebø, P. O.	SEG Expanded Abstracts	1998	Inversion of 4D seismic with best feasible approximation
Terrell, Martin J.	SEG Expanded Abstracts	2002	Seismic monitoring of a CO2 flood at Weyburn field, Saskatchewan, Canada: demonstrating the robustness of time-lapse seismology
Theune, Ulrich	SEG Expanded Abstracts	2003	Feasibility study of time-lapse seismic monitoring for heavy oil reservoir development — The rock-

			physical basis
Tiwari, U.	SEG Expanded Abstracts	2005	Estimation of effective pressure and water saturation by viscoelastic inversion of synthetic time-lapse seismic data for a gas sandstone reservoir
Toinet, Sylvain	SPE International	2004	4D Feasibility and Calibration Using 3D Seismic Modeling of Reservoir Models
Tura, A.	The Leading Edge	2001	An introduction to this special section: Instrumented Oil Fields
Tura, A.	SEG Expanded Abstracts	1999	Estimating pressure and saturation changes time-lapse AVO data
Tura, A.	SEG Expanded Abstracts	2003	Time-lapse seismic: Are we there yet?
Vasco, Don W.	Geophysics	2004	Seismic imaging of reservoir flow properties: Time-lapse pressure changes
Vasco, Don W.	Geophysics	2005	On the use of quasi-static deformation to understand reservoir fluid flow
Vasco, Don W.	Geophysics	2004	Seismic imaging of reservoir flow properties: Time-lapse amplitude changes
Vauthrin, Robert	SEG Expanded Abstracts	1999	Improvements in 4D legacy data quality and repeatability through reprocessing, Lena Field
Veire, Helene Hafslund	SEG Expanded Abstracts	1998	Estimation of reservoir fluid volumes through 4D seismic analysis on Gullfaks
Veire, Helene Hafslund	SEG Expanded Abstracts	2003	Stochastic inversion of pressure and saturation changes from time-lapse seismic data
Vesnaver, A. L.	SEG Expanded Abstracts	2001	Target-oriented time-lapse analysis by AVO and tomographic inversion
Vesnaver, A. L.	Geophysics	2003	Time-lapse tomography
Vidal, Sandrine	SEG Expanded Abstracts	2001	Feasibility study of time-lapse parameters estimate for mean effective stress and saturation changes in gas storage
Voutay, Olivier	SEG Expanded Abstracts	2002	Seismic interpretation with new attributes extracted from a prestack multicube analysis
Waggoner, J. R.	SPE International	2000	Quantifying the Economic Impact of 4D Seismic Projects
Waggoner, J. R.	SPE International	1998	Lessons Learned From 4D Projects
Waggoner, J. R.	SPE International	2002	Improved Reservoir Modeling With Time-Lapse Seismic in a Gulf of Mexico Gas Condensate Reservoir
Waggoner, J. R.	SPE International	1998	Lessons Learned from 4D Projects
Waggoner, J. R.	SPE International	2002	Improved Reservoir Modeling With Time-Lapse Seismic in a Gulf of Mexico Gas Condensate Reservoir
Wagner, Sean	SEG Expanded Abstracts	2004	Gas saturation calculated from patchy and homogeneous models at Foinaven Field
Waite, Michael W.	The Leading Edge	1997	Seismic monitoring of the Duri steamflood: Application to reservoir management

Waite, Michael W.	SEG Expanded Abstracts	2002	Probabilistic risk assessment from fuzzy seismic information, well measurements, and inferences of spatial continuity: Hamaca Field, Venezuela
Wang, Zhijing	Geophysics	1998	Seismic monitoring of a CO2 flood in a carbonate reservoir: A rock physics study
Wang, Zhijing	The Leading Edge	1997	Feasibility of time-lapse seismic reservoir monitoring: The physical basis
Wapenaar, Kees	SEG Expanded Abstracts	2001	Elastodynamic reciprocity theorems for time-lapse seismic methods
Wapenaar, Kees	SEG Expanded Abstracts	2000	One-way acoustic reciprocity and its applications in multiple elimination and time-lapse seismics
Watanabe, Toshiki	SEG Expanded Abstracts	2004	Differential waveform tomography for time-lapse crosswell seismic data with application to gas hydrate production monitoring
Weathers, Lloyd R.	The Leading Edge	1998	Wavelet control allows differencing of 3-D from 2-D
Weisenborn, Toon	The Leading Edge	2005	Time-lapse seismic in Gannet A: One more lead firmly integrated
Wever, A.	SEG Expanded Abstracts	2004	Criteria for source and receiver positioning in time-lapse seismic acquisition
Whitcombe, David N.	SEG Expanded Abstracts	2001	Systematic application of 4D in BP's NW Europe operations
Winterstein, Don	The Leading Edge	1998	9-C time-lapse VSP monitoring of steam injection at Cymric Oil Field
Wu, J.	SPE International	2005	Improving Water Saturation Prediction With 4D Seismic
Wu, Jianbing	SEG Expanded Abstracts	2004	Establishing spatial pattern correlation for interpreting time lapse seismic amplitudes
Xu, Haibin	The Leading Edge	2001	Integrating reservoir engineering and satellite remote sensing for (true) continuous time-lapse reservoir monitoring
Yuh, Sung H.	SEG Expanded Abstracts	2000	Effects of pressure and fluid saturation changes on time-lapse AVO response
Yuh, Sung H.	SEG Expanded Abstracts	2001	Time-lapse seismic monitoring of CO2 sequestration in hydrocarbon reservoirs
Yuh, Sung H.	SEG Expanded Abstracts	1999	A feasibility study of time-lapse seismic monitoring using stochastic reservoir models
Yuh, Sung H.	SEG Expanded Abstracts	2002	Uncertainty analysis in time-lapse seismic modeling
Zeeman, Jan Harry	SEG Expanded Abstracts	2001	Time-lapse GPR measurement to study the imaging operator
Zhang, Yajun	SEG Expanded Abstracts	2004	Time-lapse impedance inversion using hybrid data transformation and the spike deconvolution method
Zheng, Ye	SEG Expanded Abstracts	2002	Integrating seismic fracture analysis with migration
Zhou, Chengdang	SPE - Petroleum Exploration & Development Institute	2000	A Feasibility Study of Time-Lapse (4D) Seismic Monitoring of Water Injection Recovery Processes
Zou, Ying	The Leading Edge	2003	Time-lapse well log analysis, fluid substitution, and AVO
Zou, Ying	SEG Expanded Abstracts	2003	Seismic modelling for a heavy oil reservoir time-lapse study

Zou, Ying	SEG Expanded Abstracts	2004	Time-lapse seismic analysis of a heavy oil cold production field, Lloydminster, Western Canada
Zou, Ying	SEG Expanded Abstracts	2002	Time-lapse well log analysis, fluid substitution and AVO